Searching For Simple Symmetric Venn Diagrams

by

Abdolkhalegh Ahmadi Mamakani
B.Sc., Isfahan University of Technology, 1994
M.Sc., Amirkabir University of Technology, 1998

A Dissertation Submitted in Partial Fulfillment of the
Requirements for the Degree of

DOCTOR OF PHILOSOPHY

in the Department of Computer Science

Searching For Simple Symmetric Venn Diagrams

by

Abdolkhalegh Ahmadi Mamakani
B.Sc., Isfahan University of Technology, 1994
M.Sc., Amirkabir University of Technology, 1998

Supervisory Committee

Dr. Frank Ruskey, Supervisor
(Department of Computer Science)

Dr. Wendy Myrvold, Departmental Member
(Department of Computer Science)

Dr. Sue Whitesides, Departmental Member
(Department of Computer Science)

Dr. Peter Dukes, Outside Member
(Department of Mathematics and Statistics)

Supervisory Committee

Dr. Frank Ruskey, Supervisor
(Department of Computer Science)

Dr. Wendy Myrvold, Departmental Member
(Department of Computer Science)

Dr. Sue Whitesides, Departmental Member
(Department of Computer Science)

Dr. Peter Dukes, Outside Member
(Department of Mathematics and Statistics)

ABSTRACT

An *n-Venn diagram* is defined as a collection of n finitely intersecting closed curves dividing the plane into 2^n distinct regions, where each region is in the interior of a unique subset of the curves. A Venn diagram is *simple* if at most two curves intersect at any point, and it is *monotone* if it has some embedding on the plane in which all curves are convex. An n-Venn diagram has *n-fold rotational symmetry* if a rotation of $2\pi/n$ radians about a centre point in the plane leaves the diagram unchanged, up to a relabeling of the curves. It has been known that rotationally symmetric Venn diagrams could exist only if the number of curves is prime. Moreover, non-simple Venn diagrams with rotational symmetry have been proven to exist for any prime number of curves. However, the largest prime for which a simple rotationally symmetric Venn diagram was known prior to this, was 7.

In this thesis, we are concerned with generating simple monotone Venn diagrams, especially those that have some type(s) of symmetry. Several representations of these diagrams are introduced and different backtracking search algorithms are provided

based on these representations. Using these algorithms we show that there are 39,020 non-isomorphic simple monotone 6-Venn diagrams in total. In the case of drawing Venn diagrams on a sphere, we prove that there exists a simple symmetric n-Venn diagram, for any $n \geq 6$, with the following set(s) of isometries : (a) a 4-fold rotational symmetry about the polar axis, together with an additional involutional symmetry about an axis through the equator, or (b) an involutional symmetry about the polar axis together with two reflectional symmetries about orthogonal planes that intersect at the polar axis. Finally, we introduce a new type of symmetry of Venn diagrams which leads us to the discovery of the first simple rotationally symmetric Venn diagrams of 11 and 13 curves.

Contents

List of Tables

List of Figures

ACKNOWLEDGEMENTS

I would like to express my deepest gratitude to my supervisor Dr. Frank Ruskey for his excellent guidance and support. Without his valuable advice, encouragement and unconditional financial and spiritual support this research would have never been completed.

I would also like to thank Dr. Wendy Myrvold for her collaboration on some topics of this thesis and also for verifying part of the results. In addition, I would like to thank Dr. Rick Mabry at Louisiana State University in Shreveport and Dr. Mark Weston for verifying the correctness of the first simple symmetric 11-Venn diagram.

This research was supported in part by a fellowship from the University of Victoria .

Finally, I must express my special appreciation to my wife, Jilla, for her sacrifice, unwavering support and everlasting love.

DEDICATION

To my mother, may her soul rest in peace.

Chapter 1

Introduction

It has been said that a picture is worth a thousand words. Diagrams and pictures, particularly when they become conventional notations, are used to deliver information in a clear and understandable way without even using any words. Good examples are the traffic signs alongside the roads used to deliver information to drivers in a fast and clear way. In fact, archaeological findings from the cave paintings and stone carvings indicate that the use of diagrams and symbols has been of human interest since ancient times.

Diagrams have played a prominent role in the history of mathematics. Records obtained from Babylonian clay tablets indicate the use of mathematical diagrams in solving quadratic equations about 4000 years ago [44, 48]. Diagrams were also an integral part of geometric proofs in Ancient Greek mathematics [43]. The big advantage of diagrams is their ability to visualize the concepts that are hard to clearly explain using only words. A closed curve, for example, is a convenient way of explaining the concept of inclusion or exclusion. Therefore, it is easier to understand a mathematical proof when it is accompanied with an appropriate diagram.

Venn diagrams are named after the English logician John Venn (1834-1923) [51], who developed them as a visual system of representing logical propositions and their relationships. They are used in set theory to illustrate all possible cases of logical relations between a finite number of sets. However, Venn diagrams are interesting mathematical objects in their own right, and their combinatorial and geometric properties are the subject of many papers in recent years.

Symmetry is a fundamental concept in mathematics that can be observed in many aspects of our daily life. It is abundant in nature and it has always been a source of inspiration for man-made objects. Symmetry is an important feature when it comes

to the aesthetics of a diagram, because most people find symmetric diagrams more appealing than asymmetric ones. Furthermore, symmetric diagrams are more understandable because the human eye naturally recognizes symmetric patterns faster. Another significant property is that every symmetric diagram contains a basic part, known as the fundamental domain, from which the entire diagram can be created. Therefore, when symmetry is involved in searching for a class of Venn diagrams, for example, it leads to a dramatic decrease in problem size and searching time.

There has been a growing interest in research on symmetric Venn diagrams in recent years. Aside from the aesthetic qualities and interesting combinatorial and geometric properties of Venn diagrams, part of the interest in Venn diagrams is due to the fact that their geometric dual graphs are planar spanning subgraphs of the hypercube. Therefore, symmetric drawings of Venn diagrams imply symmetric drawings of the spanning subgraphs of the hypercube. Some recent work on finding symmetric structures embedded in the hypercube is reported by Jordan [37] and Duffus, McKibbin-Sanders and Thayer [13].

1.1 Overview

When studying a specific class of Venn diagrams, some of the natural questions that come to mind are:

- Enumeration of Venn diagrams in that class with a given number of curves.
- Existence of a general method for constructing a Venn diagram in that class for any given number of curves.

The main motivation of this research is to answer such questions.

Symmetric Venn diagrams have been proven to exist for any prime number of curves, but in the case of *simple* ones, that is, those for which no three curves intersect in a common point, the symmetric diagrams that have been found prior to this work are of at most seven curves. In this thesis we study a particular class of simple Venn diagrams, called *monotone*, that can be drawn on the plane using convex curves. The main contributions of the thesis are as follows :

- Providing several representations of simple monotone Venn diagrams and developing different backtracking search algorithms based on these representations.

- Generating all different simple monotone Venn diagrams of six curves.
- Providing a general approach for constructing simple symmetric Venn diagrams on the sphere with an isometry group of order 8.
- Introducing a new type of symmetry of Venn diagrams and using it to generate the first simple rotationally symmetric Venn diagrams of 11 and 13 curves.

The rest of thesis is organized as follows. In Chapter 2 we first review basic definitions and notation that are used throughout the rest of the thesis. The second part of Chapter 2 contains a history of research on Venn diagrams. In Chapter 3, different representations of simple monotone Venn diagrams are provided. We use these representations in Chapter 4 to generate simple monotone Venn diagrams of six curves and simple monotone symmetric Venn diagrams of seven curves. A general method of constructing simple symmetric Venn diagrams on a sphere with isometry group of order eight is provided in Chapter 5. Chapter 6 introduces a new type of symmetry of simple Venn diagrams, called *crosscut symmetry*, which enabled us to discover the first simple symmetric Venn diagrams of 11 and 13 curves. The last chapter contains conclusions and some open problems in this area.

Chapter 2

Background

In this chapter, we introduce the basic terminology that we use throughout this dissertation. First we briefly review the necessary definitions from the topology of the plane. For more detailed and formal definitions, the reader may refer to any standard textbook on this topic, such as [19, 34]. Then we describe the definition of Venn diagrams and their characteristics. We follow Grünbaum [22], and Ruskey and Weston [46] for definitions in this part of the thesis.

2.1 Jordan curves

Points are the most fundamental elements of the Euclidean plane. Each point in the plane is uniquely specified by a pair (x, y) of real numbers in the Cartesian coordinate system. This means we can identify the plane with an infinite set of pairs of real numbers. Formally, plane is defined as the infinite set

$$\mathbb{R}^2 = \{(x, y)|x, y \in \mathbb{R}\}.$$

This definitions allows us to represent objects in the plane as subsets of $\mathbb{R}^2$. In this dissertation we are interested in non-self-intersecting closed curves known as *Jordan curves* or *simple closed curves*.

Definition 2.1.1. Let ψ be a continuous map from the real interval $[0, 1]$ to $\mathbb{R}^2$ such that it is one-to-one on $[0, 1)$, that is, for any $a, b \in [0, 1)$, if $\psi(a) = \psi(b)$ then $a = b$. The image of ψ is called a *simple closed curve* or a *Jordan curve* in plane if $\psi(0) = \psi(1)$. If $\psi(0) \neq \psi(1)$ then the image of ψ is called an *arc* in the plane and $\psi(0)$ and $\psi(1)$ are the *endpoints* of the arc.

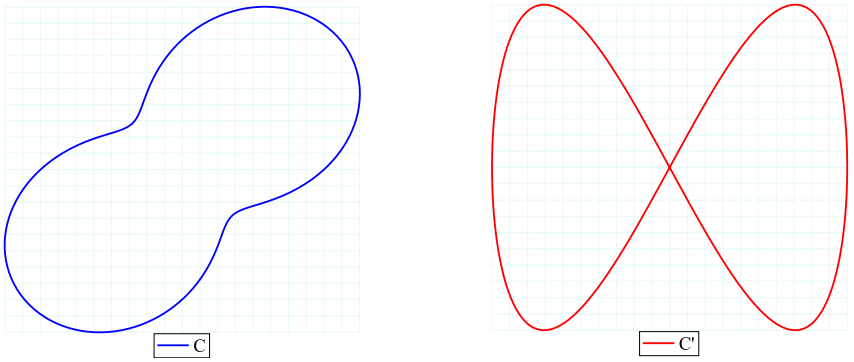

(a) A Jordan curve

(b) A self-intersecting curve

Figure 2.1: Examples of closed curves.

For example, the following mapping gives the Jordan curve of Figure 2.1(a).

$$\psi(t) = \left(\sin(2\pi t)\left(2+\sin(4\pi t)\right), \cos(2\pi t)\left(2+\sin(4\pi t)\right)\right), \qquad t \in [0,1]$$

Figure 2.1(b), however, shows an example of a self-intersecting curve obtained by the continuous mapping $\varphi(t) = (\sin(2\pi t), \sin(2\pi t)\cos(2\pi t))$, where $t \in [0,1]$.

Another example of a plane subset is an open disk of radius r (not including the boundary circle) centered at some point (a,b). It consists the following set of points.

$$\left\{(x,y) \in \mathbb{R}^2 | (x-a)^2 + (y-b)^2 < r^2\right\}$$

Let p be a point in the plane. Any open disk that contains p specifies a set of points in the plane that is usually known as a *neighborhood* of p. The concept of neighborhood is essential in understanding topological properties of the plane subsets.

Definition 2.1.2. Given a point p and subset A of the plane, we say p is *near* A if every neighborhood D of p contains a point of A, that is, $A \cap D \neq \emptyset$.

Using the notion of neighborhood, now we can define the open and closed subsets of the plane.

Definition 2.1.3. A subset S of the plane is called *open* if for every point p in S there exists a neighborhood of p that is entirely contained in S.

Again consider the simple closed curve C in Figure 2.1(a). Let A include all points of the interior of C (not including curve C). Set A is open, because there is no point in A that is near the complement set $\mathbb{R}^2 \backslash A$.

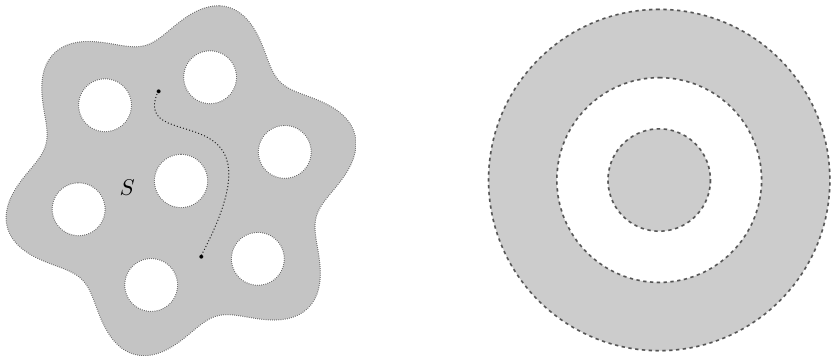

(a) Connected (b) Disconnected

Figure 2.2: Examples of plane subsets.

A plane subset is *closed* if its complement is open. The curve C in Figure 2.1(a) is a closed set which specifies the *boundary* of an open set A. It is defined as the set of all points near both A and its complement $\mathbb{R}^2 \backslash A$. For example, the boundary of a circular disk of radius r, centered at origin, is the set of points $\{(x, y) \in \mathbb{R}^2 | x^2 + y^2 = r^2\}$.

Another important property of plane subsets is *connectedness*. Consider the plane subsets in Figure 2.2, for example. The open set S in (a) is *connected* because it is possible to connect any two points of S with an arc entirely contained in it. On the other hand, the plane subset in (b) is *disconnected* because it consists of two disjoint open sets; neither of which contains a point near the other.

Definition 2.1.4. A plane subset S is *connected* if whenever it is partitioned into two nonempty subsets A and B such that $A \cap B = \emptyset$ and $S = A \cup B$, then there is always some point in A near B and vice versa.

We close this section with a fundamental result in topology known as *the Jordan curve Theorem*. It states that for any Jordan curve C in the plane, the complement $\mathbb{R}^2 \backslash C$ is composed of two disjoint connected open sets, the bounded interior of C and the unbounded exterior. For the rest of this dissertation we denote the interior and exterior of a given Jordan curve C by $\text{int}(C)$ and $\text{ext}(C)$, respectively.

2.2 Venn diagrams

As mentioned in the previous section, a Jordan curve partitions the plane into two open sets. Now consider two Jordan curves A and B in the plane. There are four

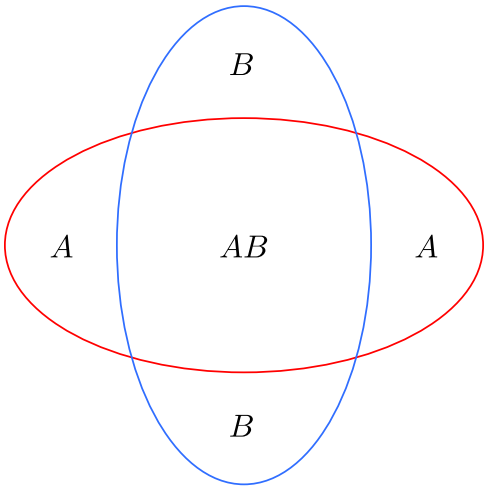

Figure 2.3: A diagram of two curves.

possible open plane subsets given by intersections of the interior and exterior of A and B, namely, $\text{ext}(A) \cap \text{ext}(B), \text{ext}(A) \cap \text{int}(B), \text{int}(A) \cap \text{ext}(B)$ and $\text{int}(A) \cap \text{int}(B)$. We refer to a collection of n Jordan curves in the plane as an *n-diagram*. In general, in an n-diagram there can exist at most 2^n sets given by intersections of the interiors and exteriors of the curves. For ease of reading we simply specify each such set by concatenating the labels of those curves that have points of their interiors in the set. For example, in a diagram of three curves A, B and C in the plane, AC specifies the set $\text{int}(A) \cap \text{ext}(B) \cap \text{int}(C)$.

Depending on the arrangement of the curves, some of the sets of a diagram may be empty and/or disconnected. Figure 2.3, for example, shows a diagram of two curves where set A consists of two disjoint open sets, as does B. In a diagram, a maximal connected open subset of the plane is called a *region*. The diagram of Figure 2.3, therefore, contains four sets and six regions.

For a family of curves in the plane, it is possible to extend the definitions to the cases where the curves intersect in infinitely many points. However, in this thesis we assume that there are only a finite number of points where the curves intersect. We use specific terms for a collection of Jordan curves depending on the existence and/or connectedness of the sets. We follow Grünbaum [22], and Ruskey and Weston [46] for definitions of these terms.

Definition 2.2.1. A collection $\mathcal{D} = \{C_1, C_2, \ldots, C_n\}$ of n Jordan curves in the plane is called an *n-Venn diagram* if none of the 2^n possible open sets $X_1 \cap X_2 \cap \cdots \cap X_n$

is empty or disconnected, where $X_i \in \{\text{int}(C_i), \text{ext}(C_i)\}$.

Each set $X_1 \cap X_2 \cap \cdots \cap X_n$, as above, in an n-Venn diagram corresponds to exactly one region of the diagram. Therefore, an n-Venn diagram has 2^n regions. In a general diagram, however, this is not true because some sets may be disconnected and consist of more than one region.

Definition 2.2.2. A diagram $\mathcal{D} = \{C_1, C_2, \ldots, C_n\}$ is called an *independent family* if none of the open sets $X_1 \cap X_2 \cap \cdots \cap X_n$ is empty, where $X_i \in \{\text{int}(C_i), \text{ext}(C_i)\}$.

There are at least 2^n regions in an independent family. There is another class of diagrams called *Euler diagrams* where the number of regions is at most 2^n, as not all the $X_1 \cap X_2 \cap \cdots \cap X_n$ sets are necessarily nonempty, but they all must be connected.

Definition 2.2.3. A diagram $\mathcal{D} = \{C_1, C_2, \ldots, C_n\}$ is an *Euler diagram* if every open set $X_1 \cap X_2 \cap \cdots \cap X_n$ is connected, where $X_i \in \{\text{int}(C_i), \text{ext}(C_i)\}$.

Figure 2.4 shows different diagrams of two curves. The diagram in (a) is a 2-Venn diagram because it has four regions and each one corresponds to one of the four possible intersections of the interior and exterior of the curves. Diagrams (b) and (c) are Euler diagrams since $\text{int}(A) \cap \text{int}(B)$ is empty in (b) and $\text{ext}(A) \cap \text{int}(B)$ is empty in (c). Figure 2.4(d) is an independent family that is not a Venn or Euler diagram because both $\text{ext}(A) \cap \text{ext}(B)$ and $\text{int}(A) \cap \text{int}(B)$ are disconnected.

We also classify diagrams based on the maximum number of curves that intersect at any point in the plane. A diagram is called *simple* if no more than two curves intersect at any given point; otherwise it is *nonsimple*. Furthermore, the intersections of the curves must be transverse; that is, in a simple Venn diagram no two curves are tangent at any point of intersection but they must cross each other.

Definition 2.2.4. A Venn diagram is *simple* if at any point of intersection exactly two curves cross each other.

Figure 2.5(a) shows the well-known and unique simple 3-Venn diagram. But the 3-Venn diagram of Figure 2.5(b) is nonsimple since there are points at which three curves intersect.

Let r be a region in a diagram. For any curve C of the diagram, we say C contains r if it has r in its interior, i.e, $r \subseteq \text{int}(C)$. We can associate a label to each region of a diagram that indicates the curves that contain the region. For Venn and Euler diagrams this label is unique since each region is in the interior of a unique subset of the curves.

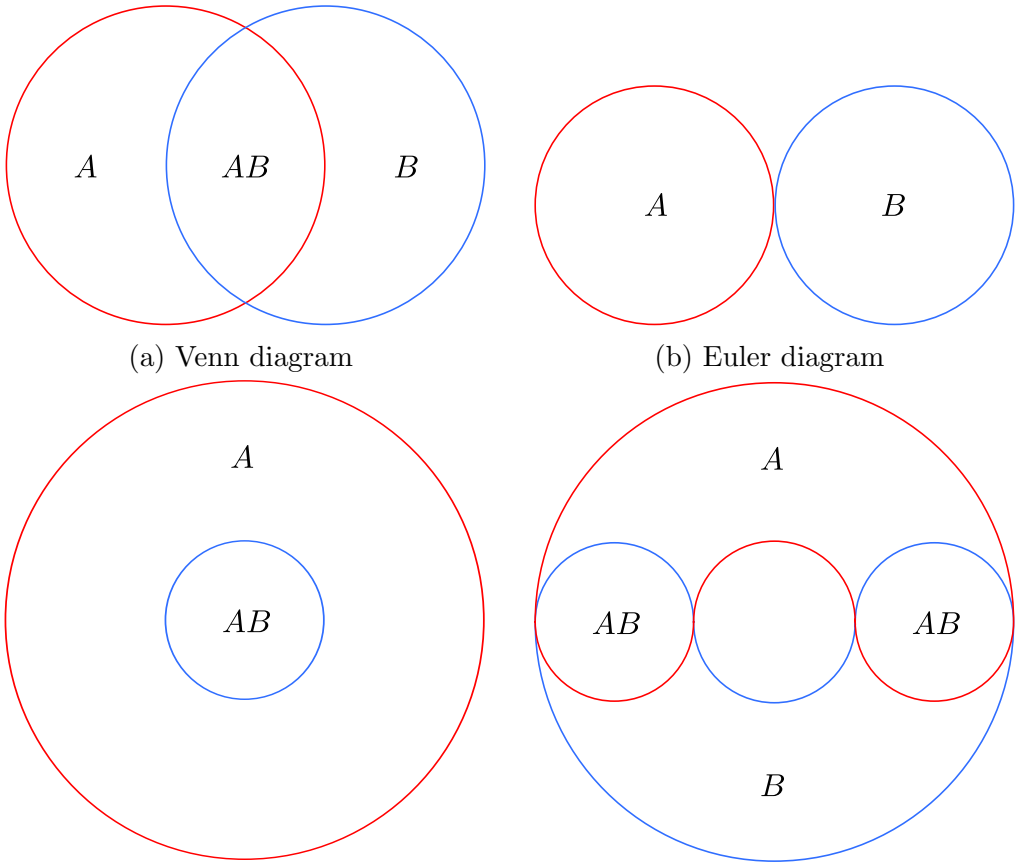

(a) Venn diagram (b) Euler diagram

(c) Euler diagram (d) Independent family

Figure 2.4: Different types of diagrams of two curves.

Definition 2.2.5. The *rank* r of a region R in a diagram $\mathcal{D} = \{C_1, C_2, \ldots, C_n\}$ is the binary number $(b_{n-1}b_{n-2}\cdots b_0)_2$ where $b_i = 1$, $0 \leq i < n$, if C_{i+1} contains R and $b_i = 0$, otherwise.

The number of 1's in the rank of a region is called the *weight* of the region and it indicates the number of curves that contain it. In an n-Venn diagram, for example, the weight of the outermost region is 0 and the weight of the innermost region is n. In a diagram of n curves, we call a region of weight k, $0 \leq k \leq n$, a *k-region* for short. Two regions in a diagram are *adjacent* if their ranks differ by exactly one bit.

Definition 2.2.6. An n-Venn diagram is *monotone* if every k-region is adjacent to at least one $(k+1)$-region (for $0 \leq k < n$) and is also adjacent to at least one $(k-1)$-region (for $0 < k \leq n$).

A simple 4-Venn diagram is shown in Figure 2.6 where each region is labeled by

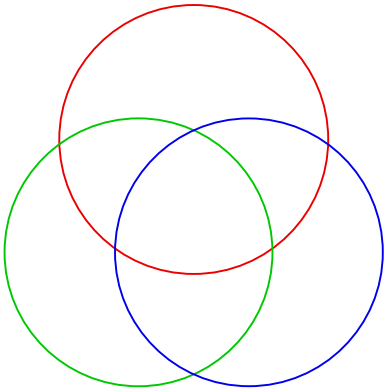

(a) A simple 3-Venn diagram

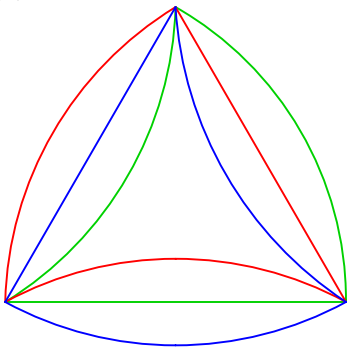

(b) A nonsimple 3-Venn diagram

Figure 2.5: Examples of simple and nonsimple Venn diagrams.

the curves containing it. The weight of the region that is only in the interior of curve D is 1 but it is not adjacent to any regions of weight 0. Therefore the diagram is nonmonotone. A Venn diagram in which every region of weight 1 is adjacent to the region of weight 0 is called an *exposed Venn diagram*. In other words, in an exposed Venn diagram every curve touches the outermost region. It is easy to see that every monotone Venn diagram is exposed.

2.3 Venn diagrams on the sphere

Part of this thesis is about constructing simple Venn diagrams on the sphere with a particular type of symmetry. Therefore, here we introduce some basic terminology related to spheres and also some transformations between spherical and Euclidean spaces that are necessary for understanding certain representations of spherical Venn diagrams. A more detailed study of spherical Venn diagrams may be found in We-

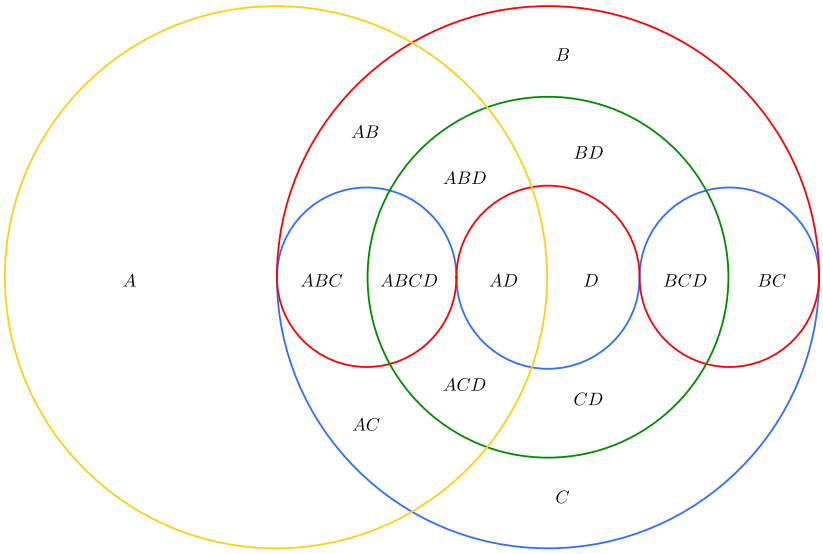

Figure 2.6: An example of a nonmonotone 4-Venn diagram.

ston's Ph.D. thesis [55].

Definition 2.3.1. A *sphere* of *radius* r is a surface in three-dimensional Euclidean space defined by the set of all points that are located at the same distance r from a given point in space known as the *center* of the sphere. For example, a sphere of radius r centered at the origin $(0, 0, 0)$ is defined as the set of all points $(x, y, z) \in \mathbb{R}^3$ such that $x^2 + y^2 + z^2 = r^2$.

Any straight line that passes through the center of a sphere intersects it at two points which are called *antipodal points*. Two particular antipodal points of the sphere are distinguished as the *north* and *south poles*. The line through the north and south poles is called the *primary axis of rotation* of the sphere. The intersection of a sphere with a plane passing through its center is a circle on the sphere called a *great circle*. If the plane is the one perpendicular to the primary axis of rotation, then the great circle is the unique *equator*. All great circles that pass through the poles and are called *circles of longitude*. The circles of longitude together with the circles parallel to the equator, which are called the circles of latitude, are often used to specify the location of a point on the surface of the sphere.

Passing through every point p on a sphere there exists a unique circle of latitude and also a unique circle of longitude. The half of the longitude circle through p to the poles is called the *meridian* of p. For convenience let assume that the radius of the sphere is 1. Then, the location of a point p on the sphere is indicated by (ϕ, θ),

where ϕ is the angle subtended by the arc along the meridian of p to the point where the meridian of p intersects the equator; θ is the angle subtended by the arc along the equator from the intersection of a reference meridian, which is called *the prime meridian*, to the point that the meridian of p intersects the equator (see Figure 2.7).

The Jordan Curve Theorem holds for Jordan curves on the sphere, as well. But we must be clear about the interior and exterior of a Jordan curve on the sphere, because unlike the plane, where the exterior of a Jordan curve is unbounded, both the interior and exterior of a Jordan curve on the sphere are bounded. Knowing the interior and exterior of the curves, we can use the same definition of Venn diagrams on the plane for a collection of Jordan curves on the sphere. For a Venn diagram on the sphere it is enough to indicate either the outermost region or innermost region to specify the interior and exterior of all curves.

When studying Venn diagrams on a sphere, it is often useful to map the surface of sphere to the plane so that it is possible to see the entire diagram as one piece. A function which describes how to assign the points on a sphere to points on the plane is known as a *projection*. Projections are used by cartographers to create a flat map of the earth. It is not possible to map a spherical object to the plane without distortions in shape, area or angle to some degree. Therefore, depending on which geometric property needs to be preserved, different projections may be used. A projection that preserves the angular relationships is said to be a *conformal projection*. Here we introduce two types of projections.

Definition 2.3.2. Consider the sphere $x^2 + y^2 + (z-1)^2 = 1$ in $\mathbb{R}^3$ with the point $(0, 0, 2)$ as the north pole (the south pole is located at the origin point $(0, 0, 0)$). The *stereographic projection* is a function λ that assigns every point p on sphere, other than the north pole, to the point q on the xy-plane such that the points p, q and the north pole lie on a straight line.

Figure 2.7 illustrates the stereographic projection[1]. The longitude angle (θ in spherical coordinates) is preserved throughout the projection. The latitude circles of the sphere are mapped to circles on the plane, centered at the origin, and the longitude circles are mapped to lines through the origin. In general, the streographic projection maps the point (ϕ, θ) in spherical coordinates to the point (r, θ) on the

[1]Figure modified from [50]

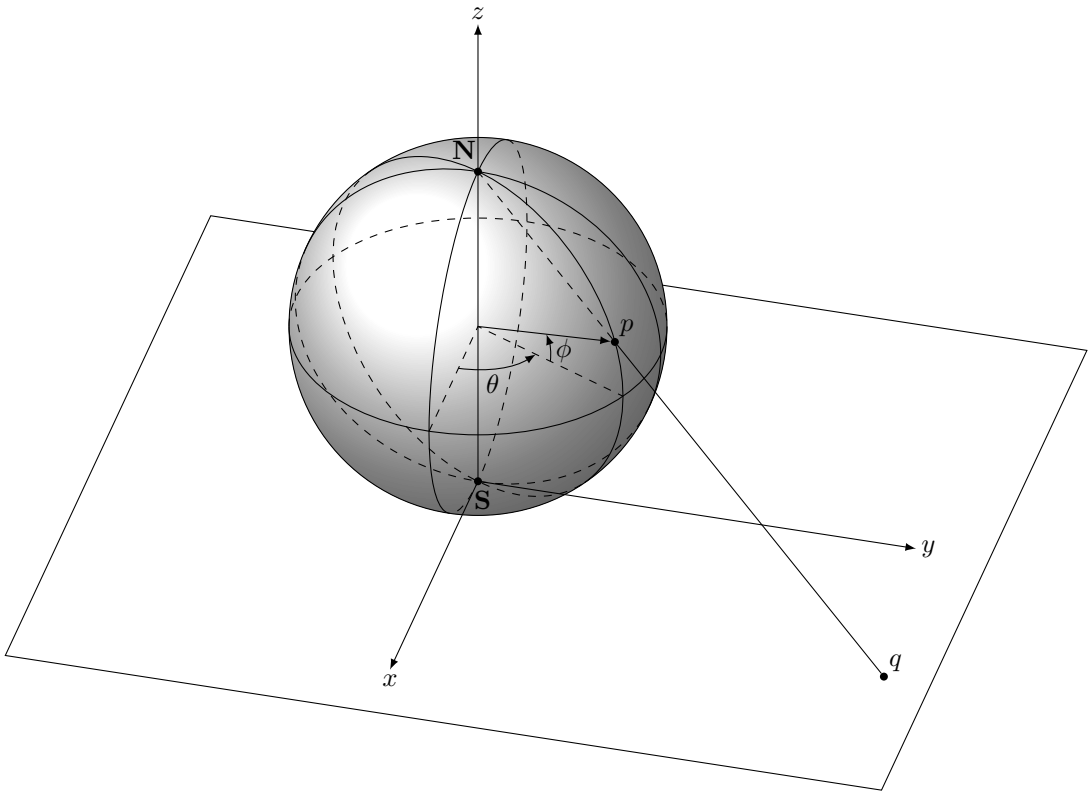

Figure 2.7: Stereographic projection of a sphere to the plane.

plane in polar coordinates, where

$$r = 2\tan\left(\frac{\phi}{2} + \frac{\pi}{4}\right).$$

Given a Venn diagram on the sphere, depending on which region is chosen as the outermost region, it may be projected to different Venn diagrams on the plane. Different Venn diagrams on the plane that are obtained from the same spherical Venn diagram via stereographic projection are sometimes said to be in the same *class* [11]. We will say that a spherical Venn diagram is *monotone* if it has some monotone projection. However, other projections of a monotone diagram are not necessarily monotone.

Imagine a Venn diagram being projected onto a sphere, with the south pole of the sphere tangent to a point inside the innermost region of the diagram, and such that the outermost region of the projected diagram contains the north pole. A rotation of the sphere by π radians about an equatorial axis, which is called a *polar-flip*, interchanges the insides and outsides of all the curves. Therefore, by projecting the diagram back to the plane another Venn diagram is obtained, which we refer to as the *polar-flip* of the original Venn diagram.

Another conformal projection, which is mostly used in navigation systems, is the cylindrical projection. Imagine a cylinder wrapped around the sphere such that the entire circumference of the cylinder is tangent to the sphere along the equator. Now map each point on the sphere to a point on the cylinder such that the line through these points intersects the axis of rotation at a right angle. Then the cylindrical projection of the sphere is the flat image on the plane obtained by unrolling the cylinder. A more formal definition of this projection is given below.

Definition 2.3.3. Given the unit sphere S, a *cylindrical projection* maps a point $p = (\phi, \theta)$ on the surface of S to the point q on the plane with $x = \theta$ and $y = \phi$. Therefore, the surface of S is mapped to a rectangular surface on the plane bounded by the horizontal lines $y = \pm 1$ and the vertical lines $x = 0$ and $x = 2\pi$.

A cylindrical projection is illustrated in Figure 2.8. The image of every longitude circle of the sphere is a vertical line from $y = -1$ to $y = +1$ and the latitude circles are mapped to horizontal lines between $x = 0$ and $x = 2\pi$. The horizontal line through the origin is the image of the equator and the two horizontal lines at $y = -1$ and $y = 1$ are the images of the south pole and the north pole of the sphere respectively.

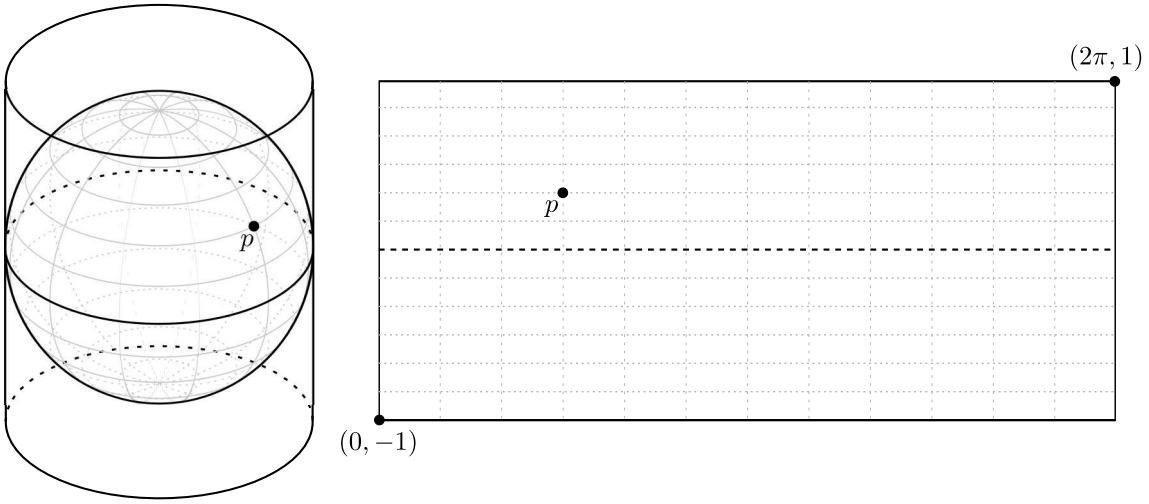

Figure 2.8: Cylindrical projection of a sphere to the plane.

2.4 Graphs

In this section we define some basic terms from graph theory which we need later to describe and study Venn diagrams as graphs. We follow West [54] in the definitions of these terms. In the second part of this section, we discuss embeddings of graphs in the plane.

Definition 2.4.1. A *graph* $G(V, E)$ consists of a vertex set $V = \{v_1, v_2, \ldots, v_n\}$ and an edge set $E = \{e_1, e_2, \ldots, e_m\}$, where each edge e_i, $1 \leq i \leq m$, is associated with a distinct unordered pair of vertices (v_j, v_k), where $1 \leq j, k \leq n$. Vertices v_k and v_j are called the *endpoints* of edge e_i and edge e_i is said to be *incident* to vertices v_j and v_k.

For a graph $G(V, E)$, we use $V(G)$ and $E(G)$ to denote the vertex set and edge set of G respectively. A *subgraph* of graph G is a graph G' such that $V(G') \subseteq V(G)$ and $E(G') \subseteq E(G)$. A *spanning subgraph* of G is a subgraph G' of G for which $V(G') = V(G)$.

In a graph $G(V, E)$, two vertices u and v are *adjacent* if they are the endpoints of an edge in the graph. A *loop* in a graph is an edge that has the same vertex as both of its endpoints. If there are multiple edges in the graph, with the same pair of endpoints, then they are called *multi-edges*. A graph with no loops and no multi-edges is called a *simple graph*. In this dissertation we work with graphs with no loops. To avoid confusion with simple Venn diagrams, we use the term *multi-graph* to refer to the graphs with multi-edges whenever it is needed, and for the remaining cases the reader may assume that the graphs are simple.

The *degree* of a vertex in a graph is the number edges that are incident to the vertex. A graph is k-regular if all vertices of the graph are of degree k. A *path* of length k in a graph $G(V, E)$ is a sequence $v_0, v_1, \ldots, v_k$ of $k + 1$ distinct vertices such that for $i \in \{1, 2, \ldots k\}$, $(v_{i-1}, v_i) \in E$. The graph G is *connected* if for any two vertices u and v there exists a path in G from u to v. A graph that remains connected after removal of any set of at most $k - 1$ vertices is called a *k-connected* graph.

Planar embeddings

A natural way to represent a graph is to draw it on a surface (the plane for example) where the vertices of the graph are shown as points on the surface and the edges are represented by arcs connecting the points corresponding to the vertices of the graph.

Definition 2.4.2. A *planar embedding* of graph $G(V, E)$ is a function ϕ that maps every vertex of G to a distinct point and maps every edge $e = (u, v)$ of G to an arc with endpoints $\phi(u)$ and $\phi(v)$ on the plane such that the arcs do not intersect except at common endpoints.

A graph G is *planar* if it has a planar embedding. Therefore, it is possible to draw a planar graph on the plane without any edges crossing. A particular embedding of a planar graph is called a *plane graph*. We often use a common name for both a planar graph and its embedding and the points and the arcs of the embedding are simply called the vertices and edges of the graph. In addition to the vertices and edges, a plane graph also has a set of *faces* denoted by F, where each *face* is a maximal connected open subset of the plane which has no point in common with any edges or vertices of the graph. The *size* of a face is the number of edges that bound the face. We sometimes refer to a face of size k as a k-face.

It is often useful to describe the combinatorial structure of a plane graph without actually drawing it. Such a description consists of a cyclic ordering of the adjacent vertices for each vertex listed in clockwise direction. The collection of cyclic orderings of adjacent vertices is called a *rotation system* of the graph (see Figure 2.9 for an illustration).

A planar graph may have different embeddings in the plane. Given the rotation systems of two planar embeddings, it is possible to check if they are isomorphic in polynomial time [53, 36, 35, 40, 49].

Definition 2.4.3 ([5])**.** Let $G_1 = (V_1, E_1, R_1)$ and $G_2 = (V_2, E_2, R_2)$ be two plane graphs, where R_1 and R_2 are the rotation systems of G_1 and G_2 respectively. We say the two plane graphs are *isomorphic* if there exists a bijective mapping φ from V_1 to V_2 that preserves the combinatorial structure; that is, if $(t_1\ t_2\ \cdots\ t_k) \in R_1$ is the cyclic ordering of the edge-ends incident to $v \in V_1$ then $(\varphi(t_1)\ \varphi(t_2)\ \cdots\ \varphi(t_k)) \in R_2$ is the cyclic ordering of edge-ends incident to $\varphi(v) \in V_2$.

For every plane graph G there is a *dual plane graph* G^* that is constructed as follows:

- For every face f_i of G, a vertex v_i^* is added to G^* (the vertices of G^* are placed inside the faces of G).
- Let e be an edge of G with f_i and f_j as the faces on two sides of e (f_i and f_j could be the same face). The *dual edge* e^* of e is an edge in G^* that connects

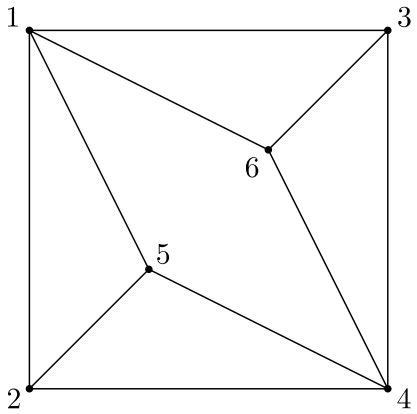

1 : (2 3 6 5)
2 : (1 5 4)
3 : (1 4 6)
4 : (2 5 6 3)
5 : (1 4 2)
6 : (1 3 4)

Figure 2.9: An example of a rotation system of a plane graph.

the vertices v_i^* and v_j^* corresponding to the faces f_i and f_j (each edge of G^* crosses its dual edge in G exactly once).

Figure 2.10 illustrates the construction of an embedding of a dual graph of the plane graph of Figure 2.9; the small white circles represent the vertices of the dual graph and dual edges are shown by the dotted lines.

2.5 Permutations

Consider the n-set $S = \{1, 2, \ldots, n\}$ which we denote as $[n]$ for convenience. An arrangement of the elements of S in some order is called a permutation of S. More formally, a permutation of S is a one-to-one and onto mapping $\pi : S \mapsto S$. There are exactly $n!$ permutations of the n-set $[n]$. The set of all permutations of n is denoted by $\mathbb{S}_n$. A permutation π of $[n]$ is often represented by the sequence $\pi(1), \pi(2), \ldots, \pi(n)$, known as "one-line" notation. For example, $3, 1, 2, 5, 4$ is a permutation of $\{1, 2, 3, 4, 5\}$. The other common notation for writing permutations is *cycle notation*. A k-cycle in a permutation π is a sequence $a_1, a_2, \ldots, a_k$ of k distinct elements, written as $(a_1\ a_2\ \cdots\ a_k)$, such that $\pi(a_i) = a_{i+1}$, for $i \in \{1, 2, \ldots, k-1\}$ and $\pi(a_k) = a_1$. In cycle notation every permutation is written as a product of disjoint cycles. For example, the permutation $5, 6, 1, 4, 3, 2$ may be written as $(153)(26)(4)$ in cycle notation. A *fixed point* in a permutation π of $[n]$ is an element $x \in [n]$ for which $\pi(x) = x$.

Of the particular interest are *involutions* and *circular permutations*. An *involution* is a permutation π such that $\pi(\pi(i)) = i$ for every element i in $[n]$. Therefore,

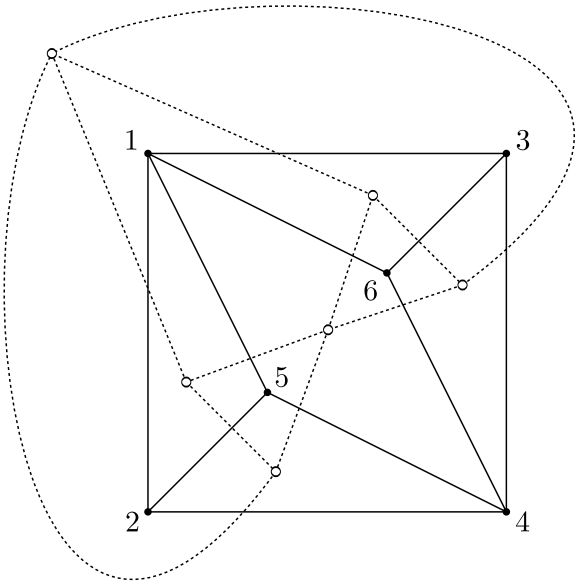

Figure 2.10: The dual graph of the plane graph of Figure 2.9

.

the maximum length of a cycle in an involution is 2. A *circular permutation* is a permutation that has one n-cycle. For every permutation π of $[n]$ there is a unique permutation π^{-1} such that $\pi(\pi^{-1}(i)) = \pi^{-1}(\pi(i)) = i$ for every element i in $[n]$. This permutation is called the *inverse* of the permutation π. Therefore, an involution can be defined as a permutation that is its own inverse. More information and some fast algorithms for generating permutations may be found in [39, 45, 2].

2.6 Transformations

One of the problems that we study in this thesis is enumerating Venn diagrams. There are no general formulas known for counting Venn diagrams. Therefore, our approach is to generate all possible candidates to find the number of Venn diagrams with a specific property. However, we first need to agree on a clear definition that tells us when two given Venn diagrams are actually the same. To do this, we must show how to transform one diagram to the other without changing intrinsic properties of the diagram.

Definition 2.6.1. Let D and R be two subsets of the plane. A *continuous transformation* from D to R is a function with domain D and range R such that for

any point $p \in D$ and set $A \subseteq D$, if p is near A, then $f(p)$ is near $f(A)$ where $f(A) = \{f(q)|q \in A\}$.

A Jordan curve, for example, is defined as any subset of the plane that can be continuously transformed to the unit circle. Understanding continuous transformations, we now can define when two Venn diagrams are isomorphic. When speaking about the isomorphism of Venn diagrams, the polar-flips are sometimes not considered (see [11, 46] for example). However, here we broaden the definition to include the polar-flips as well.

Definition 2.6.2. Two Venn diagrams are *isomorphic* if one can be changed to the other, its mirror image or its polar-flip using a continuous transformation of the plane.

Isometries

When studying the symmetries of Venn diagrams on the plane and sphere, we are particularly interested in transformations that preserve distance of any given pair of points on the underlying surface. These transformations are called *isometries*.

Definition 2.6.3. Let $d(p, q)$ denote the distance of a pair of points p and q on a surface S. A continuous transformation f of S is called an *isometry* if for each pair of points $p, q \in S$, $d(p, q) = d(f(p), f(q))$.

For an isometry f of a surface S if there exists a point $p \in S$ such that $f(p) = p$ then p is said to be an *invariant point* of f. For any surface the trivial isometry is the *identity* transformation where all points of the surface are invariant. If f and g are two isometries, then the composition of f and g, defined as $(f \circ g)(p) = f(g(p))$, for every point p, is also an isometry. Isometries of the plane include translations, rotations, reflections and glide reflections.

A *translation* is an isometry that shifts every point in the plane in a given direction. Direction and length of movement are specified by a translation vector. More precisely, given the vector $\vec{v} = (v_x, v_y)$, T_v is the *translation* along $\vec{v}$ if for any point $p(x, y)$, $T_{\vec{v}}(p) = (x + v_x, y + v_y)$.

A *rotation* is an isometry $R_{c,\theta}$ that rotates every point in the plane about a centre point c by an angle θ, $0 \leq \theta < 2\pi$. When the centre of rotation is not explicitly specified, the origin at $(0, 0)$ is considered as the centre point and rotation is defined by

$$R_\theta(x, y) = (x\cos(\theta) + y\sin(\theta), y\cos(\theta) - x\sin(\theta)) .$$

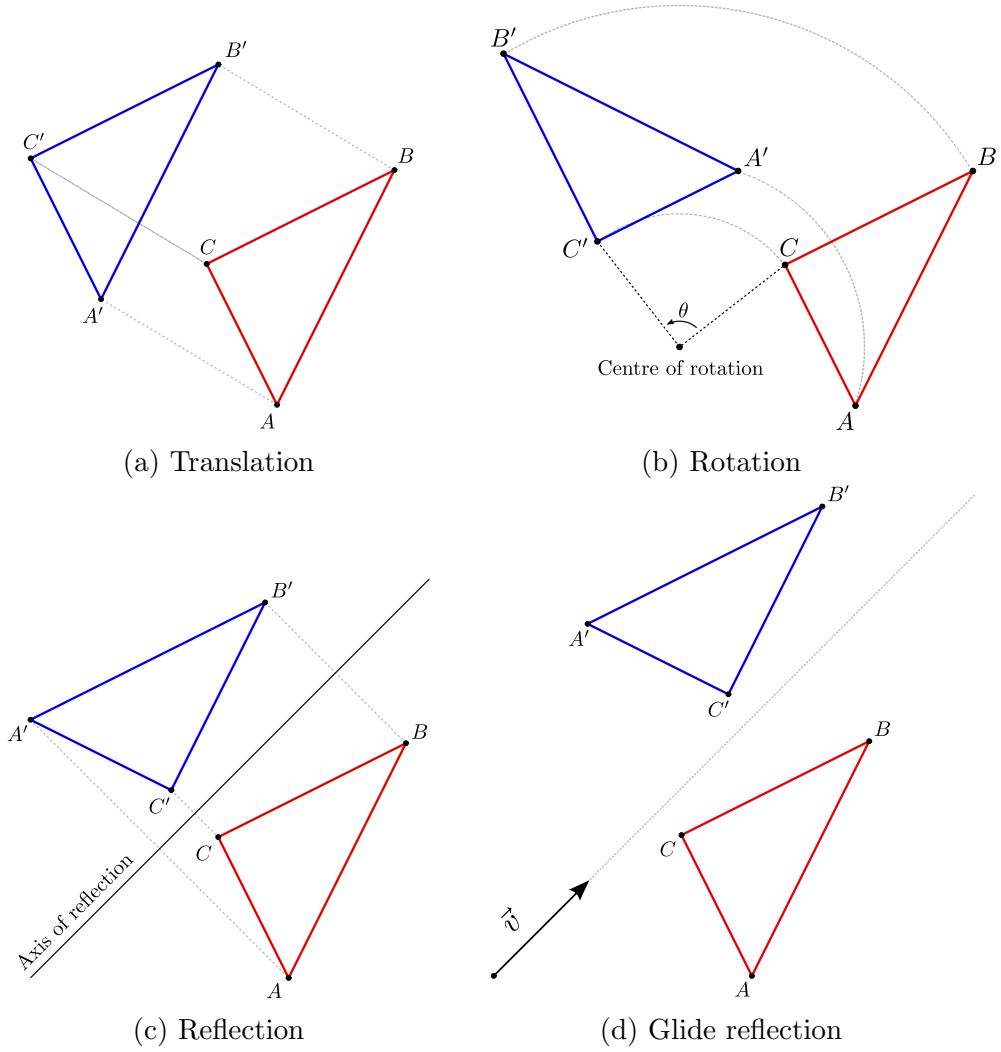

Figure 2.11: Examples of plane isometries.

When the centre of rotation is a point $c = (x, y)$ other than origin, $R_{c,\theta}$ is defined as a composition of three transformations : a translation $T_{-\vec{v}}$ along the vector $-\vec{v} = (-x, -y)$, a rotation R_θ about the origin and a translation $T_{\vec{v}}$ along vector $\vec{v} = (x, y)$, i.e., $R_{c,\theta}(p) = T_{\vec{v}}(p) \circ R_\theta(p) \circ T_{-\vec{v}}(p)$ for any point $p \in \mathbb{R}^2$. A particular case of rotation is $R_{c,\pi}$ (a rotation through π radians) which is called a *half-turn*.

Reflections are another type of isometry of the plane. Given a line L in the plane, a *reflection* F_L maps a point p to a point $q = F_L(p)$ such that the line pq is perpendicular to line L and q has the same distance from L as p. The line L is called the *axis of reflection*. One may think of this line as a mirror reflecting points to the opposite side. Reflections have infinitely many invariant points (the entire axis of

reflection).

The last type of plane isometries are *glide reflections*. A glide reflection is defined as a composition of a reflection across a line with a translation along the same line. More precisely, a glide reflection $G_{c,\vec{v}}$ is defined by

$$G_{c,\vec{v}}(p) = T_{\vec{v}}(p) \circ F_L(p), \quad \text{for } p \in \mathbb{R}^2,$$

where L is the line through point c and parallel to vector $\vec{v}$. Glide reflections have no invariant points.

Figure 2.11 shows examples of different types of plane isometries. Consider the triangle ABC in the figure. As it is shown, for rotation and translation, both ABC and its image have the same orientation; but in the case of reflection and glide reflection the orientation of the image is reversed. In general an isometry is *direct* if it preserves the orientation and it is said to be *opposite* if it reverses the orientation. This leads us to the following definition of congruence of Jordan curves.

Definition 2.6.4. Two Jordan curves C and C' are said to be *congruent* if there exists a direct isometry that maps C to C'.

There are also three types of isometries of the sphere :

- *Rotation* about an axis through the centre of sphere. In spherical coordinates, a rotation of ψ radians about the axis through the poles, moves a point (θ, ϕ) to point $(\theta, (\phi + \psi) \bmod 2\pi)$. A special case of rotation is a *polar-flip*, introduced earlier in this chapter, where the angle of rotation is π and the axis of rotation intersects the equator at two antipodal points.

- *Reflection* across a plane through the center of sphere. A reflection across the equatorial plane for example, maps point $p = (\theta, \phi)$ to point $(-\theta, \phi)$ in spherical coordinates.

- *Rotary reflection* which is a composition of a rotation about an axis through the centre followed by a reflection across a plane through the centre and orthogonal to the axis of rotation. A particularly simple type of rotary reflection is obtained when the rotation is by π radians. In that case, each point is mapped to the corresponding antipodal point on the opposite side of the sphere; we refer to this isometry as an *inversion*.

2.7 Symmetry groups

In this section we first review some basic notions from group theory to understand the symmetry of Venn diagrams. Then we introduce some symmetries of diagrams that we will be studying in the next chapters.

Definition 2.7.1. A *group* is set G together with a binary operation $*$ that satisfies the following axioms :

- The set G is *closed* under operation $*$, i.e., for every $a, b \in \mathsf{G}, a * b \in \mathsf{G}$.
- The operation is *associative*, i.e., for every $a, b, c \in \mathsf{G}, a * (b * c) = (a * b) * c$.
- G contains an *identity* element, i.e., there exists an element $e \in \mathsf{G}$ such that for every $a \in \mathsf{G}, a * e = e * a = a$.
- Each element in G has an *inverse*, i.e., for every $a \in \mathsf{G}$ there exists an element $a^{-1} \in \mathsf{G}$ such that $a * a^{-1} = a^{-1} * a = e$.

A group is *finite* if it contains a finite number of elements. The number of elements of a (finite) group G is called the *order* of the group and is denoted by $|\mathsf{G}|$.

For a geometric object in the plane, a *symmetry* is defined as an isometry that maps the object to itself. For diagrams in particular, since the curves are labeled, depending on how the curves are mapped under the symmetry, we may have different types of symmetries. However, here we only consider those cases where a diagram remains invariant after applying the symmetry, except for a relabeling of the curves. This type of symmetry is usually known as *curve preserving symmetry* or *colour symmetry* (see [55] for example, for more details about the symmetry of diagrams).

Definition 2.7.2. Let $D = \{C_1, C_2, \ldots, C_n\}$ be a diagram on the plane. An isometry f of D is called a *symmetry* of D if there exists a permutation $\pi \in \mathbb{S}_n$ such that $f(C_i) = C_{\pi(i)}$, for $1 \leq i \leq n$.

Definition 2.7.3. Let D be a diagram on a surface. The set of all symmetries of D forms a group which is called the *symmetry group* of D, where the operation of the group is composition of the symmetries.

The symmetry group of an object allows us to create the entire object by applying some isometries in the group to a given minimal part of the object.

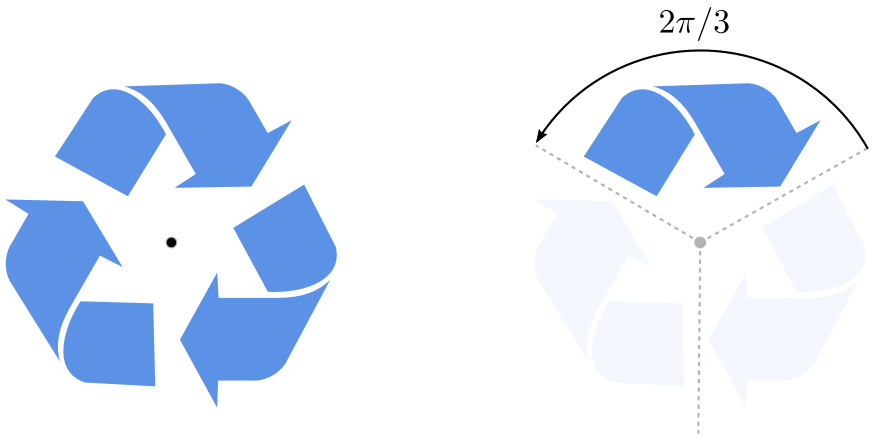

(a) An object with 3-fold rotational symmetry (b) A fundamental domain of the object

Figure 2.12: An example of rotational symmetry

Definition 2.7.4. Let V be a Venn diagram on the plane with symmetry group G. A *fundamental domain* of V is a minimal subset S of the plane such that for any point p in the plane there exists exactly one point $q \in S$ and some isometry $f \in \mathsf{G}$ where $f(q) = p$.

2.7.1 Rotational symmetry

In general an object in the plane is said to have *n-fold rotational symmetry* if it looks the same after a rotation of $2\pi/n$ radians about a point in the plane. Consider the "recycle sign" in Figure 2.12(a) for example. A rotation of $2\pi/3$ radians about the center point fixes the sign. A rotation of $4\pi/3$ radians does not change the recycle sign either, as it has the same effect of applying two consecutive rotations of $2\pi/3$ radians. After applying three consecutive rotations every point of the sign maps to itself. Therefore, the recycle sign has a symmetry group of order 3 with the isometries $\{I, R_{2\pi/3}, R_{4\pi/3}\}$.

The same concept of rotational symmetry can be applied to Venn diagrams if we ignore the label (color) of the curves.

Definition 2.7.5. An n-Venn diagram $V = \{C_1, C_2, \ldots, C_n\}$ is *rotationally symmetric* if there exists a point c on the plane and a permutation π such that $R_{c,2\pi/n}(C_i) = C_{\pi(i)}$.

If the curves of a rotationally symmetric n-Venn diagram are labeled $C_1, C_2, \ldots, C_n$ in counterclockwise direction, based on the order of touching the outermost region of the diagram, then $R_{c,2\pi/n}(C_i) = C_{i+1}$, for $1 \leq i < n$ and $R_{c,2\pi/n}(C_n) = C_1$. Therefore, the permutation associated with a rotationally symmetric n-Venn diagram can be taken to be the circular permutation $(1\ 2\ \cdots\ n)$.

The symmetry group of a rotationally symmetric n-Venn diagram contains n isometries, namely, $I, R_{c,2\pi/n}, R_{c,4\pi/n}, \ldots, R_{c,2(n-1)\pi/n}$. A rotation of $2k\pi/n$ radians is equivalent to repeating a rotation of $2\pi/n$ radians k times, that is, $R_{c,2k\pi/n} = R^k_{c,2\pi/n}$, for $0 \leq k \leq n$, where $R^0_{c,2\pi/n} = R^n_{c,2\pi/n} = I$.

If every element of a group G is a power of some fixed element $\rho \in \mathsf{G}$, then G is called a *cyclic group* denoted by $\langle\rho\rangle$ and ρ is called the *generator* of G. If $\langle\rho\rangle$ is finite then there must be some positive power of ρ which is equal to the identity. Let n be the smallest positive integer for which $\rho^n = I$. Then the finite group $\langle\rho|\rho^n = I\rangle = \{I, \rho, \rho^2, \ldots, \rho^{n-1}\}$ is a cyclic group of order n and is denoted C_n. Therefore, the symmetry group of a rotationally symmetric n-Venn diagram is the cyclic group $\mathsf{C}_n = \langle R_{c,2\pi/n}\rangle$.

A *sector* of a rotationally symmetric object in the plane with symmetry group C_n, is the part of the object bounded by two rays issuing from the point of rotation toward infinity and forming a wedge of angle $2\pi/n$ radians. The simple symmetric 7-Venn diagram in Figure 2.13 consists of seven sectors indicated by dotted lines. A sector of a rotationally symmetric object, also is referred to as a *pie-slice*, forms a fundamental domain of the object. For example, a fundamental domain for the recycle sign from Figure 2.12 is specified in Figure 2.12(b).

2.7.2 Dihedral symmetry

Consider the regular hexagon of Figure 2.14. In addition to six rotations, a reflection about any of the six specified lines leaves the hexagon unchanged. Therefore, the symmetry group of the regular hexagon consists of twelve symmetries :

- Six rotations $R_0, R_1, R_2, R_3, R_4, R_5$, where R_i is the rotation of angle $2i\pi/6$ radians about the centre of polygon.
- Six reflections $F_0, F_1, F_2, F_3, F_4, F_5$, where F_i is the reflection about a line through the centre making an angle of $i\pi/6$ radians with a fixed line through the centre and one corner of the hexagon.

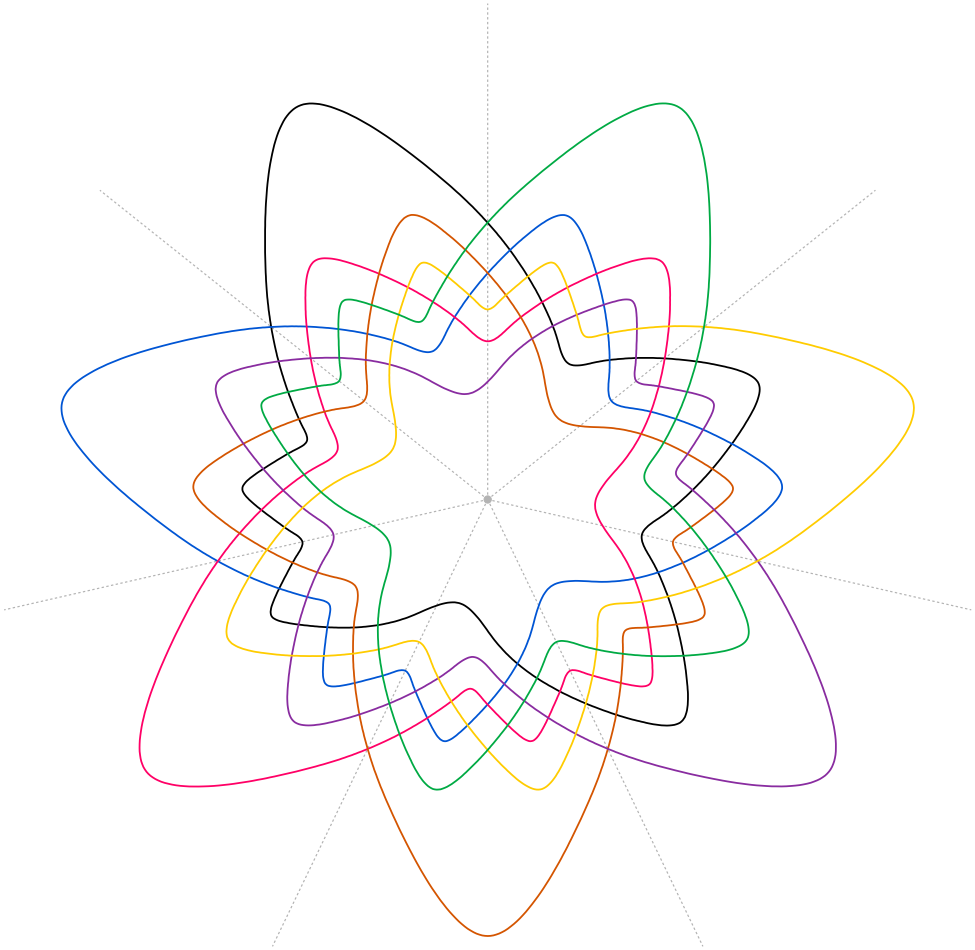

Figure 2.13: An example of a simple symmetric 7-Venn diagram.

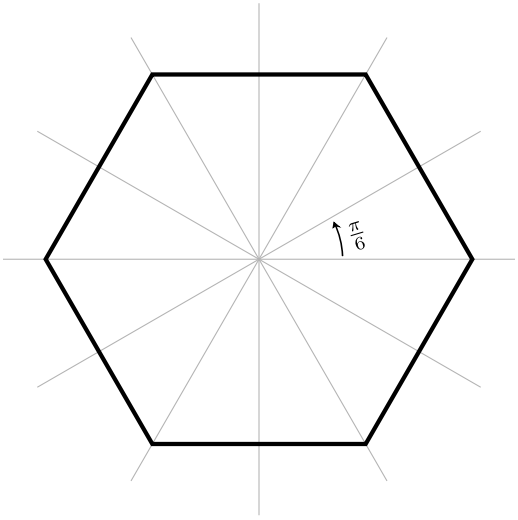

Figure 2.14: Six axes of symmetry of a regular hexagon.

In general, an object in the plane with n-fold rotational symmetry is said to have *dihedral symmetry* if there exist two lines intersecting at an angle of π/n through the centre of rotation such that the object is left unchanged after a reflection about the lines. The symmetry group of a geometric object with dihedral symmetry, an n-sided regular polygon for example, is a group of order $2n$ containing n rotations and n reflections, which is called the *dihedral group* and is denoted D_n.

2.7.3 Polar symmetry

The two types of symmetries mentioned earlier are applied to spherical diagrams as well, except that rotations happen about an axis through the centre of the sphere and reflections are done about a plane through the centre. There is another type symmetry which is easier to understand when considering diagrams on a sphere.

Definition 2.7.6. A diagram D on the sphere is said to be *polar-symmetric* if there exists an axis on the equatorial plane passing through the centre of sphere such that a rotation of π radians about it leaves the diagram unchanged up to a relabeling of the curves.

It is easier to visually check the polar-symmetry of a Venn diagram on the plane by projecting the diagram onto a sphere. Let V be a Venn diagram on the plane. If the innermost region of V contains a point p such that projecting the diagram onto the sphere with the south pole of sphere tangent to p produces a polar-symmetric

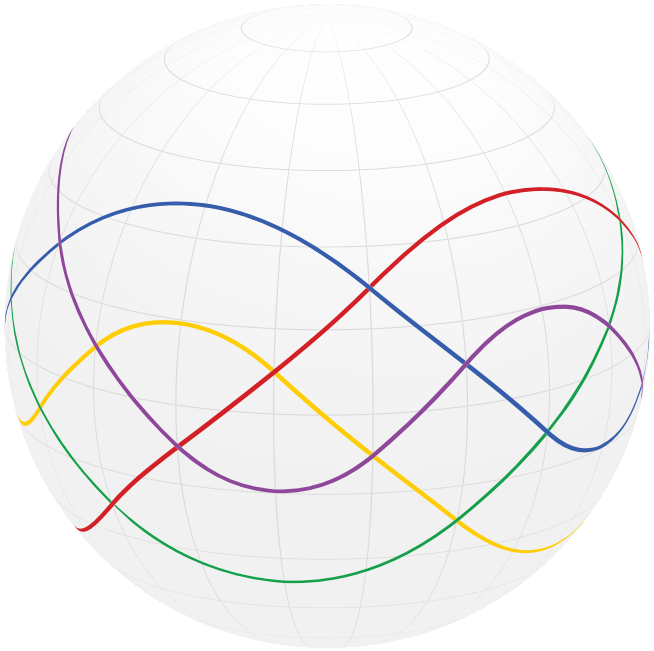

Figure 2.15: Simple symmetric 5-Venn on a sphere.

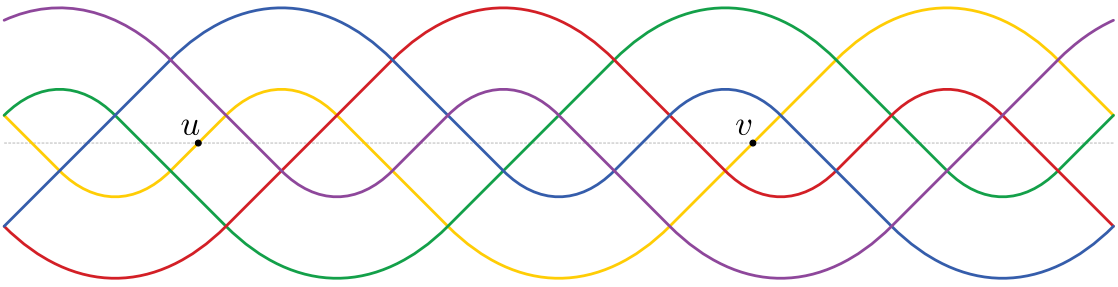

Figure 2.16: Cylindrical representation of the simple symmetric 5-Venn.

diagram then the original diagram V on the plane is also polar-symmetric. In that case there must be an equatorial axis such that a polar-flip about it leaves the spherical diagram unchanged. Therefore, the result of projecting the spherical diagram back to the plane after the polar-flip is the same as the original diagram V.

Figure 2.15 shows the unique simple rotationally symmetric 5-Venn diagram on the sphere. A careful look at the cylindrical representation of the diagram in Figure 2.16 reveals that it is polar-symmetric as well. The antipodal points u and v indicate where the equatorial axis intersects the surface of sphere. A rotation of π radians about this axis leaves the diagram fixed up to a relabeling of the curves. Because of the rotational symmetry there are exactly five such equatorial axes and therefore the symmetry group of this diagram is of order 10 since it is isomorphic to D_{10}.

2.8 History of research in Venn diagrams

Diagrams and pictures have been used for describing mathematical concepts and reasoning for a long time. The origin of diagrammatic reasoning is unknown. However, the first records of diagrammatic representations involving closed curves, as Martin Gardner states in [20], dates back to at least the Middle Ages. According to a survey on the history of logic diagrams by Margaret Baron [3], the analysis of logical propositions using lines, circles and ellipses was first studied by Gottfried Wilhelm Leibniz(1646-1716). However, as Baron states, it was the brilliant Swiss mathematician Leonard Euler(1707–1783) who introduced and popularized the use of circles in syllogistic reasoning. In his "letters to a German princess" as lessons in logic and knowledge [17], Euler introduced a geometrical system for describing and analyzing logical propositions, which is known today as Euler diagrams.

In the nineteenth century, diagrammatic reasoning was a popular topic in England, and Euler's use of circles in logical analysis was followed by many mathematicians. In 1880 John Venn(1834–1923) showed that the Euler's circles are not good enough to illustrate all possible relations among propositions and formalized a more comprehensive representation of propositions using closed curves [51]. He also provided an inductive approach to construct his diagrams, proving their existence for any number of curves. Figure 2.17 illustrates his construction for a diagram of 5 curves.

Several other methods have been provided for the construction of Venn diagram in the last century, see [1, 4, 42, 22] for example, of which Anthony Edwards' inductive construction [15, 16] is the best known. Figure 2.18 illustrates Edwards' method of

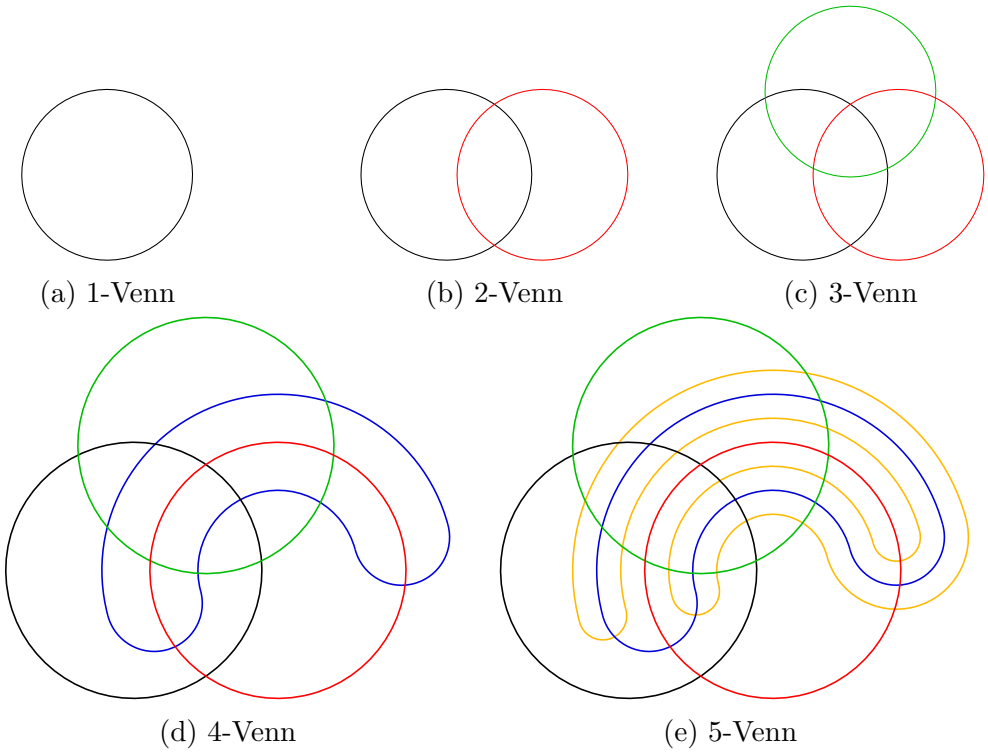

(a) 1-Venn (b) 2-Venn (c) 3-Venn

(d) 4-Venn (e) 5-Venn

Figure 2.17: John Venn's inductive approach of constructing n-Venn diagrams for $n = 1, 2, \ldots, 5$.

constructing a simple 6-Venn diagram. It starts with two rectangles and a circle in the middle. For $n \geq 4$, every new curve is twisted around the central circle in such a way that it divides every region into two parts. Edwards' diagrams are easier to understand and have some symmetries, especially when they are drawn on a sphere. Edwards' construction is explored further in Chapter 5.

Rotational symmetry of Venn diagrams was studied by David Henderson in 1960 when he was an undergraduate at Swarthmore College. In 1963, Henderson [33] showed two examples of constructing symmetric Venn diagrams of five curves using irregular pentagons and quadrilaterals. He also claimed that he had found a symmetric 7-Venn diagram using hexagons, but he could not reproduce it later. But more importantly, Henderson showed the following interesting connection between Venn diagrams and prime numbers.

Theorem 2.8.1 ([33]). *If there exists a rotationally symmetric n-Venn diagram then n must be prime.*

The intuitive reason behind this is as follows: Consider an n-Venn diagram with

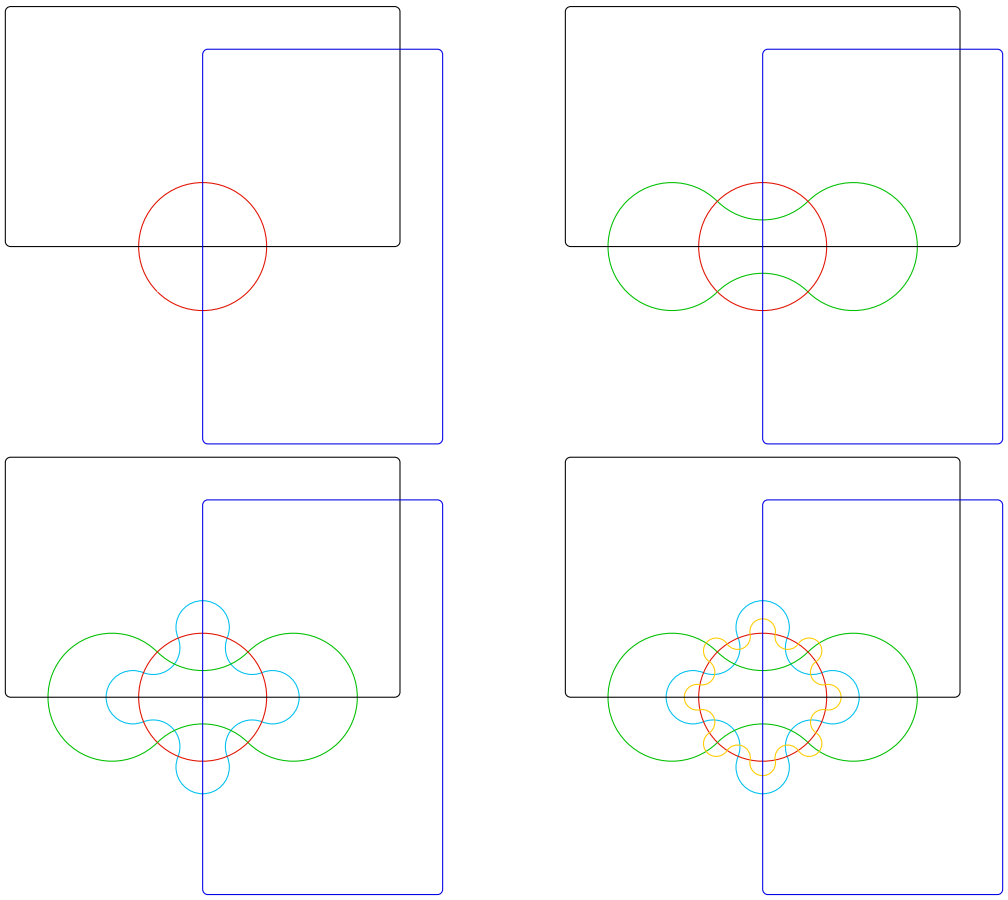

Figure 2.18: Edwards' construction of a 6-Venn diagram.

n-fold rotational symmetry. The centre of rotation must lie in the innermost region of weight n. A rotation of $2\pi/n$, maps a region of weight k and rank $r = (b_{n-1} \dots b_1 b_0)_2$ onto another region of weight k with rank $(b_0 b_{n-1} \dots b_1)_2$, for $0 \leq k \leq n$. The region of weight 0 (the outermost region) and the region of weight n (the innermost region) map onto themselves. Therefore, n must divide the number of regions of weight k, for $1 \leq k \leq n-1$. By a theorem of Leibnitz [32], n divides $\binom{n}{k}$ only if n is prime.

However, there were some ambiguities in Henderson's argument in [33]. For example, he did not mention the connectedness of the regions, which is an important property of Venn diagrams. Recently, Wagon and Webb [52] clarified some details of Henderson's argument, giving a complete geometric proof of his theorem.

Recent advances and achievements in research on Venn diagrams are largely indebted to Branko Grünbaum's pioneering work in this area. He published a series of papers on this topic, starting with the award-winning paper from 1975 [22]. In this paper, Grünbaum studied several problems on independent families and Venn

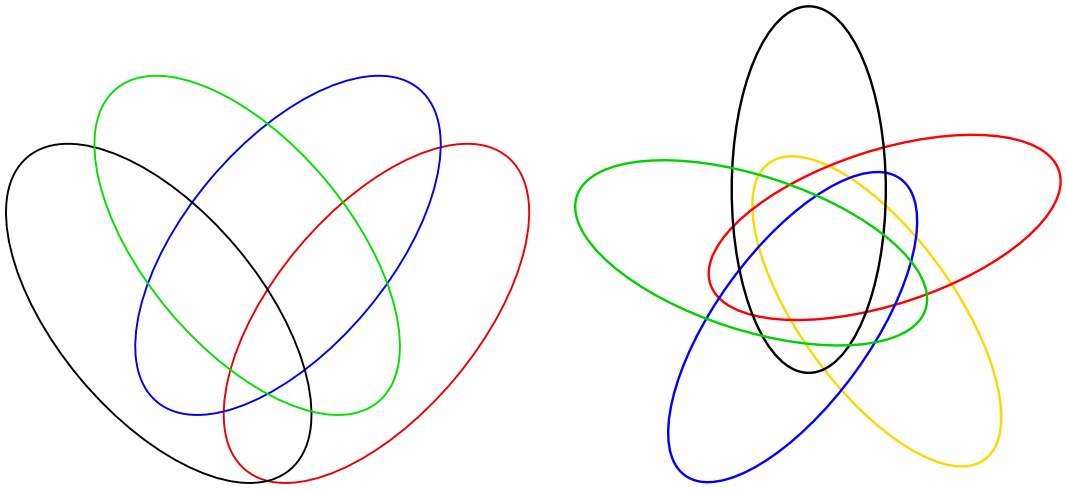

(a) 4-Venn by John Venn (b) Symmetric 5-Venn by Grünbaum

Figure 2.19: Examples of Venn diagrams of congruent ellipses.

diagrams of convex curves. Based on an earlier construction of More [42], he provided an inductive construction of a simple n-Venn diagram using convex polygons where the last added convex polygon has 2^{n-2} sides. Grünbaum also proved a lower bound for the number of sides of convex polygons forming a Venn diagram and he gave examples of Venn diagrams of convex polygons with minimum number of sides for $n = 3, 4, 5$. Later, in 2007, Carroll, Ruskey and Weston [9] improved this lower bound and gave an optimum lower bound for Venn diagrams of up to seven convex polygons.

As another problem, Grünbaum studied Venn diagrams and independent families of congruent curves. Venn himself constructed a diagram of four ellipses, shown in Figure 2.19(a), but he conjectured that there are no Venn diagrams of five congruent ellipses. Grünbaum was the first who discovered the symmetric 5-Venn diagram of five ellipses shown in Figure 2.19(b). He also provided several examples of symmetric independent families of convex polygons such as a symmetric independent family of four triangles, a symmetric independent family of six quadrangles and a symmetric independent of seven hexagons. Giving these examples, he conjectured that symmetric independent families of convex polygons exist for any number of sets [22]. More examples of 5-Venn diagrams of congruent ellipses and several problems and conjectures on the existence and enumeration of Venn diagrams of a given type were introduced by Grünbaum in a paper from 1992 [23].

Although in [22], Grünbaum mistakenly conjectured that symmetric Venn dia-

grams for more than five curves do not exist, he later discovered examples of symmetric 7-Venn diagrams (both monotone and nonmonotone) himself [24]. He is also probably the first one who noticed the polar symmetric Venn diagrams, referring to them as *spherical* [24] or *self-complementary* [25] Venn diagrams. Other examples of symmetric 7-Venn diagrams were discovered independently by Anthony Edwards, Carla Savage, Peter Winkler and Frank Ruskey [46]. The list of all monotone simple 7-Venn diagrams with rotational and polar symmetry was first reported by Anthony Edwards in [14]. Using a computer search, Ruskey showed that there are exactly 23 monotone simple symmetric 7-Venn diagrams [46], up to isomorphism. His results were also verified separately by Cao and Mamakani [8, 41]. A list of 33 nonmonotone simple symmetric 7-Venn diagram was also reported in [46] and and it has been conjectured that this list is complete.

Grünbaum's studies of Venn diagrams raised many questions and conjectures about Venn diagrams that provided the motivation for further studies in this area. In a series of papers in the 1990's, Hamburger, Chilacamarri and Pippert [11, 10, 29, 12] analyzed different properties of Venn diagrams using graph theory. In their studies, they developed new methods of generating Venn diagrams with a small number of curves. Using these methods, they counted all Venn diagrams of three curves showing that there are only two symmetric 3-Venn diagrams. They also showed that there are 20 nonisomorphic simple 5-Venn diagrams on a sphere, of which 11 are convex and 9 are nonconvex.

Hamburger was also the first one who constructed a symmetric 11-Venn diagram [27]. His approach was based on choosing a set of necklace representatives, which he called a *generator*, to construct a fundamental domain of the dual of the 11-Venn diagram. However, his diagram was highly nonsimple, containing only 462 intersection points, compared to 2046 intersection points in a simple 11-Venn diagram. In collaboration with Sali and Petruska, Hamburger also produced several other examples of nonsimple symmetric 11-Venn diagrams, with different numbers of intersection points [30, 31, 26, 28].

In 2004, Griggs, Killian and Savage (GKS) [21] showed that, given any symmetric chain decomposition in the Boolean lattice, it is always possible to construct a monotone Venn diagram with a minimum number of vertices. It has been proven by Bultena and Ruskey that such an n-Venn diagram has $\binom{n}{\lfloor n/2 \rfloor}$ vertices [7]. The most important contribution of GKS in [21], however, was to prove that symmetric Venn diagrams exist for any prime number of curves. Having the minimum number

of vertices, like Hamburger's 11-Venn diagram, their diagrams are also maximally nonsimple. There are exactly n points in the resulting diagrams, where all n curves cross. Some progress towards simplifying the GKS construction is reported in [38], but that could never succeed in producing truly simple diagrams.

Chapter 3

Representations of simple monotone Venn diagrams

In this chapter we are restricting our attention to the special (and most studied) class of Venn diagrams; diagrams that are both simple and monotone (drawable with convex curves [6]). Figure 3.1 shows several Venn diagrams of this type with different numbers of curves. We introduce several different representations of these diagrams. Although these representations are somewhat similar in nature and there are efficient algorithms for getting from one representation to the other, we used them to implement independent generating algorithms for each class of studied Venn diagrams. This chapter is joint work with Frank Ruskey and Wendy Myrvold and it has been published in [41].

3.1 Venn diagrams as graphs

A Venn diagram can be represented by a plane graph in which the intersection points of the Venn diagram are the vertices of the graph and the sections of the curves that connect the intersection points are the edges of the graph. Thinking of a Venn diagram as a graph has many benefits and will provide us with one of our fundamental representations. In this representation the faces of the graph are the regions of the diagram.

Another planar graph that we can associate with each Venn diagram is its planar dual, which is called its *Venn dual*. The rank and weight of each vertex in the dual graph are equal to the rank and weight of the associated face(region) in the Venn

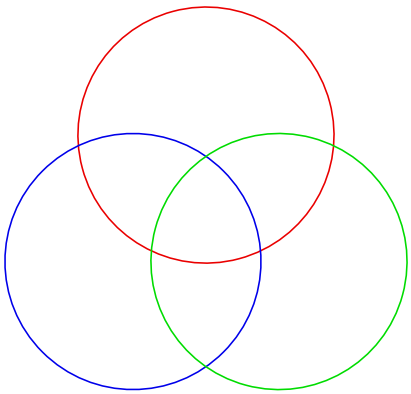

(a) A 3-Venn diagram whose curves are circles.

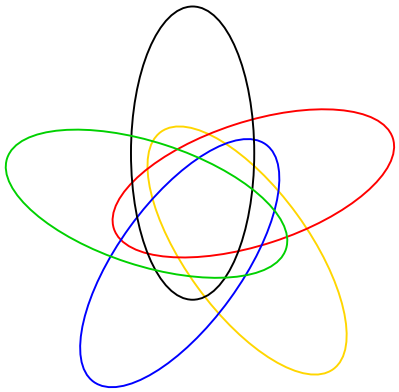

(b) A 5-Venn diagram whose curves are ellipses.

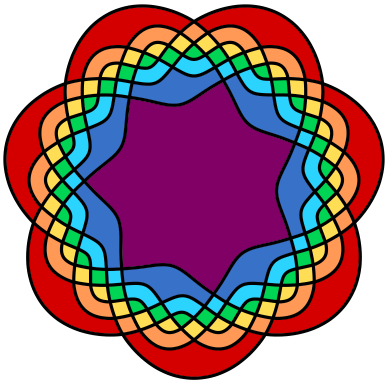

(c) A simple symmetric 7-Venn known as "Adelaide" [14].

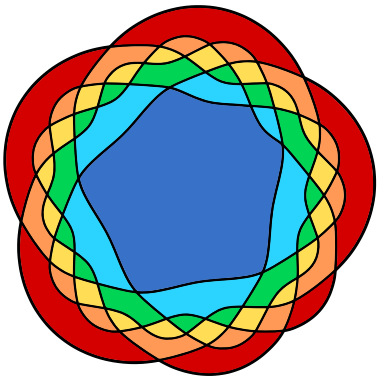

(d) A simple monotone polar-symmetric 6-Venn diagram.

Figure 3.1: Some examples of simple monotone Venn diagrams.

diagram. Figure 3.2 shows the Venn graph and Venn dual of the Venn diagram of Figure 3.1(a), where the vertices of the Venn dual are labeled with the rank of the corresponding regions of the diagram. In a simple Venn diagram, every vertex has degree four. Therefore, every face of the dual graph of a simple Venn diagram is a quadrilateral, and hence the dual is a maximal bipartite planar graph.

For a plane graph with f faces, v vertices and e edges, Euler's formula [54] states that $f + v = e + 2$. The graph of an n-Venn diagram has 2^n faces. In a simple Venn diagram each vertex of this graph has degree 4; *i.e.* $e = 2v$, so a simple n-Venn diagram has $2^n - 2$ vertices (i.e., intersection points). The graph of a Venn diagram has the following properties.

Lemma 3.1.1 ([11]). *A simple Venn diagram on three or more curves is a 3-connected graph.*

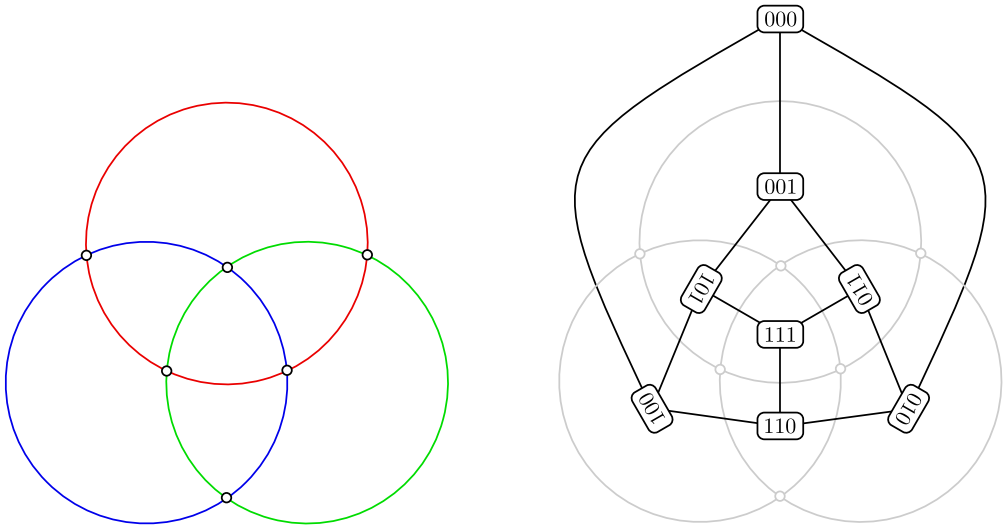

(a) Venn Graph (b) Venn dual

Figure 3.2: A Venn graph and its dual

Lemma 3.1.2 ([11])**.** *There are no two edges on a face of a Venn diagram that belong to the same curve.*

Lemma 3.1.3 ([11])**.** *In a simple Venn diagram on three or more curves there are no faces of size two.*

Lemma 3.1.4. *In a simple Venn diagram with more than three curves, there are no two faces of size 3 adjacent to another face of size 3.*

Proof. Suppose there is a Venn diagram $\mathcal{V}$ that has two 3-faces adjacent to another 3-face. Then as we can see in Figure 3.3, there are two faces (the shaded regions) in the diagram with the same rank, which contradicts the fact that $\mathcal{V}$ is a Venn diagram. □

3.2 Representing Venn Diagrams

In this section we introduce the representations that are used when we generate simple monotone Venn diagrams. First we introduce Grünbaum encodings and we prove that each Grünbaum encoding identifies a simple exposed Venn diagram up to isomorphism. In the second part we discuss the binary matrix representation, where

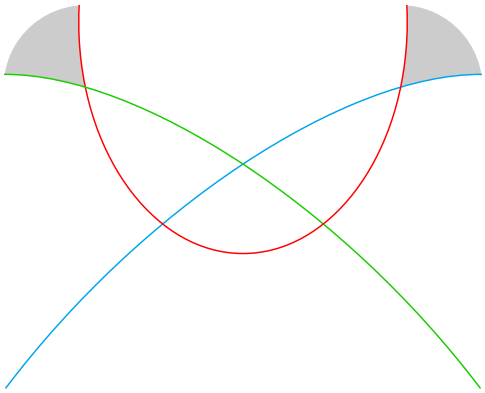

Figure 3.3: A single 3-face adjacent to two other 3-faces; the shaded regions have the same rank.

each 1 in the matrix represents an intersection point of the corresponding Venn diagram. Having the matrix representation of a diagram, it is easy to check if it is a Venn diagram or not. In the third part we show how to represent simple monotone Venn diagrams using integer compositions. We use this representation to generate all polar-symmetric convex 6-Venn diagrams. Finally, we discuss representing simple convex Venn diagrams using a finite sequence of exchanges of curve labels. We generate all simple convex 6-Venn diagrams using this method.

Grünbaum Encoding

Grünbaum encodings were introduced by Grünbaum as a way of hand-checking whether two symmetric Venn diagrams are distinct [46]. We generalize this concept here to all Venn diagrams, symmetric or not, and then focus on the special properties that they have when the diagram is symmetric. The Grünbaum encoding of a simple exposed Venn diagram consists of $4n$ strings, four for each curve C_i. Call the strings w_i, x_i, y_i, z_i for $i = 0, 1, \ldots, n-1$. In fact, given any one of the w, x, y, z strings of a Venn diagram V, we can compute the other three from it. However, we need these four strings to compute the lexicographically smallest string as the unique Grünbaum encoding representative of V. Given the lexicographically smallest Grünbaum encoding of two Venn diagrams, then we can check if they are isomorphic or not.

Starting from one of the curves in the outermost or innermost regions, we first label the curves from 0 to $n-1$ in the clockwise or counterclockwise direction. The starting curves of these labelings are chosen arbitrarily, and thus there can be several Grünbaum encodings of a given Venn diagram. Table 3.1 indicates whether the

Table 3.1: Grünbaum encoding. (a) Conventions for Grünbaum encoding. (b) Partial Grünbaum encoding of the symmetric 5-Venn diagram of Figure 3.1(b).

	cw	ccw
outermost	w	y
innermost	x	z

(a)

$w:$	1,3,2,4,1,4,2,4,1,3,1,4
$x:$	1,4,2,4,1,3,1,4,1,3,2,4
$y:$	1,4,2,4,1,3,1,4,1,3,2,4
$z:$	1,3,2,4,1,4,2,4,1,3,1,4

(b)

labeling starts on the inside or outside and whether the curve is considered to be oriented clockwise or counterclockwise. To get the w_i strings we arbitrarily pick a curve and label it 0. It intersects the outer face in exactly one segment; the remaining curves are labeled $1, 2, \ldots, n-1$ in a clockwise direction. Now that each curve is labeled, we traverse them, recording the curves that each intersects, until it returns, back to the outer face. Thus w_i is a string over the alphabet $\{0, 1, \ldots, n-1\} \setminus \{i\}$. The strings x_i, y_i, z_i are produced in a similar manner, except that we are starting on on the inner face, or traversing in a counterclockwise direction, or both, as indicated in Table 3.1(a). In Table 3.1(b), we show part of the Grünbaum encoding of Figure 3.1(b).

For curve i, each string of the Grünbaum encoding starts with $(i+1)$ and ends with $(i-1)$ (both mod n). Since each one of w, x, y or z may use a different labeling of the same curves, there are permutations that map the labelings of one to the labelings of the other. Given a Grünbaum encoding $\{w, x, y, z\}$, let the permutations π, σ and τ map the curve labels of w to the curves labels of x, y, z, respectively. Let ℓ_i denote the length of string w_i and let $w_i[k]$ be the kth element of w_i where $k = 0, 1, \ldots, \ell_i - 1$. We can get $y_{\sigma(i)}$ by

$$y_{\sigma(i)}[k] = \sigma(w_i[\ell_i - k - 1]).$$

To obtain $x_{\pi(i)}$ and $z_{\tau(i)}$, we first determine the unique index p of w_i where all curves have been encountered an odd number of times (and thus we are now on the inner face). We then have

$$x_{\pi(i)}[k] = \pi(w_i[(k+p) \bmod \ell_i]),$$

and

$$z_{\tau(i)}[k] = \tau(w_i[(p-k-1+\ell_i) \bmod \ell_i]).$$

In the case of a rotationally symmetric Venn diagram we only need the four

strings w_0, x_0, y_0, z_0 to specify the Grünbaum encoding, since the others will be a trivial relabeling of these. E.g., for any other curve $i \neq 0$, $w_i = w_0 + i \pmod{n}$. The other three strings of curve i can be obtained in the same manner from the corresponding strings of curve 0.

The following lemma gives the length of each string of the Grünbaum encoding of a simple symmetric Venn diagram.

Lemma 3.2.1. *Each string of the Grünbaum encoding of a simple symmetric n-Venn diagram has length* $(2^{n+1} - 4)/n$.

Proof. Clearly each string will have the same length, call it L. Recall that a simple symmetric n-Venn diagram has $2^n - 2$ intersection points. By rotational symmetry every intersection point represented by a number in the encoding corresponds to $n-1$ other intersection points. However, every intersection point is represented twice in this manner. Therefore, $nL = 2(2^n - 2)$, or $L = (2^{n+1} - 4)/n$. □

Let g be a Grünbaum string; i.e., $g \in \{w, x, y, z\}$. Each intersection point of curves i and j is represented by an entry of value j in g_i and an entry of value i in g_j. So each element of g_i of value j uniquely corresponds to an element of g_j of value i and vice versa. We call the corresponding elements of g_i and g_j *twins*. Consider an intersection of curve i with curve j represented by $g_i[k]$, that is, $g_i[k] = j$. We denote this intersection point by $g_i(k)$. For any curve c other than i and j, let η_c be the number of occurrences of c in g_i up to and including $g_i[k]$, starting from the first element of g_i. That is, let $\eta_c = |\{l : 1 \leq l \leq k \text{ and } g_i[l] = c\}|$, where for a given set S, $|S|$ denotes the cardinality of S. For each of the four Grünbaum strings of curve i, the parity of η_c shows whether $g_i(k)$ is in the interior or exterior of curve c. For example, for $g = w$ or $g = y$, if η_c is odd then $g_i(k)$ is in the interior of curve c and if η_c is even then $g_i(k)$ is in the exterior of curve c. The *rank* of $g_i(k)$ is defined to be the binary number $\text{rank}(g_i(k)) = (r_{n-1} \cdots r_1 r_0)_2$ where $r_k = 0$ if $k = i, j$ and otherwise $r_k = \eta_k \mod 2$.

Lemma 3.2.2. *Let g be a Grünbaum string of an n-Venn diagram, where $n \geq 3$. For each pair of curves (i, j), if $g_i[k] = j$ for some k, then there is a unique index l such that* $\text{rank}(g_j(l)) = \text{rank}(g_i(k))$.

Proof. Since $g_i[k] = j$, there is a corresponding intersection point P where i and j intersect. Thus, when following curve j we will also encounter P, and so there must be an l such that $g_j[l] = i$.

To show uniqueness, we argue by contradiction, and assume that for some $m \neq l$, there is another entry in g_j such that $\text{rank}(g_j(m)) = \text{rank}(g_j(l))$. This entry must correspond to a second point of intersection P' of curves i and j. Let R be the region of the Venn diagram that is interior to exactly the same set of curves as P and P', and let r be the rank of R. Thus both P and P' must be on the boundary of R. Thus, by Lemma 3.1.2, R must be a 2-face. But this is a contradiction, since Lemma 3.1.3 states that there are no 2-faces in a Venn diagram if $n \geq 3$. □

Theorem 3.2.3. *Given a Grünbaum encoding G of a simple exposed n-Venn diagram V, we can recover V from G, up to isomorphism of Venn diagrams.*

Proof. It is known that a plane embedding of a 3-connected planar graph is unique, once the outer face has been identified [56]. We will present a constructive proof which shows that the Grünbaum encoding determines an embedding of the diagram on the sphere. Assume that the given Grünbaum encoding is $\{w_i, x_i, y_i, z_i\}_{i=1}^{n}$. We use a three-step algorithm to construct the rotation system that uniquely represents the Venn diagram. In the first two steps we associate a vertex label with each intersection point $w_i(k)$ for all i and k, and then based on those labels, we create the rotation system in step three.

- **Step one :** Starting with w_0, for each $w_i[k]$ with $w_i[k] > i$, we associate a new vertex label with the intersection point $w_i(k)$. At the end of this step there are $2^n - 2$ distinct vertex labels since every intersection occurs exactly twice in w. At the end of this step vertex labels have been assigned to all intersections of curves i and j, where $0 \leq i < j \leq n - 1$.

- **Step two :** We now associate vertex labels with the remaining entries of w; but we must be careful to provide the correct label, since the same pair of curves can intersect multiple times. Let v be the vertex label associated with $j = w_i[k]$ where $i < j$. We need to uniquely locate the value of ℓ such that $i = w_j[\ell]$ is the twin of $w_i[k]$. By Lemma 3.2.2 there will be a unique value of ℓ such that $\text{rank}(w_i[k]) = \text{rank}(w_j[\ell])$, which can be determined by a simple scan of w_j. We then associate v with $w_j[\ell]$. After scanning each w_i, every entry in w has an associated vertex label, which we hereafter just refer to as a vertex.

- **Step three :** In this step we construct a circular list of four edge ends for each vertex. Let w_i' denote the string w_i, but with each entry $w_i[k]$ replaced with its

associated vertex. Assume that curves i and j intersect at vertex v_1 as is shown below

$$w_i' \ : \ \cdots \ v_0 \ v_1 \ v_2 \ \cdots$$
$$w_j' \ : \ \cdots \ v_3 \ v_1 \ v_4 \ \cdots$$

By computing the parity of the number of intersections between i and j along w_i, we can determine whether curve i is moving into the interior of curve j at v_1, or whether it is moving into the exterior. Since each w_k is being traversed in a clockwise direction starting at the unbounded face, the interior of w_k is always to its right. Thus, if the parity is odd, then we are moving into the interior, and if the parity is even, then we are moving into the exterior. In the former case the circular list of edge ends adjacent to v_1 must be

$$v_1 : v_0, v_4, v_2, v_3$$

and in the latter case, the circular order must be

$$v_1 : v_0, v_3, v_2, v_4.$$

Using the same method for each vertex, we get a rotation system that uniquely identifies an embedding of the Venn diagram, up to isomorphism.

The rotation system only depends on which string of $w,\ x,\ y$, or z is chosen as the first string of Grünbaum encoding. Since there exist permutation mappings to deduce all other strings from any of $w,\ x,\ y$, or z, all rotation systems that arise from the three steps are equivalent up to isomorphism. Therefore, the Grünbaum encoding uniquely identifies the Venn diagram. □

To end this section we note that the Grünbaum encoding can be used to determine whether a Venn diagram is polar symmetric or whether it has antipodal symmetry (in both instances, given that the north and south poles have been fixed). The diagram is polar symmetric if there are integers k and k' such that $w_i = z_{i+k}$ and $x_i = y_{i+k'}$, where index computations are taken mod n. Similarly, the diagram has antipodal symmetry if there are integers k and k' such that $w_i = x_{i+k}$ and $y_i = z_{i+k'}$, where index computations are taken mod n.

3.3 The matrix representation

Every simple monotone n-Venn diagram is exposed, i.e., every 1-region is adjacent to the empty region. So the empty region surrounds a set of $\binom{n}{1}$ 1-regions. The set of all regions of weight i in a simple monotone Venn diagram is called *the ring* i. Of the four regions incident to an intersection point in a simple Venn diagram, a pair of nonadjacent regions are in the interior of the same number of curves; therefore they belong to the same ring. The number of containing curves of the other two differs by two. An intersection point is said to be part of ring i if of the four incident regions, two are in ring i and the other two are in rings $i-1$ and $i+1$. In a simple monotone Venn diagram each intersection point connects two consecutive regions in a ring. Therefore, the number of intersection points in ring i is the same as the number of regions in ring i, which is $\binom{n}{i}$. The rings have different colours in Figure 3.1(c).

Thus a simple monotone $n-$Venn diagram can be represented by a $(n-1)\times(2^n-2)$ binary matrix with exactly one 1 in each column, where each 1 in the matrix represents an intersection point in the Venn diagram. Row i of the matrix corresponds to ring i of the Venn diagram, which will thus contain $\binom{n}{i}$ 1's. Furthermore, there are no two adjacent 1s in any row, because there are no 2-faces in a simple Venn diagram, for $n > 2$

Figure 3.4 shows the matrix representation of 1/7-th of the symmetric 7-Venn diagram of Figure 3.1(c).

Because of the property of symmetry, a symmetric n-Venn diagram can be partitioned to n identical circular sectors, where each sector is specified by two rays from the point of symmetry offset by a central angle of $2\pi/n$ radians. Therefore, having an nth of the matrix, which we call the *slice matrix*, is enough to represent the diagram. We simply copy the slice matrix n times to get the entire matrix representation.

Given a slice matrix of a simple monotone symmetric Venn diagram, any circular shift of this matrix by some number of columns is also a slice matrix of the same Venn diagram. A slice matrix of a simple monotone symmetric Venn diagram with a 1 in the first entry of the first column is called a *standard slice matrix*. Let S be the standard slice matrix of a simple monotone symmetric n-Venn diagram. Then matrix representation M of the entire Venn diagram is obtained by concatenating n copies of S, that is, $M = S^n$.

Note that there are $\binom{m-k+1}{k}$ binary sequences of length m that have k 1s, with the restriction that no 1s are adjacent. Thus we can generate all possible standard

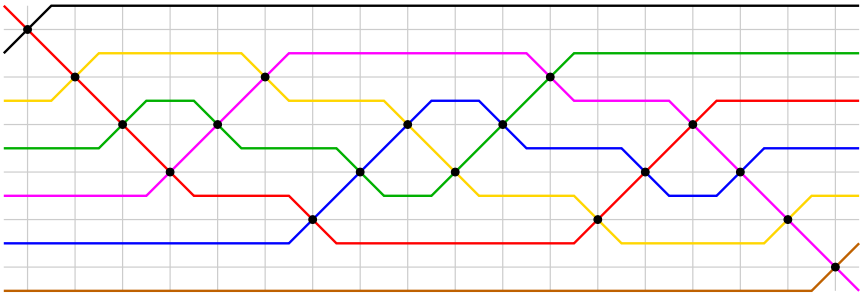

(a)

1	0	0	0	0	0	0	0	0	0	0	0	0	0	0	0	0	0
0	1	0	0	0	1	0	0	0	0	0	1	0	0	0	0	0	0
0	0	1	0	1	0	0	0	1	0	1	0	0	0	1	0	0	0
0	0	0	1	0	0	0	1	0	1	0	0	0	1	0	1	0	0
0	0	0	0	0	0	1	0	0	0	0	0	1	0	0	0	1	0
0	0	0	0	0	0	0	0	0	0	0	0	0	0	0	0	0	1

(b)

Figure 3.4: Matrix representation of one sector of the symmetric 7-Venn diagram of Figure 3.1(c), the diagram known as "Adelaide."

matrices by generating the $n-1$ distinct combinations, one combination per ring. Each combination is a selection of columns from M (see Figure 3.4(b)). In the case of $n = 7$, the number of combinations correspond to the following product of binomial coefficients:

$$\binom{18}{0} \cdot \binom{17}{3} \cdot \binom{14}{5} \cdot \binom{9}{5} \cdot \binom{4}{3} \cdot \binom{1}{1} = 686,125,440. \tag{3.1}$$

This is a large but manageable number of possibilities.

Given a matrix representation M, we need to check that there are no two regions with the same rank to check if it represents a valid Venn diagram. To compute the rank of a region, we need to know the labels of the curves that contain the region. For this purpose it is useful to consider another matrix, which we call the P-matrix. It consists of n rows and 2^n-2 columns. The initial column is the vector $[0,1,\ldots,n-1]$, and each successive column is obtained from its predecessor by swapping the two values in a column if there is a 1 in the corresponding column of matrix M, that is, if $M_{i,j} = 1$ then $P_{i,j+1} = P_{i+1,j}$ and $P_{i+1,j+1} = P_{i,j}$. For example the first 19 columns of the P-matrix for the matrix M of Figure 3.4 is given below.

0	1	1	1	1	1	1	1	1	1	1	1	1	1	1	1	1	1	1
1	0	2	2	2	2	4	4	4	4	4	4	3	3	3	3	3	3	3
2	2	0	3	3	4	2	2	2	5	5	3	4	4	4	0	0	0	0
3	3	3	0	4	3	3	3	5	2	3	5	5	5	0	4	5	5	5
4	4	4	4	0	0	0	5	3	3	2	2	2	0	5	5	4	2	2
5	5	5	5	5	5	5	0	0	0	0	0	0	2	2	2	2	4	6
6	6	6	6	6	6	6	6	6	6	6	6	6	6	6	6	6	6	4

Suppose that the vector $[p_0, p_1, \ldots, p_{n-1}]$ is a column of the P-matrix, where p_0 is the label of the outermost (top) curve and p_{n-1} is the label of the innermost (bottom) curve. Then a region at ring i, $1 \leq i \leq n-1$, in the interior of curves $p_0, \cdots, p_{i-1}$ has the rank $\sum_{k=0}^{i-1} 2^{p_k}$. If the next column of P is obtained by exchanging p_i and p_{i+1}, then we have created exactly one new region, a region with rank $\sum_{k=0}^{i} 2^{p_k} - 2^{p_{i-1}}$. Proceeding from left to right through P, we can then compute the rank of each region. Matrix P (and hence matrix M) represents a valid simple monotone Venn diagram if we get exactly $2^n - 2$ regions with distinct ranks and if the labels of the curves at the end is the same as the starting vector of the curves labels, which is $[0, 1, \ldots, n-1]$.

Crossing sequence

Recall that when testing whether a standard matrix represented a Venn diagram we used the P-matrix. But instead of storing the P-matrix as a sequence of permutations, we could simply record the row in which the intersection occurs, as is shown in Figure 3.5. If π and π' are two successive permutations then the corresponding entry in the permutation sequence is i if π' is obtained from π by exchanging $\pi(i)$ and $\pi(i-1)$. We call the resulting sequence of length $2^n - 2$ the *crossing sequence*. It is clear that there are $\binom{n}{i}$ elements of value i in the sequence, where $i \in \{1, 2, \ldots, n-1\}$. Furthermore, since we assume that the first permutation of the P-matrix is the identity, the first entry of the permutation sequence is a 1.

For a simple rotationally symmetric n-Venn diagram, the first $(2^n - 2)/n$ elements of the crossing sequence are enough to represent the diagram; the remainder of the crossing sequence is formed by $n-1$ concatenations of this sequence. For example, the crossing sequence representing one sector of the simple symmetric 5-Venn diagram is shown in Figure 3.5.

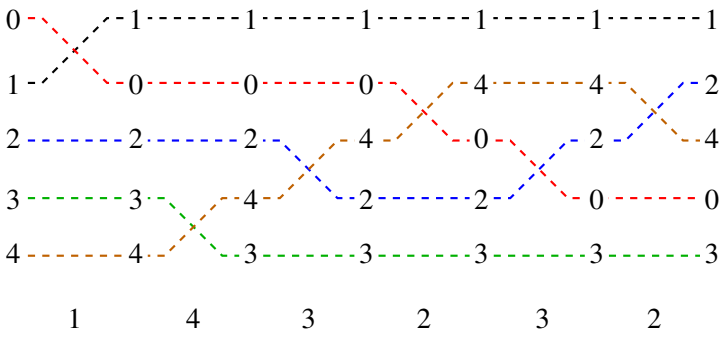

Figure 3.5: The P-matrix of one slice of Grünbaum's 5-ellipses Venn diagram. Shown below it are the first six values of the crossing sequence.

3.4 Composition representation

In this subsection we introduce a representation of Venn diagrams that is based on integer compositions. In this representation, we use a sequence of nonnegative integers to show the size of faces in each ring and also to specify the position of intersection points of the next ring relative to the position of intersection points in the current ring. A *k-composition of n* is a sequence of nonnegative integers $(a_0, a_1, \cdots, a_{k-1})$ such that $n = \sum a_i$. Let $\mathcal{C}(n, k)$ denote the set of all k-compositions of n.

In a simple monotone n-Venn diagram there are $\binom{n}{i+1}$ intersection points at ring $i+1$ that are distributed among $\binom{n}{i}$ intersection points at ring i. Starting from an intersection point at ring i, we can specify the number of intersection points at ring $i+1$ between each two consecutive intersection points of ring i using a composition of $\binom{n}{i+1}$ into $\binom{n}{i}$ parts. Consider a generic face in ring i, like that shown in Figure 3.6. It is delimited by some two intersection points that are adjacent to regions on the same ring. If there are p intersections on the lower part of the face (such intersections are adjacent to k-faces with $k \geq i$), then p will be part of the composition for ring i.

A simple monotone n-Venn diagram V can be represented by a sequence $C_V = (c_1, c_2, \ldots, c_{n-2})$ where

$$c_i \in \mathcal{C}\left(\binom{n}{i+1}, \binom{n}{i}\right).$$

The composition c_i is determined by following ring i in a circular fashion, recording for each i-face the number of intersection points that only lead to k faces, where $k > i$. Thus the underlying compositions are *circular*. To be able to recover the diagram from the compositions, we need to specify where each composition starts.

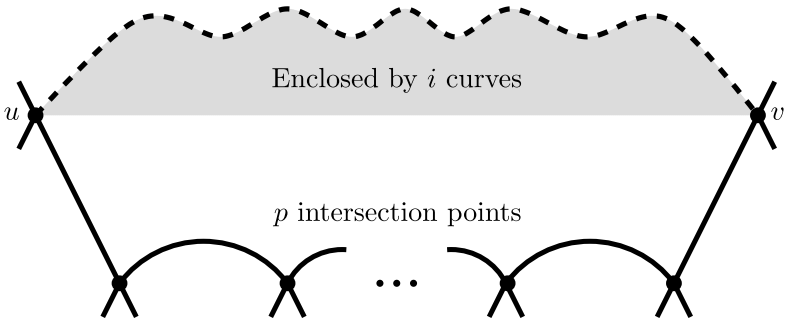

Figure 3.6: An i-face with p lower vertices.

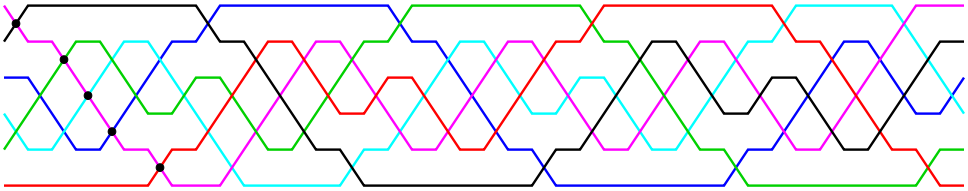

(a) Cylindrical representation of the diagram

$$\begin{pmatrix} (3,3,3,3,2,1)\ , \\ (1,1,2,1,1,2,1,1,2,1,1,2,1,1,2), \\ (1,0,1,1,1,0,1,1,1,0,1,1,1,0,1,1,1,0,1,1), \\ (1,1,0,1,0,0,1,0,0,1,0,0,1,0,0) \end{pmatrix}$$

(b) Composition representation of the diagram

Figure 3.7: Composition representation of a simple monotone 6-Venn diagram.

Given $c_i = p + q + r + \cdots$, the starting face for c_{i+1} is one that lies below the face corresponding to p, call it F. Suppose that F is joined to the rest of the ith ring by vertices u and v on its left and right, respectively. If $p > 1$, then the face is the one that lies between the first two of the lower p intersection points (see Figure 3.6). If $p = 1$, then the face is the one that lies between the lower vertex and v. If $p = 0$, then the face is the one that lies below the edge from u to v. With these conventions, we say that C_V is a *composition representation* of V. A simple monotone Venn diagram does not necessarily have a unique composition representation because starting from a different intersection point on the first ring we may get a different composition representation of the Venn diagram. Figure 3.7 shows the composition representation of the 6-Venn diagram of Figure 3.1(d). The black dots indicate where the various faces of the compositions start.

We now list several observations that will help us cut down the size of the search space of the generating algorithm.

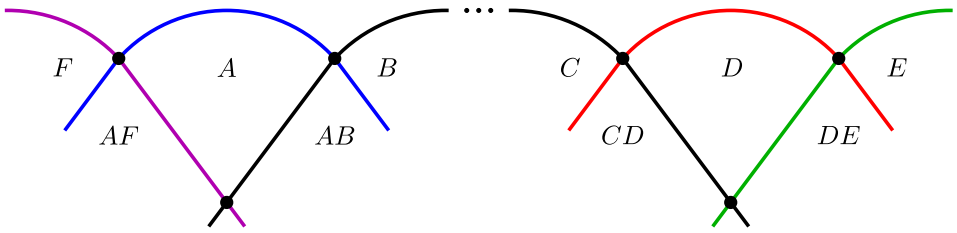

Figure 3.8: Nonadjacent 1s in the first ring composition

Remark 3.4.1. *For any simple monotone n-Venn diagram V, the largest part of c_i in the composition representation is at most $n - i - 1$.*

Proof. A region at ring i is in the interior of i curves. Since the size of a region is at most n and no two edges belong to the same curve by Lemma 3.1.2, at most $n - i$ remaining curves can be used to shape the region. As shown in Figure 3.6, to put p intersection points between the two end points of the region on the next ring, we need $p + 1$ curves, $p - 1$ curves for the bottom side and two curves for the left and right sides. So, $p \leq n - i - 1$. □

Remark 3.4.2. *In the composition representation of any simple monotone Venn diagram with more than 3 curves, there are no two nonadjacent 1s in c_1.*

Proof. If there is such a Venn diagram V, then the first ring of the Venn diagram will be like Figure 3.8, where regions A and D correspond to nonadjacent 1s in the composition, and $A \neq D$. Then $A \cap D = \emptyset$, which contradicts the assumption that V is a Venn diagram. So in the first ring composition there are at most two 1s, which must be adjacent. □

Remark 3.4.3. *There are no two consecutive 0s in c_2 for the composition representation of any simple monotone n-Venn diagram.*

Proof. By Lemma 3.1.4. □

Let $c_1 = (a_0, a_1, \ldots, a_{k-1})$ and $c_2 = (b_0, b_1, \ldots, b_{k-1})$ be two compositions of n into k parts. We say c_2 is a rotation of c_1 if there exists some integer $j \in \{0, 1, \ldots, k-1\}$ such that for every i, $0 \leq i \leq k-1$, $b_i = a_{i+j \pmod k}$. The reversal composition of c_1 is the composition $(a_{k-1}, a_{k-2}, \ldots, a_0)$.

Definition 3.4.1. Let $c_1, c_2 \in \mathcal{C}(n, k)$ be two compositions of n into k parts. We say that c_1 and r_2 are *rotationally distinct* if c_2 is not a rotation of c_1 or its reversal.

Let $\mathcal{F}_n$ denote the set of all rotationally distinct compositions of $\binom{n}{2}$ into n parts such that for any $r \in \mathcal{F}_n$ there are no two nonadjacent parts of 1 and all parts are less than or equal to $n-2$.

Lemma 3.4.4. *If c_1 is the composition corresponding to the first ring of a simple monotone n-Venn diagram, then there exists some composition $c_1' \in \mathcal{F}_n$ such that c_1 is a rotation of c_1' or its reversal.*

Proof. Given a simple monotone n-Venn diagram, suppose we get the composition representation P of V by picking a particular intersection point x in the first ring as the reference point. Now let P' be another representation of V using any other intersection point in the first ring different than x as the reference point. It is clear that c_1' in P' is a rotation of c_1 in P. Also for any composition representation P'' of the mirror of V the first composition c_1'' in P'' is a rotation of the reversal of c_1. By Remarks 3.4.1 and 3.4.2, the largest part of c_1 is $n-2$ and there are no two nonadjacent 1s in c_1. Therefore, there is a composition $c \in \mathcal{F}_n$ that is rotationally identical to c_1. □

Using the matrix representation or the composition representation we generate Venn diagrams vertically (top-to-bottom). However, crossing sequences generate Venn diagrams horizontally from left-to-right. This allows us to immediately compute the rank of regions as we move from one permutation to the next, and thus can potentially help in reducing the size of the backtracking tree, since non-Venn diagrams are recognized early.

Chapter 4

Generating simple monotone Venn diagrams

In the previous chapter, we studied different representations of simple monotone Venn diagrams. In this chapter we introduce different algorithms based on those representations to provide a complete enumeration of such diagrams for small values of n. We also want to determine diagrams that have nontrivial isometries when embedded on the sphere. The underlying techniques rely on exhaustive backtrack searches with intelligent pruning rules justified by structural theorems. Such computer searches are prone to error and so we have made considerable effort to ensure that our computations are correct by using different representations, different methods for checking isomorphism, and independent programming efforts. This chapter is joint work with Frank Ruskey and Wendy Myrvold.

Our main concern in this chapter are Venn diagrams with n curves, where $n = 6$ and $n = 7$. The case of $n = 7$ is done first, but only on those diagrams that have a 7-fold rotational symmetry, because of the overwhelming number of possibilities otherwise. We find that there are 23 nonisomorphic rotationally symmetric simple monotone 7-Venn diagrams, which corroborates the earlier results of Ruskey [46]. Of these 23, there are 6 that have an additional 2-fold "polar symmetry" (Figure 4.1), and 17 that do not (Figure 4.2).

In the case of $n = 6$, there are 39,020 nonisomorphic simple monotone 6-Venn diagrams. Of these, 375 have polar symmetry, and of those 27 have an isometry group order of 4, 6 have an isometry group order of 8 (Figure 4.3).

4.1 Generating simple symmetric convex 7-Venn diagrams

We used the matrix representation from Section 3.3 to generate all simple symmetric monotone 7-Venn diagrams. The generating algorithm is shown in Algorithm 1. A slice matrix of a simple symmetric monotone 7-Venn diagram has 6 rows and 18 columns where the number of 1s in rows $1, 2, \cdots, 6$ are $1, 3, 5, 5, 3, 1$ respectively. To generate each row we are generating restricted combinations; e.g., all bit-strings of length 18 with k 1s, no two of which are adjacent. The total number of combinations generated is the number given in (3.1).

For each generated slice matrix, we copy it n times to get a complete matrix M, which we then convert into the corresponding P-matrix. Then we check if P represents a valid Venn diagram by counting the number of distinct regions. This process was described earlier in the paper.

To eliminate isomorphic Venn diagrams, we use the Grünbaum encoding, which is easily created from the P-matrix in $O(2^n)$ time. Since the diagram is symmetric, we only need w_i for $i = 0$ and similarly, we only need x_0, y_0, and z_0 (which are easily obtained from w_0 using the permutation mappings explained earlier). We first initialize a vector ρ with the permutation of $\{0, 1, \cdots, n-1\}$ such that the curves appear on the outer boundary of the outermost ring in the order $\rho(1), \rho(2), \ldots, \rho(n-1)$. To get w_0, we scan P left-to-right and follow curve 0's intersections with other curves, translating them by ρ^{-1}. The lexicographically smallest string of $\{w_0, x_0, y_0, z_0\}$ is chosen as the representative Grünbaum encoding of the Venn diagram. Comparing the Grünbaum encodings of the previously generated Venn diagrams with the Grünbaum encoding of the current Venn diagram, we can eliminate isomorphic Venn diagrams.

Using this algorithm we found exactly 23 simple symmetric monotone 7-Venn diagrams, of which 6 are polar symmetric. See Figures 4.1 and 4.2 for attractive renderings of these diagrams.

These computations were checked by using an algorithm based on the composition representation, and using a depth-first-search labeling algorithm for the isomorphism check.

Algorithm 1 Generating all simple symmetric convex 7-Venn diagrams

```
1: procedure GenSymSeven(i)
2:     G ← {}
3:     V ← {}
4:     for each standard slice matrix M do
5:         for i ← 1, ··· , 7 do
6:             X ← X · M
7:         end for
8:         if isVenn(X) then
9:             g ← Grünbaum encoding of X
10:            if g ∉ G then
11:                G ← G ∪ g
12:                V ← V ∪ X
13:            end if
14:        end if
15:    end for
16: end procedure
```

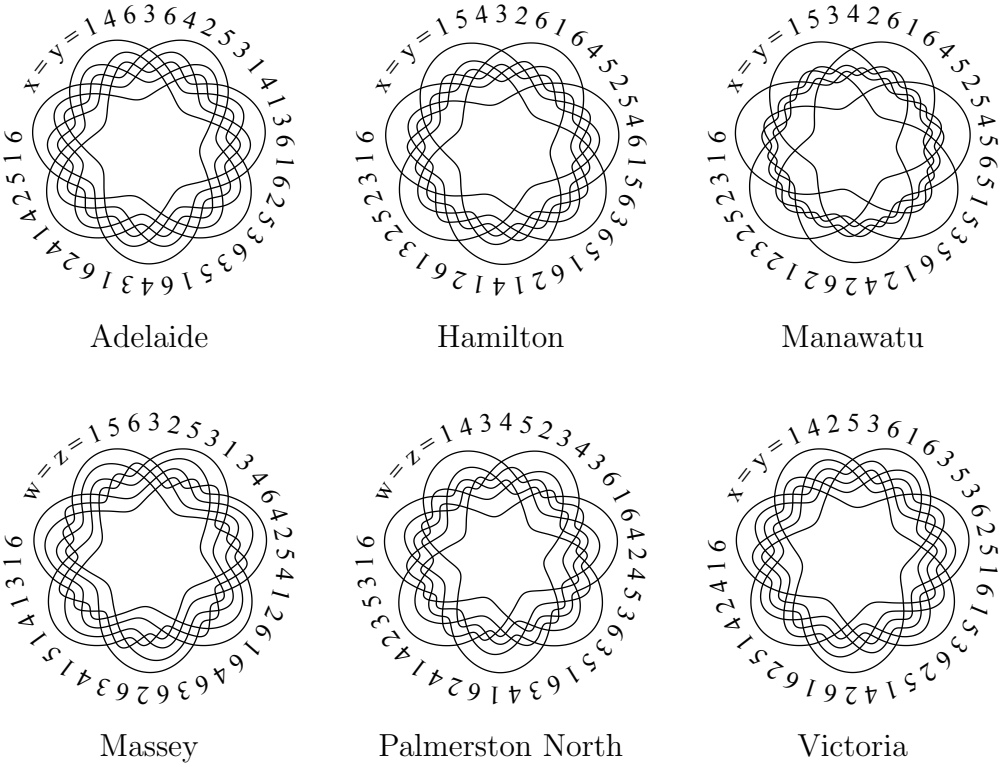

Figure 4.1: All simple monotone polar symmetric 7-Venn diagrams, using the names given to them by Edwards [14]. Around each diagram is the lexicographically smallest Grünbaum encoding.

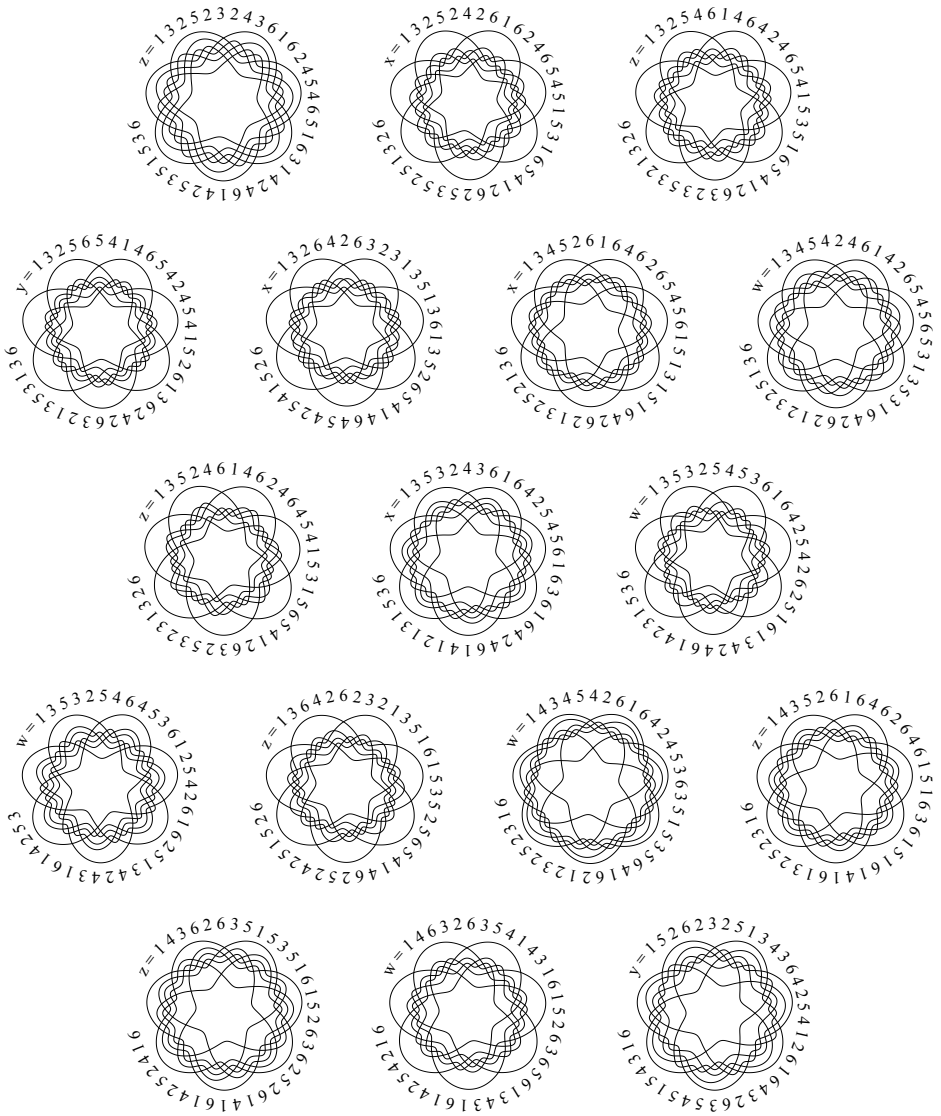

Figure 4.2: All 17 simple monotone symmetric 7-Venn diagrams that do not have polar symmetry. Around each diagram is the lexicographically smallest Grünbaum encoding.

4.2 Generating simple polar symmetric 6-Venn diagrams

Given the upper/lower half of the cylindrical representation of a polar symmetric Venn diagram, one can generate the whole diagram by creating a copy of the given half, turning it upside down and rotating it until the two parts match together. So, to generate a polar symmetric monotone Venn diagram, we need only to generate the first $\lceil \frac{n-2}{2} \rceil$ compositions.

The algorithm for generating simple convex polar-symmetric 6-Venn diagrams is described in Algorithm 2. Given the first two compositions, we create the upper and lower halves of the corresponding diagram. Two halves of the diagram can match only if gluing them using the intersection points doesn't create any faces of size 2. Given the last composition of the upper half, for each positive part a_j there are $a_j - 1$ edges that bound the corresponding face from the bottom and there is a gap between two faces corresponding to two consecutive parts of the composition. So, we can map the composition to a bit-string where each 1 represents a bounding edge of a face and each 0 represents the gap between two faces. The length of bit-string is the same as the sum of all parts of the composition. In other words, the composition $(a_1, a_2, \cdots, a_k)$ is mapped to the following bit-string.

$$\overbrace{11\cdots1}^{a_1-1\ bits}0\overbrace{11\cdots1}^{a_2-1\ bits}0\cdots0\overbrace{11\cdots1}^{a_k-1\ bits}0$$

We can find all matchings of the two halves by computing the bitwise "and" of the bit-string and its reverse for all left rotations of the reverse bit-string. Any result other than 0 means that there is at least one face of size 2 in the middle and it is rejected. Otherwise, we compute the matrix representation of the resulting diagram. The matrix can be obtained by sweeping the compositions from left to right and computing the position of each intersection point. For each pair of the first two compositions, we compute all matchings of the upper and lower halves. Checking the resulting matrix for each matching gives us all possible simple monotone polar-symmetric 6-Venn diagrams.

Using exhaustive search based on this algorithm we found 375 simple monotone polar symmetric 6-Venn diagrams. This result was independently checked by Wendy Myrvold using a separate program that is based on a different search method. Ta-

Algorithm 2 Generating all simple convex polar-symmetric 6-Venn diagrams

```
1: procedure GenPolarSix(i)
2:     for each composition (a_1, a_2, ..., a_6) ∈ F_6 do
3:         for each composition (b_1, b_2, ..., b_15) ∈ C(20, 15) do
4:             create the corresponding upper and lower halves
5:             for i ← 1, ..., 20 do
6:                 glue the upper and lower halves
7:                 if there are no parallel edges in the diagram then
8:                     compute matrix X representing the diagram
9:                     if isVenn(X) then
10:                        add X to the list of Venn diagrams
11:                    end if
12:                end if
13:                rotate lower half one point to the left
14:            end for
15:        end for
16:    end for
17: end procedure
```

Composition	Venn Diagrams	Composition	Venn Diagrams
4 4 3 2 1 1	25	2 3 4 3 2 1	5
4 3 4 2 1 1	0	4 2 2 4 2 1	0
3 4 4 2 1 1	38	3 3 2 4 2 1	9
4 4 2 3 1 1	0	2 4 2 4 2 1	0
4 3 3 3 1 1	12	3 2 3 4 2 1	3
3 4 3 3 1 1	9	4 3 2 2 3 1	9
4 2 4 3 1 1	0	3 4 2 2 3 1	15
4 3 2 4 1 1	0	4 2 3 2 3 1	0
4 4 2 2 2 1	15	3 3 3 2 3 1	9
4 3 3 2 2 1	2	3 2 4 2 3 1	0
3 4 3 2 2 1	30	4 2 2 3 3 1	12
4 2 4 2 2 1	0	3 3 2 3 3 1	4
3 3 4 2 2 1	6	4 2 2 2 4 1	0
2 4 4 2 2 1	13	4 3 2 2 2 2	15
4 3 2 3 2 1	7	4 2 3 2 2 2	22
3 4 2 3 2 1	8	3 3 3 2 2 2	6
4 2 3 3 2 1	6	4 2 2 3 2 2	1
3 3 3 3 2 1	41	3 3 2 3 2 2	21
2 4 3 3 2 1	22	3 2 3 2 3 2	3
3 2 4 3 2 1	7		

Table 4.1: Number of polar symmetric 6-Venn diagrams for $\mathcal{F}_6$

ble 4.1 shows the number of Venn diagrams for each particular composition of the first level.

4.3 Generating simple convex 6-Venn diagrams

In this part we explain the algorithm for generating all simple convex 6-Venn diagrams using the permutation representation. Starting from the identity permutation, for each permutation try all possible exchanges of adjacent curves to get the next permutation until we get a sequence of length 62 that represents a Venn diagram. The height of the recursion tree of the backtracking algorithm is 62. There are five possible choices for the first exchange and four choices for each of the other exchanges. So, there are 5×4^{61} possible sequences in total. Therefore, we need some rules to prune the search tree as much as possible to speed up the generating algorithm to make the problem tractable.

As with matrix representation, if a sequence of exchanges X represents a valid Venn diagram then any rotation of X represents the same Venn diagram. A sequence of exchanges X is *canonical* if among all rotations of X, it has the largest corresponding P-matrix. We need the canonical form to eliminate all sequences which are identical to a canonical sequence up to rotations. Given a prefix of length k of an exchange sequence $S = (s_1 s_2 \cdots s_{62})$, if there is some i, $1 < i \leq k$ such that starting at position i in S with the identity permutation we get a larger P-matrix, then S is not canonical. So we can check the canonicity for each generated prefix of exchanges and reject the noncanonical exchange sequences as soon as possible.

As another rule, if there are two exchanges that occur in two adjacent permutations of the P-matrix such that the positions of the exchanges do not intersect, then the exchange of the lower position comes first because the resulting diagram in both cases is the same. Therefore, we do not need to generate both of them.

As was mentioned before, we can compute and check the rank of regions as we move from one permutation in the P-matrix to the next. So we can cut a non-Venn diagram at the earliest stage of recursion. We can also benefit from some other simple properties of convex Venn diagrams, such as Lemma 3.1.2.

The pseudocode for generating all simple convex 6-Venn diagram is shown in Algorithm 3. Input i is the next exchange, S is the exchange sequence, and V is the list of Venn diagrams that have been found so far. The current permutation of curve labels is stored in vector C and vector $rank$ is used to store the rank of current region of each ring. The number of regions that have been visited so far is stored in rno. The vector $visited$ is used to keep track of the visited regions. We start with the identity permutation as the curve labels. So, vector $rank$ must be initialized to $[1, 3, 7, 15, 31]$, because, as was mentioned before, the rank of the region at ring i is $\sum_{k=0}^{i-1} 2^{C_k}$. Two consecutive regions at ring i only differ in $C[i]$ and $C[i+1]$. To update the rank vector, after swapping $C[i]$ and $C[i+1]$, we need to add curve $C[i]$ to the new region and exclude $C[i+1]$ from it. The rank of regions of the other rings remain unchanged. Lines 24 to 27 of the algorithm restore the variables to their state before the recursive call.

A distributed version of the algorithm takes only a few hours on a cluster of machines with 64 processors to generate all simple monotone 6-Venn diagrams. There are 39,020 such Venn diagrams in total.

Algorithm 3 Generating all simple convex 6-Venn diagrams

```
1: procedure GenSix(i, rno)
2:     if S is not canonical then
3:         return
4:     end if
5:     if rno = 62 then
6:         if C = id then
7:             V ← V ∪ S
8:         end if
9:         return
10:    end if
11:    r ← rank[i]
12:    if visited[r] = 1 then
13:        return
14:    end if
15:    visited[r] ← 1
16:    S ← S ∪ {i}
17:    C[i] :=: C[i + 1]
18:    rank[i] ← rank[i] + 2^C[i] − 2^C[i+1]
19:    for j ← i − 1, . . . , n − 1 do
20:        if j ≠ i then
21:            GenSix(j, rno + 1)
22:        end if
23:    end for
24:    rank[i] ← rank[i] − 2^C[i] + 2^C[i+1]
25:    C[i] :=: C[i + 1]
26:    S ← S \ {i}
27:    visited[r] ← 0
28: end procedure
```

4.4 Testing for symmetry

In this section, we describe how we tested each of the 39,020 planar monotone 6-Venn diagrams to determine whether they have any nontrivial automorphisms when embedded on the sphere.

It is well-known that a 3-connected planar graph has a unique embedding (under the assumption that reversing the sense of clockwise for an embedding gives an equivalent embedding). Because of this property, 3-connected planar graphs can be put into a canonical form, and it is possible to compute the automorphism group using a very simple algorithm based on a special type of breadth-first search (called a *clockwise BFS*) that runs in $O(n^2)$ time in the worst case. It is not clear who originally came up with this elegant algorithm. One place it has been explained and used is [18].

Given a rotation system for a graph, a *clockwise breadth-first search* (BFS) starts at a specified root vertex r, and has a specified neighbour f of r designated to be the first child of r. A BFS is performed with the restrictions that the neighbors of r are traversed in clockwise order starting with the first child f. When the neighbors of a non-root vertex u are visited, they are traversed in clockwise order starting with the BFS parent of u. A clockwise BFS labels each vertex with its breadth-first index.

To get the canonical form for an embedding, consider all possible selections of a root vertex, a first child, and the direction representing clockwise and choose one giving a lexicographically minimized rotation system. The selections giving an identically labeled rotation system give the automorphisms. If there are no automorphisms that have different choices for the clockwise direction, then the embedding is said to be *chiral*, and otherwise it is *achiral*.

The algorithm above gives the automorphisms that can be realized when embedding the graph on the sphere (these will be called the *spherical automorphisms*. To consider only those that map the innermost face (i.e., the full face) to itself, one trick that can be used is to embed a new vertex w inside the innermost face and connect it to all the vertices on the innermost face. Then apply the clockwise BFS but only with the selections that have w as the root vertex. These are the *planar automorphisms* (they are the automorphisms realizable for a picture of an embedding drawn on the plane).

The *polar automorphisms* are those which map the innermost face either to itself or to the external face. The trick used to compute these is to add two new vertices; w_1,

which is connected to the vertices on the innermost face, and w_2, which is connected to the vertices on the external face. Then apply the clockwise BFS selections that have either w_1 or w_2 as the root vertex.

Using the above described ideas we found that 375 of the simple monotone 6-Venn diagrams are polar symmetric, which confirms our results of generating polar symmetric 6-Venn diagrams using compositions. And 270 of the generated Venn diagrams have the (antipodal) rotary reflection symmetry. Amongst all simple convex 6-Venn diagrams, we found 27 Venn diagrams with automorphism group order of four. There are only six Venn diagrams that have an automorphism group order of eight; these are shown in Figure 4.3. In all six cases, there are two curves that intersect in only two points. Imagine each Venn diagram as being projected on a sphere such that these two curves map to two great circles that meet perpendicularly at the north and south sphere poles. The three cases on left side of Figure 4.3 have the 4-fold rotational symmetry about an axis through the poles. The three other cases have the refection symmetry across the two planes which pass through the two great circles. The other factor of 2 comes from the fact that all of these diagrams are polar-symmetric.

4.5 Concluding remarks for this chapter

In this chapter we investigated generating simple monotone Venn diagrams. We described some generating algorithms based on different representations that were introduced in the previous chapter to exhaustively list simple monotone Venn diagrams with 6 and 7 curves. Using these algorithm we showed that there are 23 simple monotone symmetric 7-Venn diagrams where amongst of them six cases are polar-symmetric. For simple monotone Venn diagrams on six curves, we showed that there are 39,020 diagrams in total, 375 of which are polar-symmetric. A list of all 375 simple convex 6-Venn diagrams with polar symmetry may be found at `http://webhome.cs.uvic.ca/~ruskey/Publications/SixVenn/PolarSixVenn.html`

Prior to this, the only spherical symmetries known were 7-fold rotations and polar flips. However, by hand we have created a spherical 7-Venn diagram with a 4-fold rotational symmetry and a polar symmetry; see Figure 4.4. The lexicographically smallest Grünbaum encoding of the diagram is shown below it. Note that because of the polar symmetry x and y (also w and z) strings of the Grünbaum encoding are identical. In the next chapter we will investigate constructing simple monotone Venn diagrams on the sphere with symmetry group of order eight in the general case when

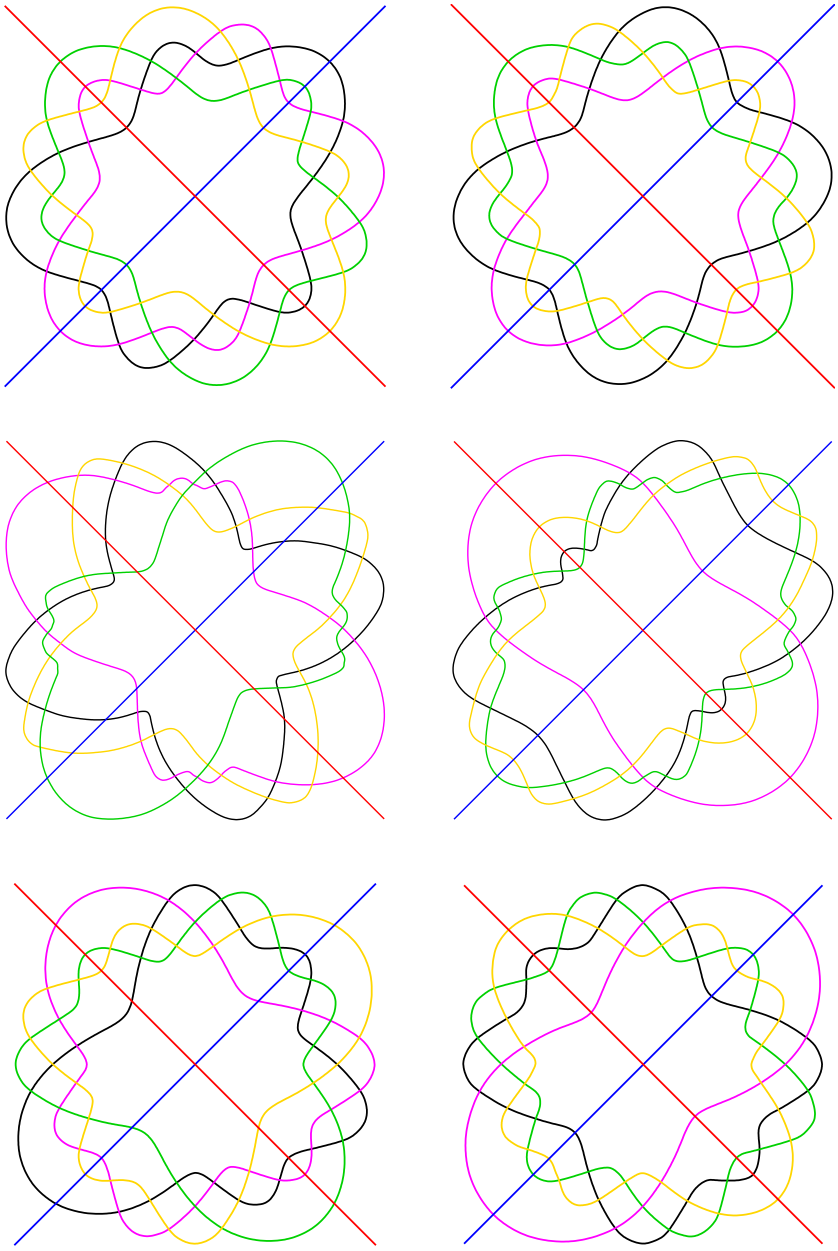

Figure 4.3: All simple convex spherical 6-Venn diagrams whose isometry groups have order 8. The diagrams on each row can be transformed, one into the other, by flipping an opposing pair of quadrants.

there is a large number of curves.

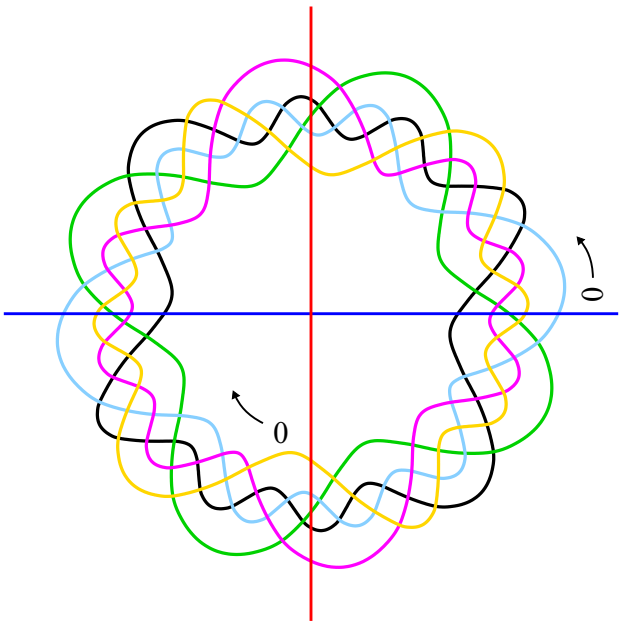

$x_0 = y_0$	1 2 4 3 4 2 1 4 1 5 3 1 2 1 4 2 3 2 4 1 2 4 3 6 1 2 4 3 4 2 1 4 1 5 3 1 2 1 4 2 3 2 4 1 2 4 3 6
$x_1 = y_1$	2 4 3 4 2 0 4 0 3 5 0 2 0 4 2 3 2 4 0 6 3 2 4 0 2 4 3 4 2 0 4 0 3 5 0 2 0 4 2 3 2 4 0 6 3 2 4 0
$x_2 = y_2$	3 1 0 4 5 3 1 0 4 1 0 3 0 1 4 0 4 3 6 4 1 4 0 1 3 1 0 4 5 3 1 0 4 1 0 3 0 1 4 0 4 3 6 4 1 4 0 1
$x_3 = y_3$	4 1 5 0 2 4 2 0 1 0 2 6 4 1 0 1 4 2 4 1 5 0 2 4 2 0 1 0 2 6 4 1 0 1 4 2
$x_4 = y_4$	5 2 1 0 3 0 1 2 0 2 6 3 2 1 2 0 1 3 1 0 2 1 0 3 5 2 1 0 3 0 1 2 0 2 6 3 2 1 2 0 1 3 1 0 2 1 0 3
$x_5 = y_5$	6 4 1 3 0 2 6 2 0 3 1 4
$x_6 = y_6$	0 2 3 4 1 5 1 4 3 2 0 5

Figure 4.4: A spherical 7-Venn diagram with a 4-fold rotational symmetry and polar symmetry. Shown below the diagram is its lexicographically smallest Grünbaum encoding.

Chapter 5

Simple spherical Venn diagrams with isometry group of order eight

In the previous chapter, we showed several examples of spherical Venn diagrams with six and seven curves that have the symmetry group of order eight. In this chapter, we provide a general method of constructing simple spherical Venn diagrams with the same type of symmetry. For each $n \geq 6$ we show how to construct simple spherical Venn diagrams of n curves embedded on the sphere with either of the following sets of isometries: (a) a 4-fold rotational symmetry about the polar axis, together with an additional involutional symmetry about an axis through the equator, or (b) an involutional symmetry about the polar axis together with two reflectional symmetries about orthogonal planes that intersect at the polar axis. In both cases (a) and (b) the order of the group of isometries is eight.

5.1 Bounded Venn diagrams

As a planar graph, any Venn diagram can be embedded on a sphere; a Venn diagram so embedded is said to be a *spherical Venn diagram*. Because of the richness of the isometry group of the sphere, it is natural to search for spherical Venn diagrams with different types of isometry. Anthony Edwards was perhaps the first to notice that some Venn diagrams could be drawn on the sphere with nontrivial symmetries [15]. A detailed study of the symmetries of Venn diagrams on the sphere was initiated by Mark Weston [55], and Ruskey and Weston [47] showed that, for any n and any isometry of the sphere of order two, there is a Venn diagram achieving that isometry.

An exhaustive search shows that the number of simple monotone spherical 6-Venn diagrams with isometry group of order eight is six and the number with isometry group of order four is 27 (see Chapter 4).

We will find it very useful to use a new variant of Venn diagrams. Consider a strip of the plane bounded by two vertical lines called L on the left and R on the right. Let $\mathcal{C} = \{C_1, C_2, \ldots, C_n\}$ be a collection of n curves in the plane such that each curve C_i lies strictly between L and R with one endpoint on L and the other endpoint on R. The two regions of the strip below and above a curve are called the *interior* and *exterior* of the curve, respectively. The collection $\mathcal{C}$ is then called a *bounded n-Venn diagram* if for each $S \subseteq \{1, 2, \ldots, n\}$ the region

$$\bigcap_{i \in S} \text{int}(C_i) \quad \cap \quad \bigcap_{i \notin S} \text{ext}(C_i) \tag{5.1}$$

is nonempty and connected.

Observe that in a bounded Venn diagram each curve must intersect every other curve at least once. The two vertical bounding lines L and R are called the *left bound* and *right bound* of the diagram. A bounded Venn diagram is *simple* if no three curves intersect at any point of the diagram and the intersection points with L and R are distinct. In this paper we are dealing only with simple diagrams unless otherwise specified. Figure 5.1 shows a bounded Venn diagram of three curves. A *boundary vertex* is a point of the diagram at which the left or right bound intersect one of the curves. The rest of the intersection points in the diagram are called *(internal) vertices*. Each bound intersects a curve in exactly one point, so there are $2n$ boundary vertices in a bounded n-Venn diagram of n curves. Furthermore, we will assume, without loss of generality, that the set of y coordinates of the boundary vertices on L is exactly the same as the set of y coordinates of the boundary vertices on R.

Each simple bounded Venn diagram V induces a permutation $\rho(V)$ which indicates the order that the curves hit the right bound. The permutation is determined by labeling the vertices $1, 2, \ldots, n$ from top to bottom along L and then reading off the permutation from top to bottom along R. If $\rho(V)$ is an involution, then it is called an *involutional bounded Venn diagram*. The bounded 3-Venn diagram of Figure 5.1 is not involutional since it induces the circular permutation (1 2 3).

Let H denote the isometry of rotation by π radians, *i.e.*, for any point (x, y), $H(x, y) = (-x, -y)$, where the bounded Venn diagram is centered at $(0, 0)$. A bounded Venn diagram has the *half turn symmetry* if it maps to itself under H

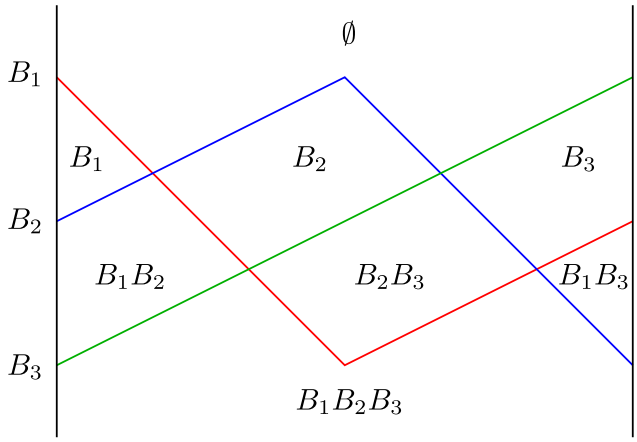

Figure 5.1: A simple bounded Venn diagram of three curves.

up to a relabeling of the curves. We call a bounded Venn diagram with half turn symmetry a symmetric bounded Venn diagram for convenience.

In the remainder of this chapter, we first review Edwards's construction of symmetric Venn diagrams on the sphere and discuss bounded Venn diagrams in more detail in Section 5.2. Then in Section 5.3 we provide general constructions of involutional simple bounded Venn diagrams which are symmetric under rotation by π radians, and use these to construct Venn diagrams with isometries of order eight on the sphere.

5.2 Simple bounded Venn diagrams

Giving a general construction of simple Venn diagrams on the plane, Anthony Edwards observed that it is possible to draw these diagrams on the sphere with some additional symmetries. Edwards's construction starts with a circle of longitude as the first curve. The 2-Venn diagram is obtained by adding another longitudinal circle orthogonal to the previous one. Adding the equator as the third curve creates a simple symmetric 3-Venn diagram. Subsequent curves are added inductively, starting from some point located on the first curve immediately below the equator and then dividing each region by alternatively intersecting the equator, above and below. Figure 5.2 (redrawn from [55]) shows a cylindrical representation of the construction of a simple 7-Venn diagram. More details and illustrations of Edwards's construction can be found in [16].

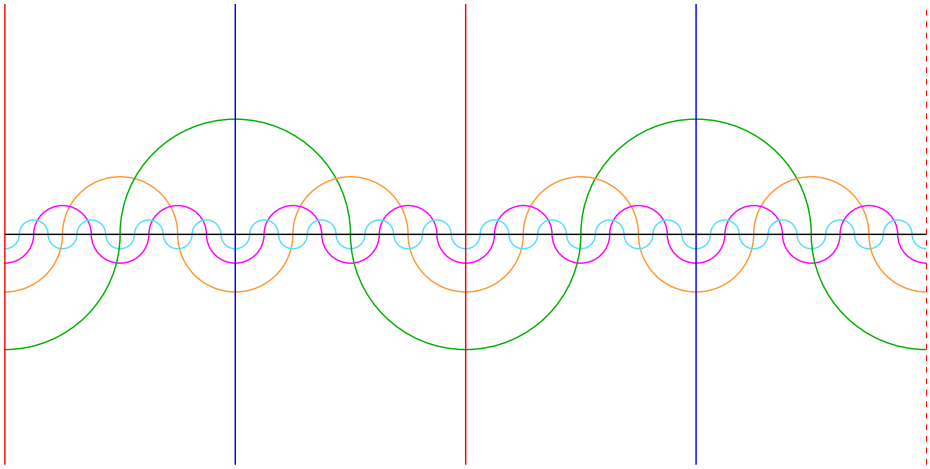

Figure 5.2: Cylindrical projection of Edwards's construction of a 7-Venn diagram.

Considering the two orthogonal longitudes as the bounds, Edwards's construction of a simple n-Venn diagram can be thought of being composed of four bounded Venn diagrams, each of $n-2$ curves. These four bounded Venn diagrams are illustrated in Figure 5.2. It is not difficult to prove that the permutation induced by the leftmost bounded Venn diagram is $(1\ 2\ \cdots\ n{-}2)$. The three subsequent slices are obtained by the successive flips of the first slice about a vertical bisecting axis. Let $\mathbb{E}$ denote the symmetry group of Edwards diagrams. The group $\mathbb{E}$ has order four based on using the following two symmetries to generate the group:

- Reflection of the sphere across one of the two planes that contain the two longitudinal circles.
- A rotation by π radians about the polar axis.

Edwards's construction shows that simple bounded Venn diagrams exist for any number of curves. Conversely, we show below that any bounded Venn diagram can be used to construct an ordinary spherical Venn diagram that preserves the symmetries of Edwards diagrams.

Lemma 5.2.1. *For every simple bounded Venn diagram V with no nontrivial isometries, there exists a simple spherical Venn diagram V' with isometry group $\mathbb{E}$ such that V is the fundamental domain of V' (in its cylindrical representation).*

Proof. Given any simple bounded Venn diagram V of $n-2$ curves with induced permutation ρ, the permutation of the horizontal flip of V is ρ^{-1}. We take four copies

of the bounded Venn diagram, flipping every other copy, as in Edwards's construction. Thus the final permutation at the rightmost bound is $\rho\rho^{-1}\rho\rho^{-1} = id$, which implies that the correct curves meet at the right boundary; this gives us $n-2$ simple closed curves. Considering the boundaries of the V as two great circles that intersect at the poles, the regions within each strip satisfy (5.1) and the regions within each strip are distinct from any other strip. Therefore the overall construction is the cylindrical representation of a simple n-Venn diagram V'. The symmetry group of V' is $\mathbb{E}$ since V has no nontrivial isometries. □

There are classes of permutations not induced by any bounded Venn diagram.

Lemma 5.2.2. *Let V be a simple bounded n-Venn diagram. If $\rho(V)$ contains the cycle $(a_1\ a_2\ \cdots\ a_k)$ where $\{a_1, a_2, \ldots, a_k\} = \{1, 2, \ldots, k\}$, then $k = n$.*

Proof. Suppose $k < n$. Let $C = \{C_1, \ldots, C_n\}$ be the set of all curves and let S be the set of the first k curves. Every pair (c, c') of curves of the two disjoint sets S and $C \backslash S$ intersect in at least two points since $\text{ext}(c) \cap \text{int}(c')$ is not empty and $\rho(c') \notin S$. Therefore, there would be two distinct boundary regions corresponding to $\bigcap_{i\in S} \text{int}(C_i) \quad \cap \quad \bigcap_{i\in C\backslash S} \text{ext}(C_i)$ which contradicts the definition of bounded Venn diagrams. □

Lemma 5.2.3. *A simple bounded Venn diagram of n curves has exactly $2^n - n - 1$ internal vertices.*

Proof. If we connect the left and right bound together at both the top and the bottom, then any bounded Venn diagram of n curves can be viewed as a planar graph where each of the $2n$ boundary vertices has degree three. Let V, F and E be the number of vertices, faces and edges of the graph and let v be the number of internal vertices. Since the diagram is simple, then the degree of each internal vertex is four. By Euler's formula, $F + V = E + 2$, where

$$V = 2n + v \quad \text{and} \quad E = \frac{4v + 6n}{2} = 2v + 3n \quad \text{and} \quad F = 2^n + 1.$$

Substituting V, E and F by the equivalent values from the above equations we have

$$2^n + 1 + 2n + v = 2v + 3n + 2.$$

Therefore $v = 2^n - n - 1$. □

Theorem 5.2.4. *There is no involutional simple bounded 3-Venn diagram.*

Proof. Suppose there is an involutional simple bounded Venn diagram Δ of three curves. Then by Lemma 5.2.2 the only possible involution of Δ is (1 3)(2) which implies that each pair of curves intersect in an odd number of points. So Δ must have an odd number of internal vertices which is a contradiction since Lemma 5.2.3 implies that a simple bounded 3-Venn diagram has four internal vertices. □

5.3 Symmetric Venn diagrams with isometry group of order eight

In his 1984 paper on Venn diagrams [57], Peter Winkler wrote "in a sense, no inductive construction can possibly fail." The reason is that if you manage to add a curve C to an existing $(n-1)$-Venn diagram to obtain an n-Venn diagram, then you can follow curve C, alternately bisecting the regions on either side, to obtain an $(n+1)$-Venn diagram. The same observation is true about bounded Venn diagrams. But such a one-curve-at-a-time construction could never be used to create a half-turn symmetric simple bounded Venn diagram because every curve would have to pass through the central point, destroying simplicity. However, below we show how to inductively add pairs of curves that avoid the central point and which are symmetric.

Given an involutional simple bounded Venn diagram, the following lemma shows how to construct a simple Venn diagram with 4-fold rotational symmetry on the sphere.

Lemma 5.3.1. *Let V be a simple bounded Venn diagram of n curves with no non-trivial isometries and with permutation ρ such that $\rho^4 = id$. There exists a simple spherical Venn diagram V' of $n+2$ curves with 4-fold rotational symmetry about the polar axis such that V is the fundamental domain of the cylindrical representation of V'.*

Proof. A 2-Venn diagram can be projected onto the sphere so that the two curves are two great circles that intersect each other perpendicularly at the two poles (see Figure 5.3). The diagram then has 4-fold rotational symmetry about an axis through the poles. Given a bounded Venn diagram V with permutation ρ, if we add a copy of V to each region of the 2-Venn diagram replacing the left and right bounds of V with the segments of the two initial curves that bound the region, then we will get

an $(n+2)$-Venn diagram V' with 4-fold rotational symmetry. The bounded Venn diagram V has no nontrivial isometries and therefore, V is the fundamental domain of the cylindrical representation of V'. □

By Lemma 5.3.1, an involutional bounded Venn diagram can be used to construct a symmetric Venn diagram on the sphere with isometry group order four. Symmetry of the bounded Venn diagram itself can give constructions of Venn diagrams with higher order of symmetry. In this section, we give general constructions of symmetric involutional bounded n-Venn diagrams, treating the n even and n odd cases separately.

Symmetric involutional bounded n-Venn diagrams with n even

Figure 5.5(a) shows a simple symmetric involutional bounded 2-Venn diagram. With this diagram as an illustration we provide a general construction of involutional simple symmetric n-Venn diagrams when n is even.

Lemma 5.3.2. *For any even number $n = 2k$, with $k \geq 1$, there is an involutional simple symmetric bounded n-Venn diagram.*

Proof. For $k = 1$, an involutional simple symmetric bounded Venn diagram is shown in Figure 5.5(a). The involution is (1 2).

Adding two curves at each step, we show below how to inductively extend this $(2k)$-Venn diagram to an involutional simple symmetric bounded $(2k+2)$-Venn diagram. Figure 5.5(b) shows an extension of the diagram of Figure 5.5(a) to a simple involutional bounded 4-Venn diagram; this diagram is the basis of our induction. Let x denote the central point where C_1 and C_2 intersect. The two areas in the figure below/above C_2 map to each other by a rotation of π radians about x. So the diagram is symmetric as well. We then add pairs of additional curves as illustrated in Figures 5.5(c) through 5.5(e).

Our main focus is on the triangular area below C_2, which we denote as Δ and which is shaded in Figure 5.5(b). The portion of the curve C_j lying in Δ is denoted $\bar{C}_j$. In our construction Δ itself should be regarded as a bounded Venn diagram, in which C_2 forms the left bound (but with the intersection of C_2 with R removed. We use the notation Δ_i to denote Δ after curve $\bar{C}_i$ has been added to it.

The curves of the pair are added one at a time; the first added curve, which will have an even index, starts at a point like u which lies on C_2 below the x but above all

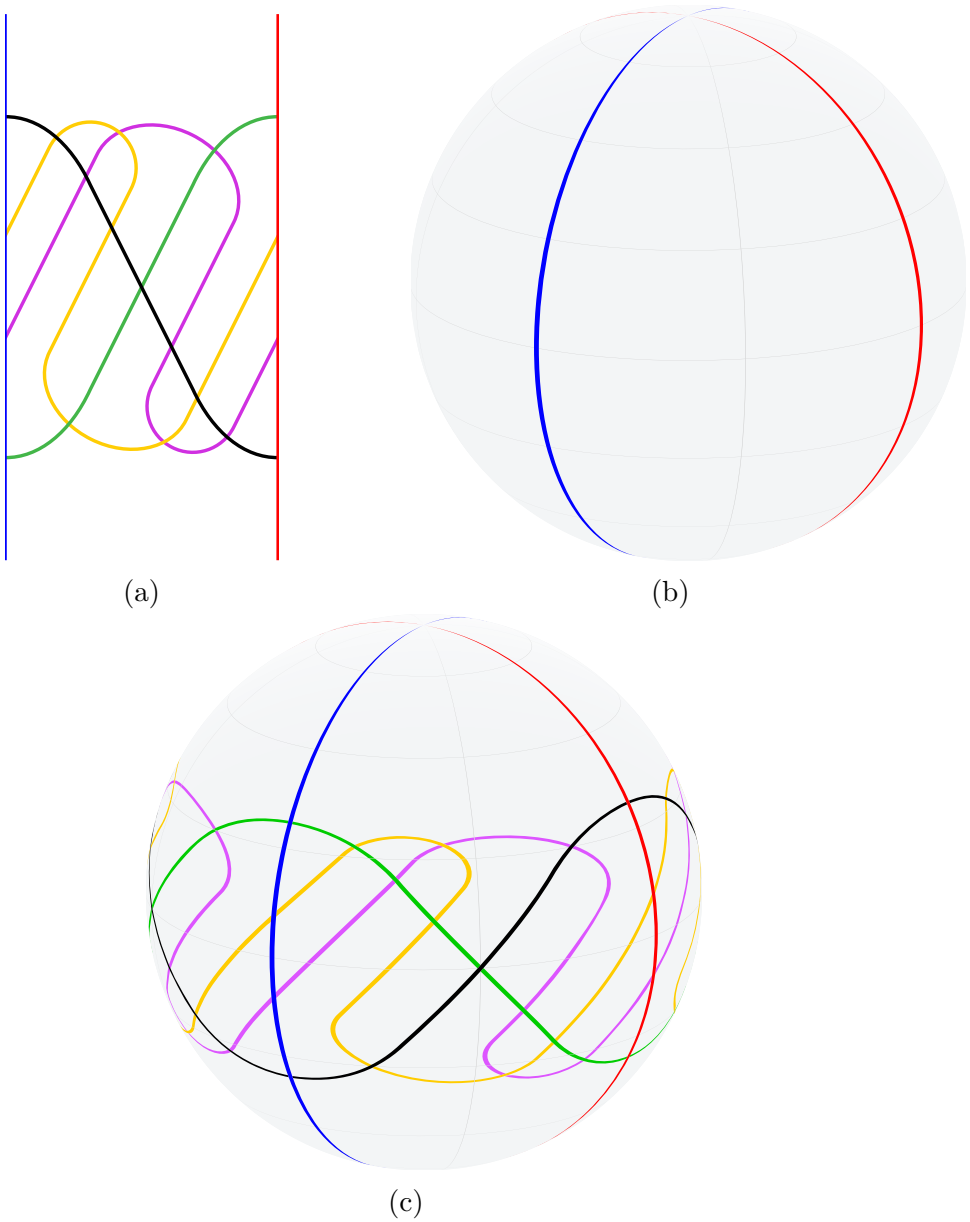

(a) (b)

(c)

Figure 5.3: Constructing a simple spherical Venn diagram with 4-fold rotational symmetry using a bounded Venn diagram V where $\rho^4(V) = id$.

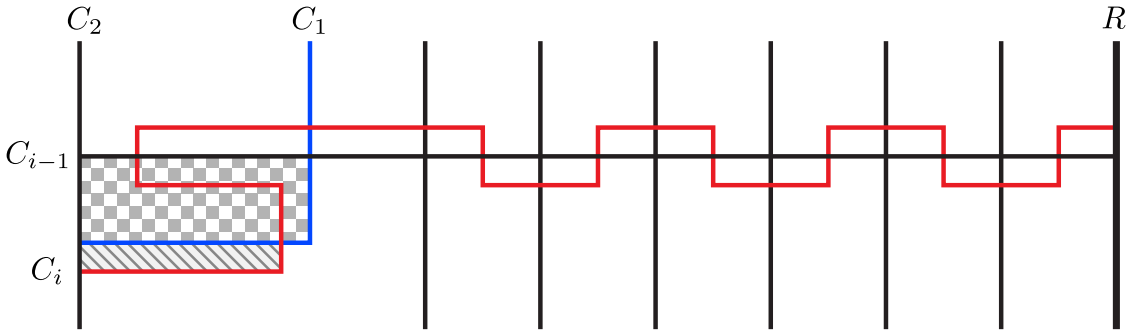

Figure 5.4: Adding curve C_i, for i odd. For i even, flip this diagram horizontally.

other curves. Similarly, the second added curve, which will have odd index, starts at a point like v which lies on C_2 but above the central point and again with no curve intersections between x and v.

It mainly uses the follow-the-last-added-curve approach, but there is a slight twist at the beginning. Imagine that the last added curve is C_{i-1} and we are now adding C_i. Stretch C_{i-1} so that it is a horizontal line segment, as shown in Figure 5.4, which also shows how C_i is added to the diagram. The checkerboard shaded region is a 3-face, bounded by C_1, C_2, C_{i-1}. We expand the inductive hypothesis to include the existence of this face. We will also assume inductively that C_{i-1} has a curve segment lying on every face of Δ.

The red curve C_i is added as shown. Clearly, given that C_{i-1} has a segment lying on every face, C_i bisects each region of Δ_{i-1} and therefore C_i will have a segment lying on each region. Therefore, if Δ_{i-1} is a bounded Venn diagram, then so is Δ_i. Also note that there is now a 3-face, the diagonally shaded region, bounded by C_1, C_2, C_i. *Ignoring* C_1, we observe inductively that the permutation induced by Δ is $(3\ 4)(5\ 6)\cdots(2k{-}1\ 2k)$.

Algorithm AddCurve(i, w_i) adds a new curve C_i to Δ_{i-1} starting at point w_i, using the method outlined above. It also returns the sequence of intersections with curve C_i that occur as a sequence $S_i[0..\ell_i]$. For example, referring to Figures 5.5(b) and 5.5(c), $S_4 = (C_1, C_3, C_1)$ and $S_5 = (C_1, C_4, C_1, C_3, C_4, C_1, C_4)$. Since C_i has one segment on each region of Δ_i we know that $\ell_i = 2^{i-2} - 1$.

Algorithm BVennEven uses Algorithm AddCurve to inductively extend the base case diagram of Figure 5.5(b) to the final involutional symmetric bounded $n{-}$Venn diagram. Figures 5.5(c) through 5.5(e) illustrate the first iteration of the algorithm to get an involutional simple symmetric bounded 6-Venn diagram.

Algorithm AddCurve(i, w) : Adding curve i to Δ starting at w.

Starting at w, draw $\bar{C}_i$ parallel to $\bar{C}_{i-1}$, then across C_1;
Draw $\bar{C}_i$ parallel to $\bar{C}_{i-1}$, then across $\bar{C}_{i-1}$;
Draw $\bar{C}_i$ parallel to $\bar{C}_{i-1}$, then across C_1
$S_i[1..3] \leftarrow (1, i-1, 1)$; $\ell_i \leftarrow 3$;
for $j \leftarrow 2$ to ℓ_{i-1} **do**
    $X \leftarrow S_{i-1}[j]$;
    Draw C_i parallel to C_{i-1} in the current region, then across X;
    Draw C_i through the region, then across C_{i-1};
    $S_i[\ell_i + 1] \leftarrow X$; $S_i[\ell_i + 2] \leftarrow C_{i-1}$; $\ell_i \leftarrow \ell_i + 2$;
end for
return (S_i, ℓ_i);

Algorithm BVennEven(k) : Inductive construction of involutional simple symmetric bounded n-Venn diagram for n even. $(n = 2k)$

$S_4 \leftarrow [C_1, C_3, C_1]$; $\ell_4 \leftarrow 3$;
for $i = 3$ to k **do**
    Start C_{2i-1} at some point u on C_2 below C_1 and above C_{2i-3};
    $(S_{2i-1}, \ell_{2i-1}) \leftarrow AddCurve(2i-1, u)$;
    Pass C_{2i-1} through the last region and connect it to right bound;
    Start C_{2i} at point $v = H(u)$ on C_2 above C_1 and below C_{2i-2};
    $(S_{2i}, \ell_{2i}) \leftarrow AddCurve(2i, v)$;
    Pass C_{2i} through the last region and connect it to right bound;
    Add $H(C_{2i-1})$ to the diagram as the continuation of C_{2i} and add $H(C_{2i})$ as the continuation of C_{2i-1}.
end for

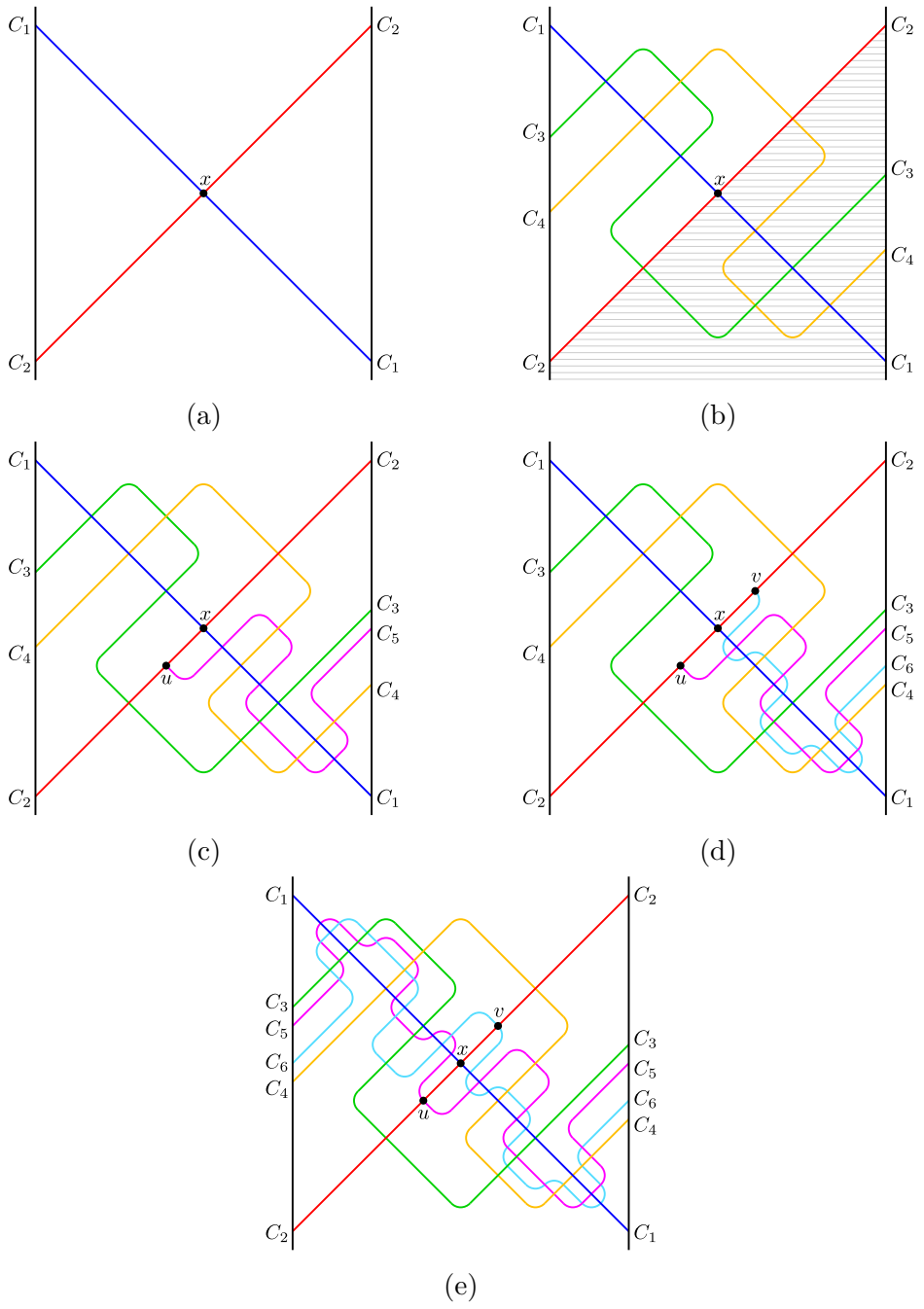

Figure 5.5: Inductive construction of an involutional simple symmetric bounded Venn diagram. (a) Bounded 2-Venn diagram. (b) Bounded 4-Venn diagram, the base case of our construction. (c) Adding half of C_{2i-1}. (d) Adding half of C_{2i}. (e) Adding $H(C_{2i-1})$ and $H(C_{2i})$.

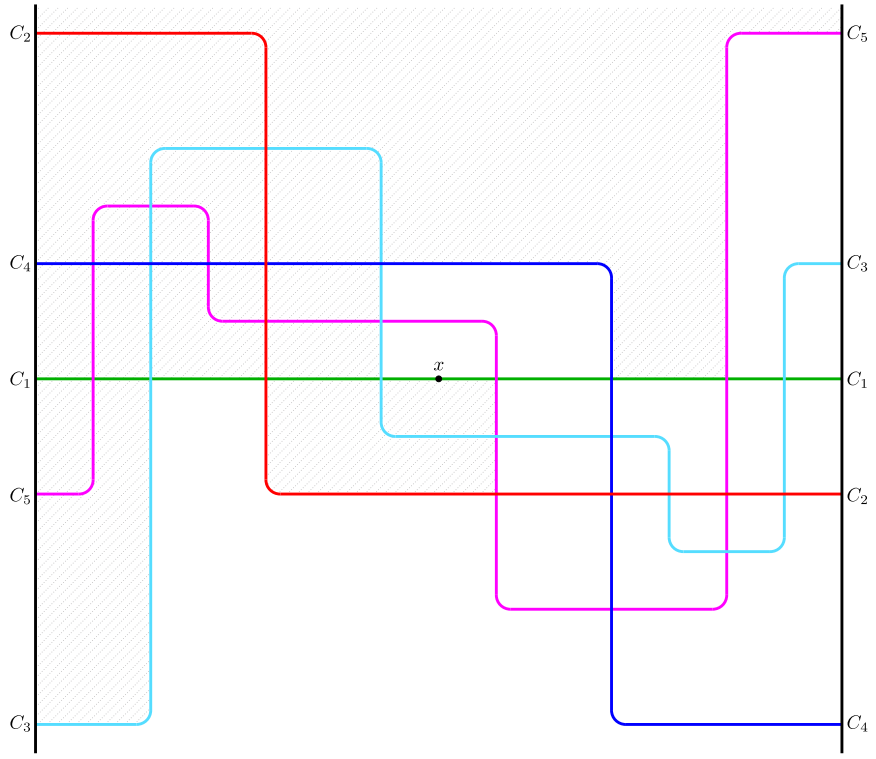

Figure 5.6: An involutional simple symmetric bounded 5-Venn diagram.

Recall that the permutation induced by Δ, ignoring C_1, is $(3\ 4)(5\ 6)\cdots(2k{-}1\ 2k)$. Thus after joining the curves of Δ and $H(\Delta)$, we are left with the identity. Since curves C_1 and C_2 are in a 2-cycle, the overall permutation is an involution. □

Symmetric involutional bounded n-Venn diagrams with n odd

We proved by Theorem 5.2.4 that there are no involutional simple bounded 3-Venn diagrams. However, using an exhaustive search program we found an involutional simple symmetric bounded 5-Venn diagram (Figure 5.6). The following lemma shows how to inductively extend this diagram to an involutional simple bounded $(2k+1)$-Venn diagram while preserving the half turn symmetry, for any $k > 2$.

Lemma 5.3.3. *For any odd number $n = 2k+1, k \geq 2$, there is an involutional simple symmetric bounded n-Venn diagram.*

Proof. For $k = 2$ there is an involutional simple symmetric bounded Venn diagram which is shown in Figure 5.6. Figure 5.7 shows the extension of the involutional bounded 5-Venn diagram of Figure 5.6 to a diagram with seven curves. The two new

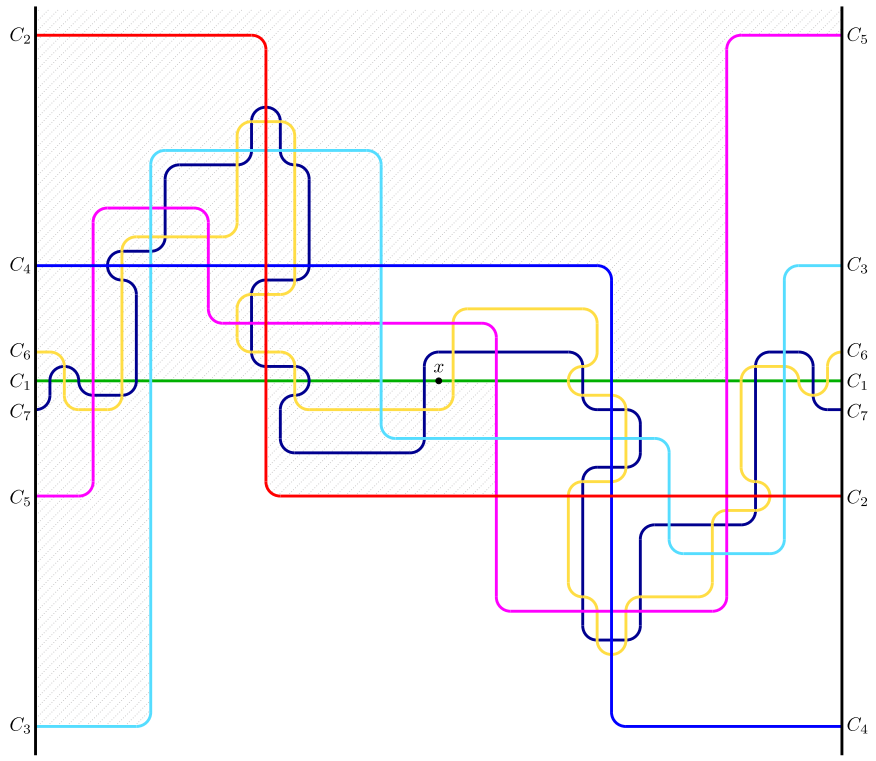

Figure 5.7: An involutional simple symmetric bounded 7-Venn diagram, the base case diagram of our construction for an odd number of curves.

curves divide each region of the bounded 5-Venn diagram into four distinct regions and thus the new diagram is a simple bounded 7-Venn diagram. The associated permutation of the new diagram is (1 6)(2 7)(3)(4)(5). So it is involutional and it has the half-turn symmetry as well, because the two specified parts of the diagram map to each other under the rotation by 180 degrees. We show how to inductively extend this diagram to an involutional simple symmetric bounded $(2k+1)$-Venn diagram, for $k > 3$ using the same sort of ideas that were used in the proof for the n even case.

Here we will use Δ to denote the shaded area in Figures 5.6 and 5.7 and we will use $\bar{C}_j$ to denote that part of C_j that is contained in Δ. The reason that we are using the 7-Venn diagram instead of the 5-Venn diagram is that C_7 has no segment on the boundary of Δ but C_5 does. Furthermore, it is easy to verify that $\bar{C}_7$ in Figure 5.7 bisects every region of Δ_6. Thus we can apply the same sort of curve-adding technique that was used in the proof of Lemma 5.3.2 to the current situation. In fact, Figure 5.4 applies again except that the left vertical line is L and the right vertical line is the remaining boundary of Δ, although the only part of that boundary that will be used is the central segment of C_1.

Using the AddCurve algorithm, similar to the even case but with left bound instead of C_2, Algorithm BVennOdd extends this diagram to the final involutional simple symmetric bounded n-Venn diagram.

Algorithm BVennOdd(k)

$S_7 \leftarrow [C_1, C_6, C_1, C_5, C_6, C_1, C_6, C_4, C_6, C_3, C_6, C_5, C_6, C_3, C_6,$
$C_2, C_6, C_3, C_6, C_4, C_6, C_2, C_6, C_5, C_6, C_2, C_6, C_1, C_6, C_3, C_6]$;
$\ell_7 \leftarrow 31$;
for $i = 4$ to k **do**
Start C_{2i} at some point u on left bound above C_1 and below C_{2i-2};
$(S_{2i}, \ell_{2i}) \leftarrow AddCurve(2i)$;
Pass C_{2i} through the last region and connect it to some point s on C_1;
Start C_{2i+1} at point $v = H(u)$ on left bound below C_1 and above C_{2i-1};
$(S_{2i+1}, \ell_{2i+1}) \leftarrow AddCurve(2i+1)$;
Pass C_{2i+1} through the last region and connect it to point $t = H(s)$ on C_1;
Add $H(C_{2i}$ as continuation of C_{2i+1} and add $H(C_{2i+1})$ as continuation of C_{2i};
end for

So given an involutional symmetric bounded Venn diagram before an iteration, it is extended to an involutional symmetric bounded Venn diagram with two more curves. Since the algorithm starts with seven curves, after $k-3$ iterations we will get an involutional symmetric bounded $(2k+1)$-Venn diagram. The associated involution of the final diagram is $(1, n-1)(2, n)(3)(4)\cdots(n-2)$. □

As we saw earlier, given an involutional bounded n-Venn diagram one can get an $(n+2)$-Venn diagram with symmetry group of order four on the sphere either using Edwards's flipping method (not to be confused with Edwards's construction) or by Lemma 5.3.1. Except for $n = 1$ and $n = 2$, the results in each of the two cases are different. Now let S be a sphere of unit radius. Given an involutional symmetric bounded n-Venn diagram D, let V_1 and V_2 be two $(n+2)$-Venn diagrams on S resulting from D using Edwards's flipping method and Lemma 5.3.1, respectively. Consider a mapping f, such that for any point $p \in S$ with latitude ϕ and longitude θ, $f(\phi, \theta) = (-\phi, \pi/2 - \theta)$. Because of the half-turn symmetry of D, both V_1 and V_2 are invariant under the mapping f up to relabeling of the curves. Therefore, they both have symmetry group order eight. As an example, Figure 5.8 shows the cylindrical projection of the two constructed symmetric 6-Venn diagrams.

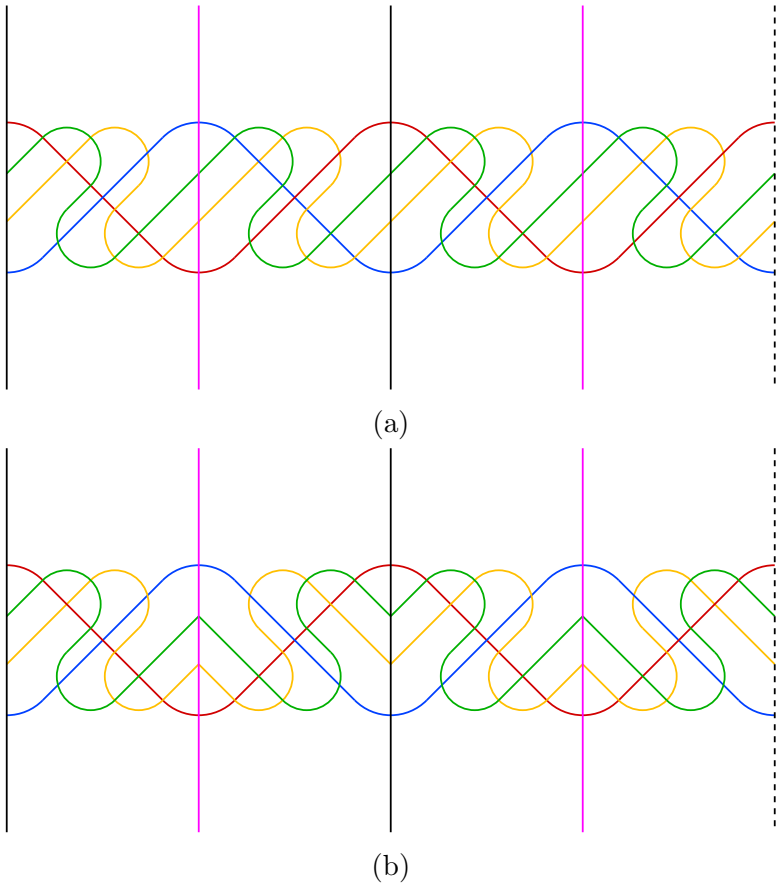

(a)

(b)

Figure 5.8: Cylindrical projections of simple symmetric 6-Venn diagrams with isometry group of order 8 using diagram of Figure 5.5(b): (a) a 6-Venn diagram with 4-fold rotational symmetry; (b) a 6-Venn diagram with two reflectional symmetries.

5.4 Concluding remarks for this chapter

Bounded Venn diagrams generalize Edwards's construction of simple Venn diagrams with symmetry group order four on the sphere. We showed here that involutional bounded Venn diagrams are fundamental domains which can be used for constructing symmetric Venn diagrams with 4-fold rotational symmetry. We provided separate constructions of involutional simple bounded n-Venn diagrams for even and odd cases by Lemma 5.3.2 and Lemma 5.3.3 respectively, where $n \neq 3$. The resulting bounded Venn diagrams in both cases have 2-fold symmetry which proves the existence of simple symmetric $(n+2)$-Venn diagrams with isometry groups of order eight.

Theorem 5.4.1. *There exists a simple symmetric n-Venn diagram on the sphere with isometry group of order 8 for $n = 2, 3, 4$ or $n \geq 6$.*

Note that the planar dual of a simple n-Venn diagram is a maximal spanning subgraph of the n-dimensional hypercube. Symmetries are preserved with primal/dual transitions. Therefore, by Theorem 5.4.1, we can equivalently say that, for any $n \neq 3$, there exists a maximal planar spanning subgraph of the $(n+2)$-dimensional hypercube with an automorphism of order eight.

Chapter 6

Simple symmetric Venn diagrams with crosscut symmetry

In this chapter we introduce a new property of Venn diagrams called *crosscut symmetry*, which is related to dihedral symmetry. Utilizing a computer search restricted to crosscut symmetry we found many simple symmetric Venn diagrams with 11 and 13 curves, which answers an existence question that has been open since the 1960's [46].

6.1 Crosscut symmetry

We define a *crosscut* of a Venn diagram as a segment of a curve that extends from the innermost region to the outermost region and "cuts" (i.e., intersects) every other curve exactly once. Except for $n = 2$ and $n = 3$, where the symmetric 2-Venn and 3-Venn diagrams have four and six crosscuts respectively, a symmetric n-Venn diagram either has n crosscuts or it has none. Referring to Figure 6.1(a), notice that each of the seven curves has a crosscut.

Lemma 6.1.1. *If $n > 3$, then a symmetric n-Venn diagram has at most one crosscut per curve.*

Proof. A curve of a Venn diagram touches a face at most once. Thus a curve in any Venn diagram cannot have three or more crosscuts, because that curve would touch the outer face (and the innermost face) at least twice. Now suppose that some curve C in an n-Venn diagram has two crosscuts. Then those crosscuts must start at the same segment of C on the outer face, and finish at the same segment of C on the innermost face. Thus, curve C contains exactly $2(n-1)$ intersections with the other

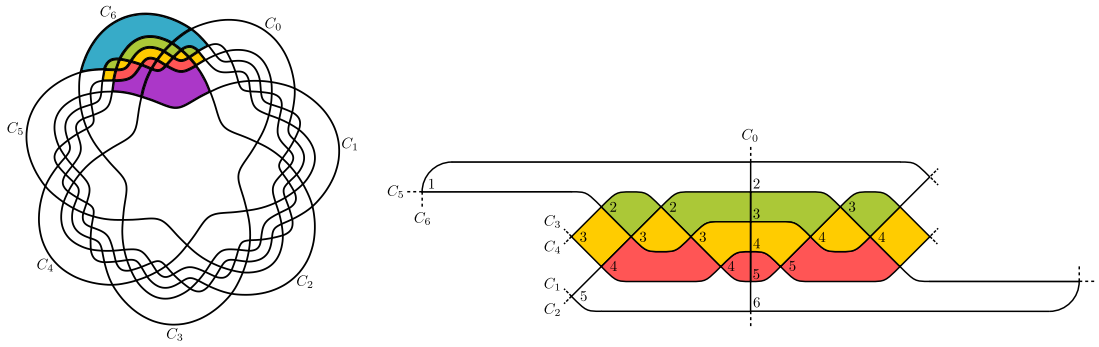

(a) (b)

Figure 6.1: (a) A simple rotationally symmetric monotone 7-Venn diagram with a cluster colored (shaded). (b) The cylindrical representation of the colored cluster of the diagram in (a), showing the reflective aspect of crosscut symmetry.

curves. If the Venn diagram is symmetric, then there must be a total of $n(n-1)$ intersection points. On the other hand, a simple symmetric Venn diagram has exactly $2^n - 2$ intersection points. Since $n(n-1) = 2^n - 2$ has a solution for $n = 1, 2, 3$, but not for $n > 3$, the lemma is proved. □

A *clump* in a Venn diagram is a collection of regions that is bounded by a simple closed path of curve segments. The *size* of a clump is the number of regions that it contains. Aside from the innermost face and the outermost face, a rotationally symmetric n-Venn diagram can be partitioned into n congruent clumps, each of size $(2^n - 2)/n$; in this case we call the clump a *cluster* — it is like a fundamental region for the rotation, but omitting the parts of the fundamental region corresponding to the full set and to the empty set. Referring again to Figure 6.1(a), a cluster has been shaded, and this cluster is redrawn in Figure 6.1(b) minus the coloring of the two topmost and the two bottommost regions. Notice that the cluster of Figure 6.1(b) has a central shaded section which has a reflective symmetry about the crosscut. The essential aspects of this reflective symmetry are embodied in the definition of crosscut symmetry, given below.

Definition 6.1.1. Given a rotationally symmetric n-Venn diagram, we label the curves as $C_0, C_1, \ldots, C_{n-1}$ according to the clockwise order in which they touch the unbounded outermost face. Assume that we have a cluster with the property that every curve intersects the cluster in a segment and that S_k denotes the cluster that contain the crosscut for curve C_k. Let $L_{i,k}$ be the list of curves that we encounter as we follow C_i in the cluster S_k in clockwise order, and let $\ell_{i,k}$ denote the length of

$L_{i,k}$. A rotationally symmetric n-Venn diagram has *crosscut symmetry* if it can be partitioned into n such clusters $S_0, S_1, \ldots, S_{n-1}$ in such a way that for every cluster S_k, for any $i \neq k$, the list $L_{i,k}$ is palindromic, that is, for $1 \leq j \leq \ell_{i,k}$, we have $L_{i,k}[j] = L_{i,k}[\ell_{i,k} - j + 1]$.

Figure 6.1(a) shows a simple rotationally symmetric 7-Venn diagram which also has crosscut symmetry. In the Survey of Venn diagrams it is known as M_4 [46]. There is only one other simple 7-Venn diagram with crosscut symmetry; it is dubbed "Hamilton" by Edwards [14]. Hamilton also has "polar symmetry" but is not used here as an example because it might cause confusion with the crosscut symmetry. Cluster S_1 of the diagram is shown in Figure6.1(b) where a segment of C_1 is the crosscut. The list of crossing curves for each curve in the cluster S_1 is shown below.

$$
\begin{aligned}
L_{0,0} &= [C_1, C_4, C_3, C_5, C_2, C_6] \\
L_{1,0} &= [C_2, C_0, C_2] \\
L_{2,0} &= [C_1, C_3, C_5, C_4, C_0, C_4, C_5, C_3, C_1] \\
L_{3,0} &= [C_4, C_2, C_4, C_0, C_4, C_2, C_4] \\
L_{4,0} &= [C_3, C_5, C_2, C_5, C_3, C_0, C_3, C_5, C_2, C_5, C_3] \\
L_{5,0} &= [C_6, C_4, C_2, C_4, C_0, C_4, C_2, C_4, C_6] \\
L_{6,0} &= [C_5, C_0, C_5]
\end{aligned}
$$

Recall the crossing sequence definition from Chapter 3 for representing simple monotone Venn diagrams. For a simple rotationally symmetric n-Venn diagram, the first $(2^n - 2)/n$ elements of the crossing sequence are enough to represent the entire diagram; the remainder of the crossing sequence is formed by $n - 1$ concatenations of this sequence. For example, the first $18 = (2^7 - 2)/7$ elements of the crossing sequence for 7-Venn diagram of Figure 6.1(a) could be the following list; we write "could" here since crossings can sometimes occur in different orders and still represent the same diagram (e.g., taking $\rho = 3, 1, 5, 2, 4$ gives the same diagram); see Remark 6.1.2.

$$\underbrace{1, 3, 2, 5, 4}_{\rho}, \underbrace{3, 2, 3, 4}_{\alpha}, \underbrace{6, 5, 4, 3, 2}_{\delta}, \underbrace{5, 4, 3, 4}_{\alpha^{r+}}$$

We encourage the reader to verify that this sequence is correct by referring to the crossing numbers shown to the right of the intersections in Figure 6.1(b).

Remark 6.1.2. *If j, k is an adjacent pair in a crossing sequence $\mathcal{C}$ and $|j-k| > 1$, then the sequence $\mathcal{C}'$ obtained by replacing the pair j, k with the pair k, j is also a crossing sequence of the same diagram.*

Define function h as $h(n) = 2(\lceil n/2 \rceil - \lfloor n/2 \rfloor)$. Clearly, $h(n) = 2$ if n is odd and $h(n) = 0$ if n is even. We use this function to describe the crossing sequence of a simple monotone Venn diagram with rotational and crosscut symmetry in the following theorem.

Theorem 6.1.3. *A simple monotone rotationally symmetric n-Venn diagram is crosscut symmetric if and only if it can be represented by a crossing sequence of the form $\rho, \alpha, \delta, \alpha^{r+}$ where*

- *ρ is $1, 3, 2, 5, 4, \ldots, n-2, n-3$; that is, $\rho(1) = 1$ and $\rho(k) = k - h(k) + 1$, for $2 \leq k \leq n-2$.*
- *δ is $n-1, n-2, \ldots, 3, 2$.*
- *α and α^{r+} are two sequences of length $(2^{n-1} - (n-1)^2)/n$ such that α^{r+} is obtained by reversing α and adding 1 to each element; that is, $\alpha^{r+}[i] = \alpha[|\alpha| - i + 1] + 1$.*

Proof. Let V be a simple monotone rotationally symmetric n-Venn diagram with crosscut symmetry. Assume that the curves of V are labeled $C_0, C_1, \ldots, C_{n-1}$ according to their clockwise order of touching the outermost region. Consider a cluster of V where a segment of C_0 forms the crosscut. Each curve of the diagram touches the outermost and innermost region exactly once. Therefore, C_{n-1} only intersects C_{n-2} at some point u on the left border of the cluster before intersecting the crosscut. Since the diagram is crosscut symmetric, $L_{n-1,0} = [C_{n-2}, 0, C_{n-2}]$ and so C_{n-1} must intersect C_{n-2} at some point v on the right border of the cluster immediately below C_0. Because of the rotational symmetry of V, the point v is the image of some point s on the left border under the rotation of $2\pi/n$ about the center of the diagram. At the point s the curves C_{n-2} and C_{n-3} intersect. Again, because of the crosscut symmetry, $L_{n-2,0} = [C_{n-1}, C_{n-3}, \ldots, C_{n-3}, C_{n-1}]$, and so there is a corresponding point t on the right border where C_{n-2} and C_{n-3} intersect. Continuing in this way, we can see that the the left and right border of a crosscut symmetric n-Venn diagram must have the "zig-zag" shape as illustrated in Figure 6.2.

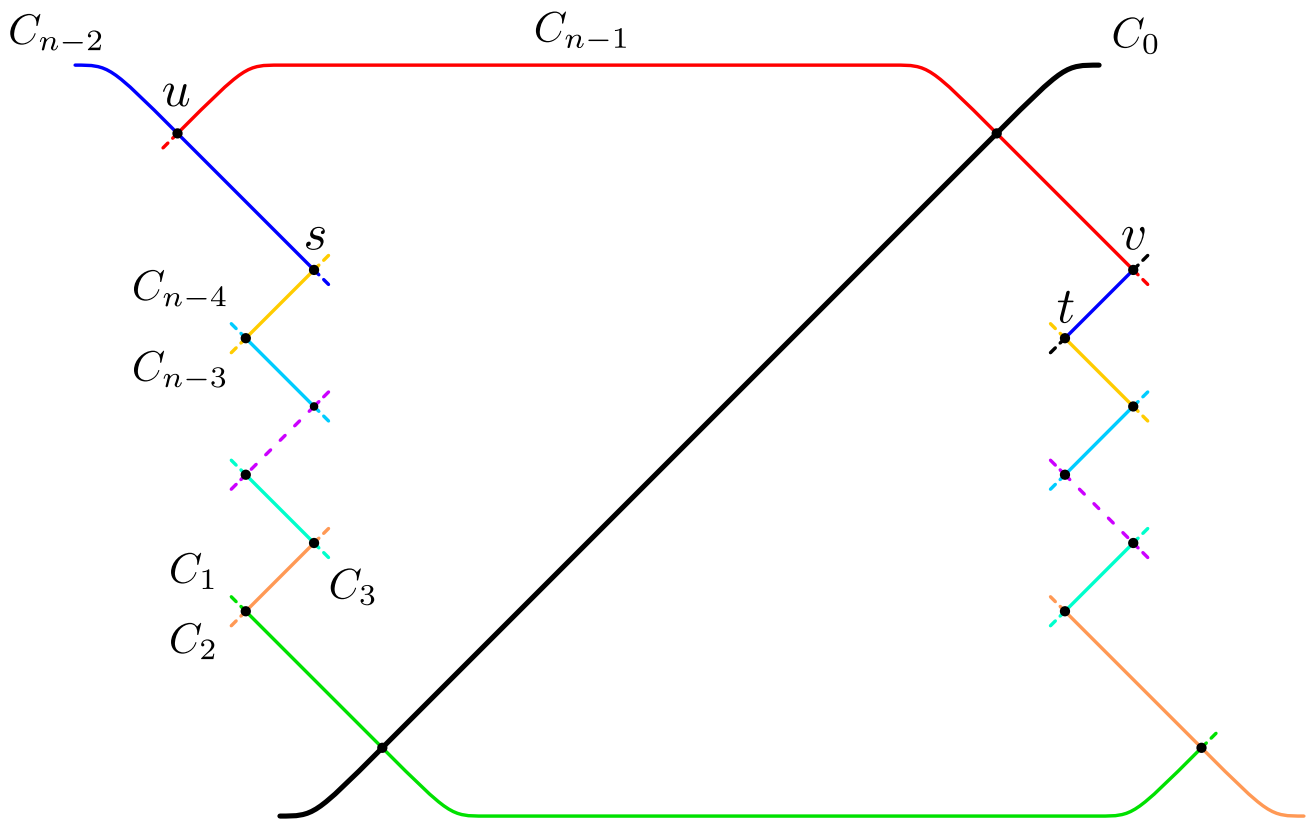

Figure 6.2: A cluster of a crosscut symmetric simple monotone n-Venn diagram (cylindrical representation).

Consider two rays issuing from the center of the diagram which cut all the curves immediately before the left zig-zag border and immediately after the right zig-zag border of the cluster. Let π and σ be the curve vectors along the rays as we move the rays in opposite directions towards the crosscut. We prove by induction that as long as the two rays do not intersect the crosscut, at each moment σ is a cyclic shift of π one element to right; therefore if $\pi(i)$ and $\pi(i-1)$ intersect on the left side, then $\sigma(i+1)$ and $\sigma(i)$ must also intersect on the right side. Initially π is the vector

$$[C_{n-2}, C_{n-1}, C_{n-4}, C_{n-3}, \ldots, C_1, C_2, C_0],$$

that is,

$$\pi(n-1) = C_0 \text{ and } \pi(k) = C_{n-k-2+h(k)}, \text{for } 0 \leq k \leq n-2,$$

and σ is the vector

$$[C_0, C_{n-2}, C_{n-1}, C_{n-4}, \ldots, C_4, C_1, C_2],$$

that is,

$$\sigma(0) = C_0 \text{ and } \sigma(k) = C_{n-k-h(k)+1}, \text{for } 1 \leq k \leq n-1.$$

According to the "zig-zag" shape of the borders, after $n-2$ crossings on the borders, π and σ will have the following values :

$$[C_{n-1}, C_{n-3}, C_{n-2}, C_{n-5}, \ldots, C_3, C_1, C_0],$$

that is,

$$\pi(0) = C_{n-1} \text{ and } \pi(k) = C_{n-k-h(k)}, \text{for } 1 \leq k \leq n-1,$$

and

$$[C_0, C_{n-1}, C_{n-3}, C_{n-2}, \ldots, C_2, C_3, C_1],$$

that is,

$$\sigma(0) = \pi(n-1) \text{ and } \sigma(k) = \pi(k-1), \text{ for } 1 \leq k \leq n-1.$$

Clearly, the $n-2$ crossings on the left border can be represented by the crossing sequence $\rho = 1, 3, 2, 5, 4, \ldots, n-2, n-3$.

Now suppose for any of the previous k intersection points, σ is always a cyclic rotation of π one element to the right and suppose the next crossing occurs between $\pi(i)$ and $\pi(i-1)$. Since $\pi(i) = \sigma(i+1)$ and $\pi(i-1) = \sigma(i)$ the next crossing on the right side of crosscut must occur between $\sigma(i+1)$ and $\sigma(i)$, for otherwise the diagram would not be crosscut symmetric. Thus, σ remains a cyclic shift of π by

one element to the right after the crossing. Therefore, by induction, each crossing of $\pi(i)$ and $\pi(i-1)$ corresponds to a crossing of $\sigma(i+1)$ and $\sigma(i)$. Let α represent the sequence of crossings that follow the first $n-2$ crossings that occur on the left border. Reversing the crossings of the right side of the crosscut, the entire crossing sequence of the cluster is

$$1,3,2,5,4,\ldots,n-2,n-3,\alpha,n-1,n-2,\ldots,2,1,\alpha^{r+},n-2,n-1,\ldots,5,6,3,4,2,$$

where $\alpha^{r+}[i] = \alpha[|\alpha| - i + 1] + 1$. Removing the $n-1$ elements representing the intersection points of the right border, we will get the required crossing sequence $\rho, \alpha, \delta, \alpha^{r+}$ of the diagram.

To prove the converse, suppose we are given a rotationally symmetric n-Venn diagram V with the crossing sequence $\rho, \alpha, \delta, \alpha^{r+}$ as specified in the statement of the theorem. Then the crossing sequence of one cluster of V is $\rho, \alpha, \delta, \alpha^{r+}, \rho, n-1$ where $\rho = [1,3,2,5,4,\ldots,n-2,n-3]$, and $\delta = [n-1,n-2,\ldots,3,2]$. The ρ sequence indicates that the cluster has the "zig-zag"-shaped borders. Therefore, by Remark 6.1.2, the crossing sequence of the cluster can be transformed into an equivalent crossing sequence

$$A = [1,3,2,\ldots,n{-}2,n{-}3,\alpha,n{-}1,n{-}2,\ldots,3,2,1,\alpha^{r+},n-2,n-3,\ldots,3,4,2].$$

Thus there is a crosscut in the cluster and

$$A\left[|A| - i + 1\right] = A[i] + 1, \qquad 1 \le i \le \frac{|A| - n + 1}{2}.$$

Using similar reasoning to the first part of the proof, it can be shown that at each pair of crossing points corresponding to $A[i]$ and $A[|A|-i+1]$, the same pair of curves intersect. So, for each curve C in the cluster as we move the rays along C in opposite directions, we encounter the same curves that intersect C and therefore the diagram is crosscut symmetric. □

Given a cluster S_i of a crosscut symmetric n-Venn diagram where a segment of C_i is the crosscut, there are the same number of regions on both sides of the crosscut. Furthermore, let r be a k-region in S_i that lies in the exterior of C_i and interior to the curves in some set $\mathcal{K}$; then there is a corresponding $(k+1)$-set region r' that is in the interior of C_i and also interior to the curves in $\mathcal{K}$.

6.2 Simple symmetric 11-Venn diagrams

By Theorem 6.1.3, having the subsequence α of a crossing sequence we can construct the corresponding simple monotone crosscut symmetric n-Venn diagram. Therefore, for small values of prime n, an exhaustive search of α sequences yield crosscut symmetric n-Venn diagrams. For example, for $n = 3$ and $n = 5$, α is empty and the only possible cases are the three circles Venn diagram and Grünbaum's 5-ellipses. For $n = 7$, the valid cases of α are $[3, 2, 4, 3]$ and $[3, 2, 3, 4]$ which correspond to Hamilton and M_4. The search algorithm is of the backtracking variety; for each possible case of α, we construct the crossing sequence $S = \rho, \alpha, \delta, \alpha^{r+}$, checking along the way whether it currently satisfies the Venn diagram constraints, and then doing a final check of whether S represents a valid rotationally symmetric Venn diagram. Using this algorithm for $n = 11$, we found more than 200,000 nonisomorphic simple monotone symmetric Venn diagrams, which settles a long-standing open problem.

Figure 6.3 shows the first simple symmetric 11-Venn diagram discovered. It was discovered on March of 2012, so following Anthony Edwards' tradition of naming symmetric diagrams [14], we name it "Newroz" which means "the new day" or "the new sun" and refers to the first days of spring in Kurdish/Persian culture; for English speakers, Newroz sounds also like "new rose", perhaps also an apt description.

Part of Newroz is magnified in Figure 6.4 to show more details. Below is the α sequence for Newroz. Given this sequence, by Theorem 6.1.3 one can construct a cluster of the diagram, which is shown in Figure 6.5.

$$[3,2,3,4,3,4,5,4,3,2,3,4,3,4,5,4,3,4,5,4,5,6,5,4,5,6,5,6,$$
$$7,6,5,4,3,2,5,4,3,4,6,5,4,5,6,7,6,7,8,7,6,5,6,5,4,3,4,5,$$
$$7,6,5,4,6,5,8,7,6,5,4,5,7,6,5,6,8,7,6,5,4,6,5,7,6,5,6,7.]$$

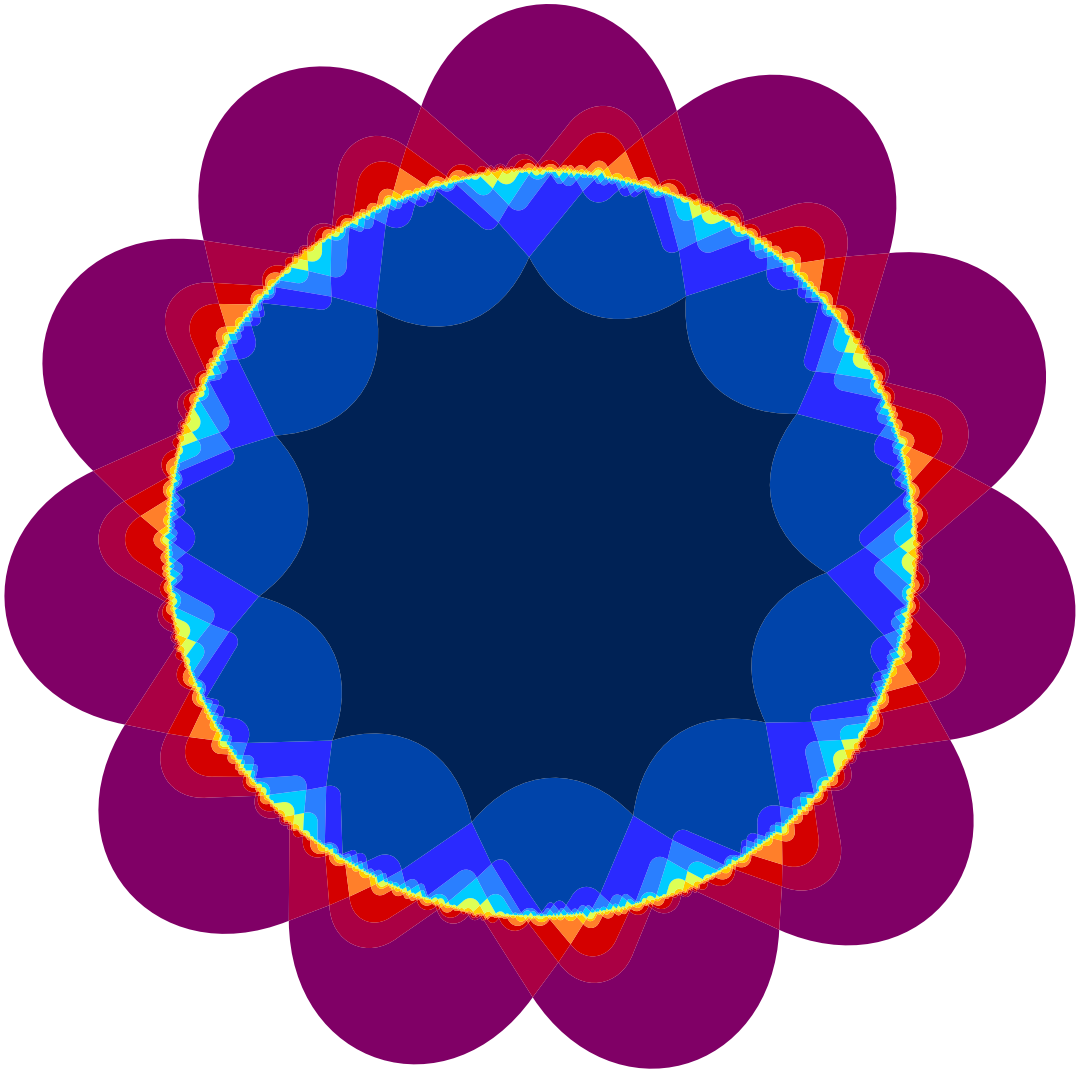

Figure 6.3: Newroz, the first simple symmetric 11-Venn diagram.

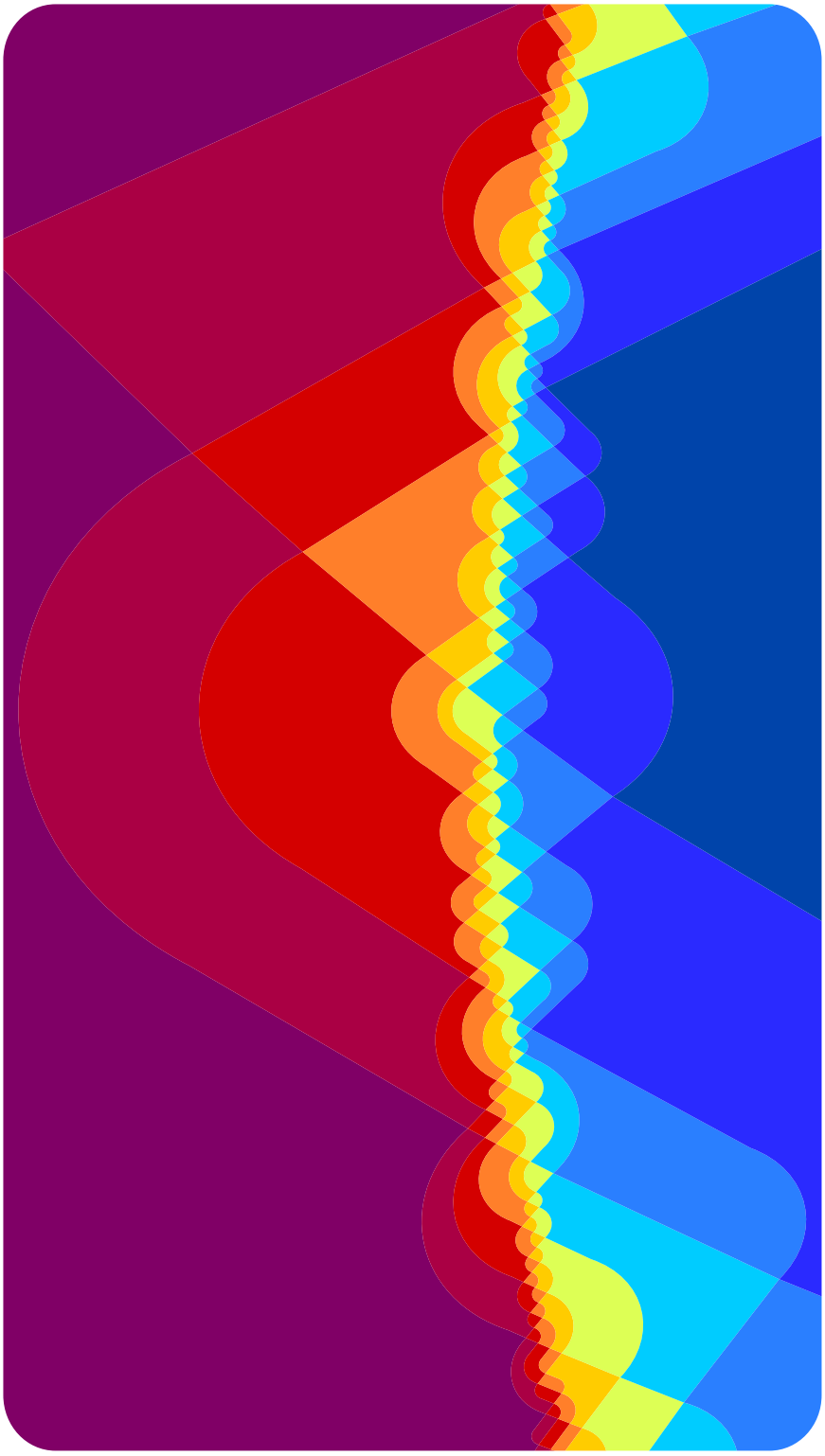

Figure 6.4: A blowup of part of Newroz

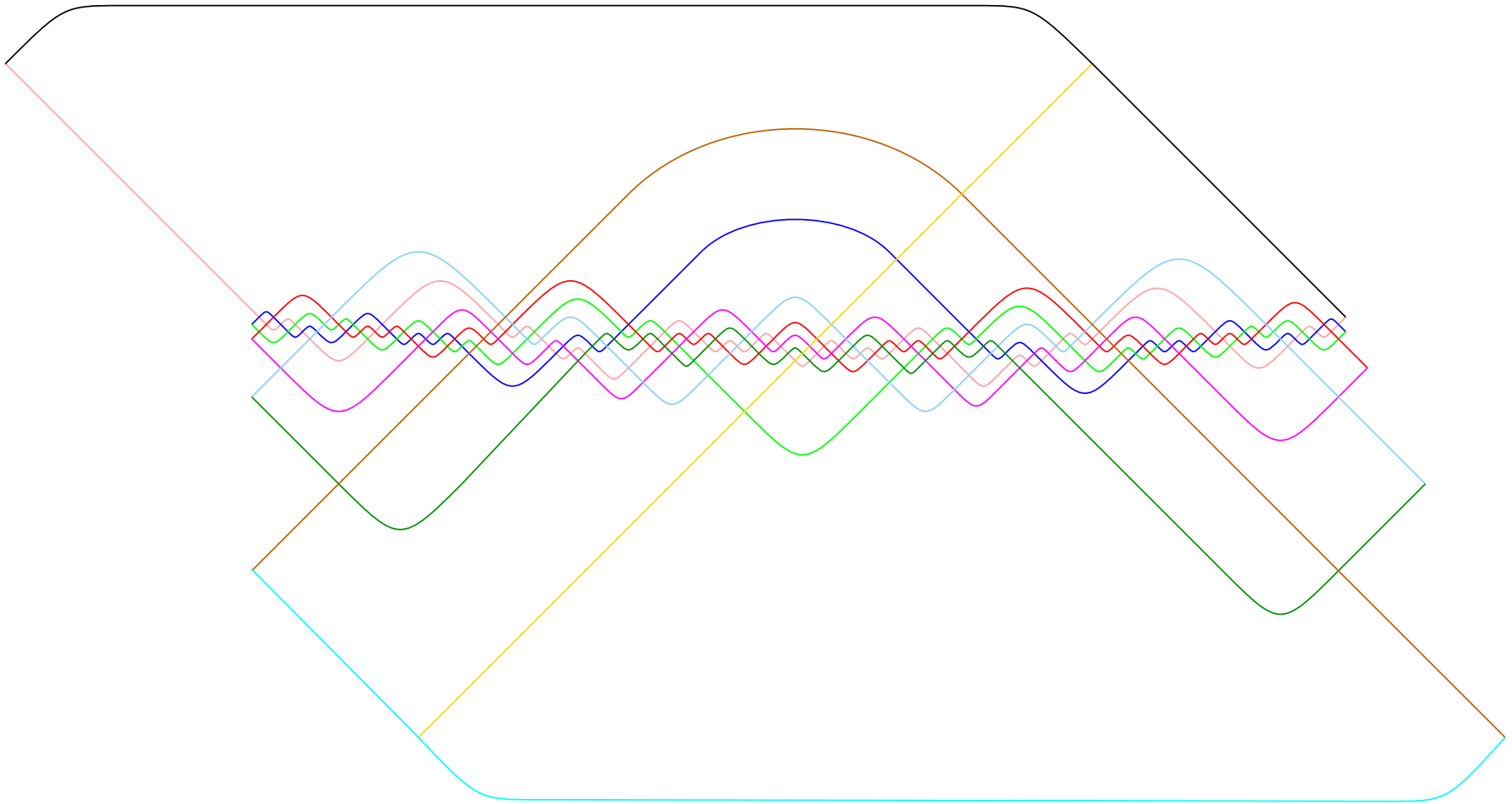

Figure 6.5: A cluster of Newroz, the first simple symmetric 11-Venn diagram.

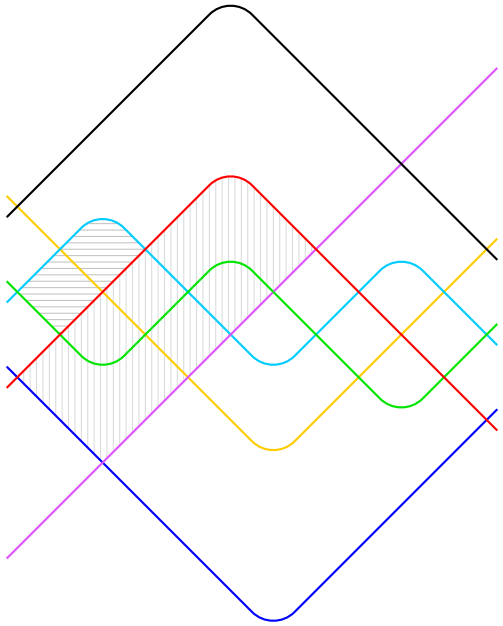

Figure 6.6: A cluster of simple symmetric 7-Venn diagram named Hamilton.

6.3 Iterated crosscut symmetry

Consider a cluster of the simple symmetric 7-Venn diagram Hamilton shown in Figure 6.6. In addition to the polar and crosscut symmetries, Hamilton has another interesting property which we call the *iterated crosscut symmetry*. As can be seen from the figure, a property similar to crosscut symmetry can be applied to the two shaded areas on the left side of the main crosscut. The horizontally shaded area contains two regions separated by a segment of the yellow curve as the crosscut. The crosscut of the vertically shaded area is a segment of the green curve intersecting the two parallel curve segments exactly once inside the shaded area.

Figure 6.7 shows the structure of the left side of a cluster of a simple symmetric n-Venn diagram with iterated crosscut symmetry. It consists of $\lfloor (n-2)/2 \rfloor$ stacked components, each one has its own crosscut symmetry, where the crosscut of the i-th component from the bottom of the stack is a segment of the curve with label $2(i+1)$.

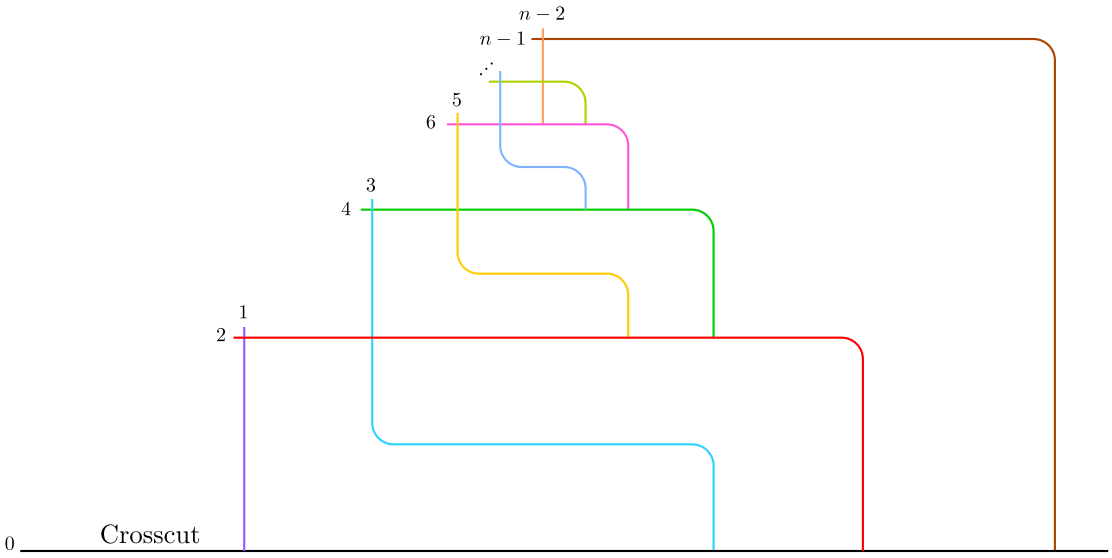

Figure 6.7: A general framework of the cluster of a simple symmetric Venn diagram with iterated crosscut symmetry.

Let $S_H = \rho_H, \alpha_H, \delta_H, \alpha_H^{r+}$ denote the crossing sequence of Hamilton where $\rho_H = 1,3,2,5,4$, $\alpha_H = 3,2,4,3$, $\delta_H = 6,5,4,3,2$ and $\alpha_H^{r+} = 4,5,3,4$. Using $\rho_H, \alpha_H, 7, \delta_H$ as a seed and restricting the backtracking search to the cases with iterated crosscut symmetry, we found several examples of simple symmetric 11-Venn diagrams with this property. Figure 6.8 shows one such 11-Venn diagram. The cylindrical representation of the cluster of the diagram is shown in Figure 6.9.

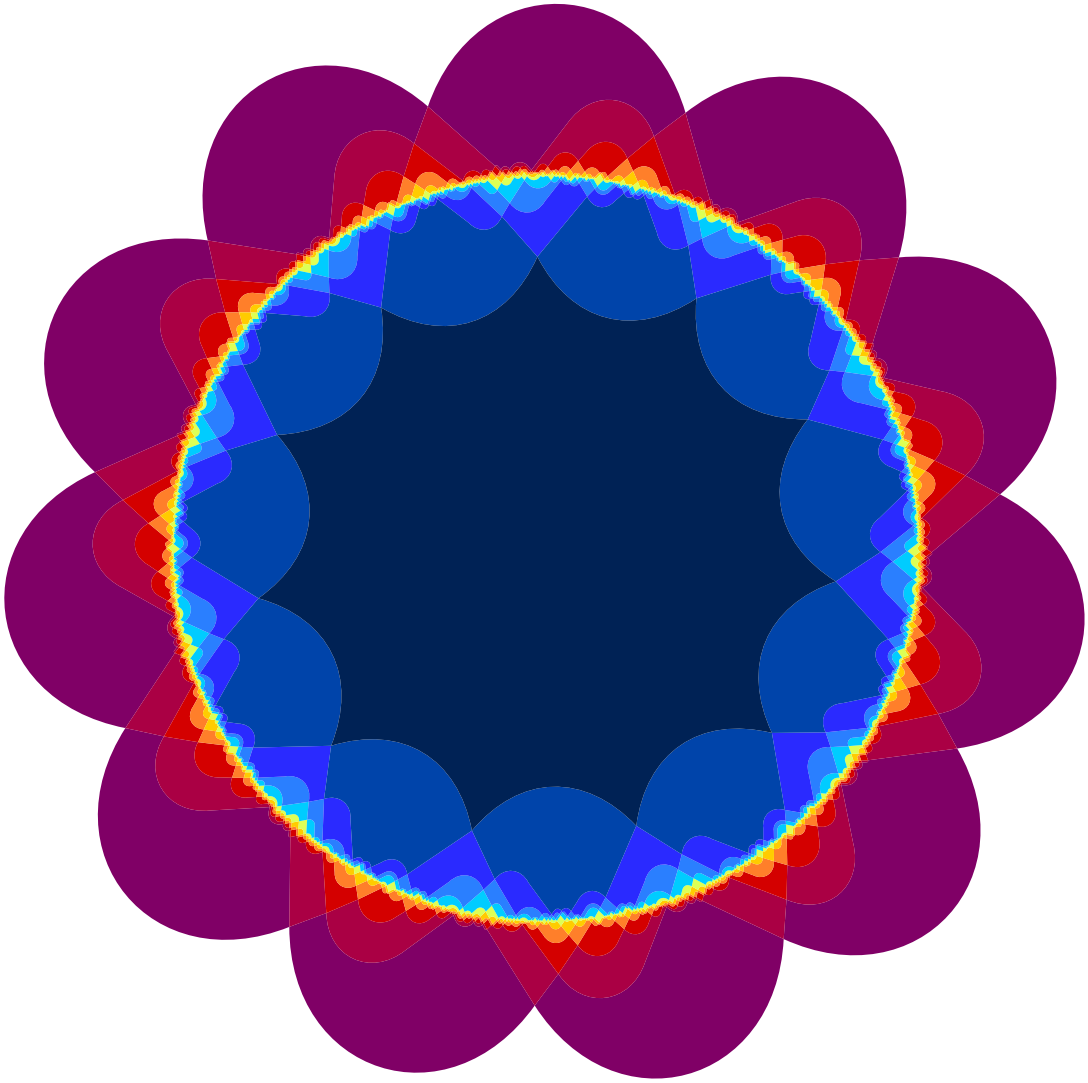

Figure 6.8: An example of a simple symmetric 11-Venn diagram with iterated crosscut symmetry.

Let $S_E = \rho_E, \alpha_E, \delta_E, \alpha_E^{r+}$ denote the crossing sequence of the diagram of Figure 6.8. Then by Figure 6.9 it is easy to verify that

$$\begin{aligned}\alpha_E = {} & 3,2,4,3,5,4,3,2,4,3,5,4,6,5,4,3,5,4,6,5,7,6,5,4,3,2,3,4,\\ & 3,4,5,4,5,6,5,4,3,6,5,6,5,4,5,4,7,6,5,4,6,5,7,6,8,7,6,5,\\ & 4,3,7,8,6,7,5,6,7,8,5,6,5,6,7,6,7,4,5,6,7,6,5,6,5,4,5,4.\end{aligned}$$

It is natural to ask if it is possible to find a simple symmetric 13-Venn diagram

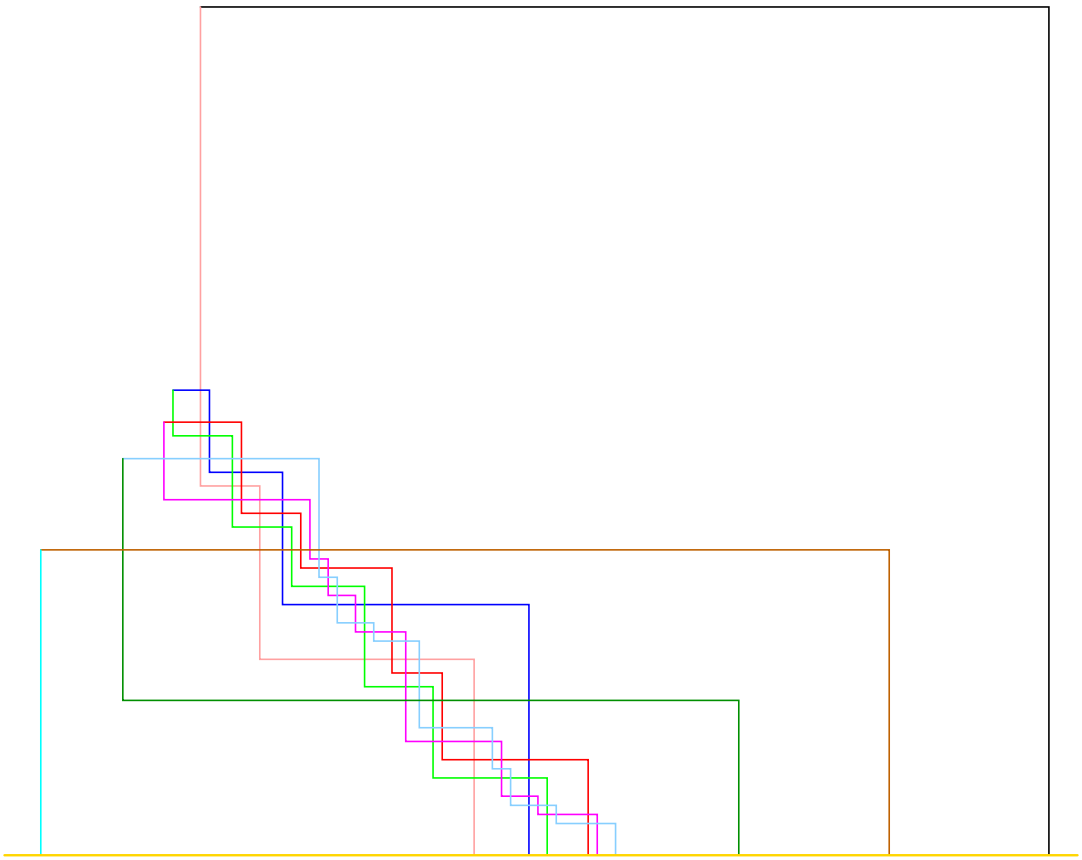

Figure 6.9: Left side of the cluster of a simple symmetric 11-Venn diagram with iterated crosscut symmetry.

using the same method that we used for searching simple symmetric 11-Venn diagrams with iterated crosscut symmetry. The answer is yes; applying the backtracking search using $\rho_E, \alpha_E, 11, \delta_E$ as a seed, we found more than 30,000 cases of simple symmetric 13-Venn diagrams that also have iterated crosscut symmetry.

The first simple symmetric 13-Venn diagram found with iterated crosscut symmetry is shown in Figure 6.10. Part of this diagram is magnified in Figure 6.11. The top four components of the iterated crosscut structure of the diagram, all together forming the first 93 regions of the cluster, come from the first half cluster of the symmetric 11-Venn diagram of Figure 6.9. This is because the α sequence of the 11-Venn diagram forms the first 84 elements of the α sequence of the 13-Venn diagram (see Table 6.1). The last component of the symmetric 13-Venn diagram, which contains $315 - 93 = 222$ regions, is shown in Figure 6.12.

$$
\begin{aligned}
\alpha_T = {} & 3,2,4,\ \ 3,5,4,3,2,4,\ \ 3,5,4,6,5,4,3,5,\ \ 4,6,5,7,6,5,4,3,2,\ \ 3,4,\\
& 3,4,5,\ \ 4,5,6,5,4,3,\ \ 6,5,6,5,4,5,4,7,\ \ 6,5,4,6,5,7,6,8,7,\ \ 6,5,\\
& 4,3,7,\ \ 8,6,7,5,6,7,\ \ 8,5,6,5,6,7,6,7,\ \ 4,5,6,7,6,5,6,5,4,\ \ 5,4,\\
& 9,8,7,\ \ 6,5,4,3,2,3,\ \ 4,3,4,5,4,5,6,5,\ \ 4,3,5,4,6,5,4,5,6,\ \ 7,6,\\
& 5,4,5,\ \ 6,5,6,7,6,5,\ \ 6,7,6,7,8,7,6,5,\ \ 4,3,5,4,6,5,7,6,5,\ \ 4,6,\\
& 5,7,6,\ \ 8,7,8,7,6,5,\ \ 4,5,6,7,6,5,4,7,\ \ 6,8,7,6,5,7,6,5,8,\ \ 7,6,\\
& 9,8,7,\ \ 6,5,4,8,7,8,\ \ 7,6,7,6,5,9,8,7,\ \ 6,8,7,6,5,9,8,7,6,10,9,\\
& 8,7,6,\ \ 5,4,3,7,8,9,10,6,7,8,9,7,8,9,10,6,7,8,7,8,9,8,9,\ \ 5,6,\\
& 7,8,9,10,7,8,9,6,7,\ \ 8,6,7,8,9,7,8,5,\ \ 6,7,8,7,6,5,6,7,8,\ \ 9,8,\\
& 9,7,8,\ \ 6,7,5,6,7,8,\ \ 6,7,5,6,4,5,6,7,\ \ 8,9,8,7,8,7,6,7,8,\ \ 7,6,\\
& 7,6,5,\ \ 6,7,8,7,6,5,\ \ 6,7,5,6,4,5,6,7,\ \ 6,5,6,5,4,5,4.
\end{aligned}
$$

Table 6.1: The α sequence of the simple symmetric 13-Venn diagram of Figure 6.10 .

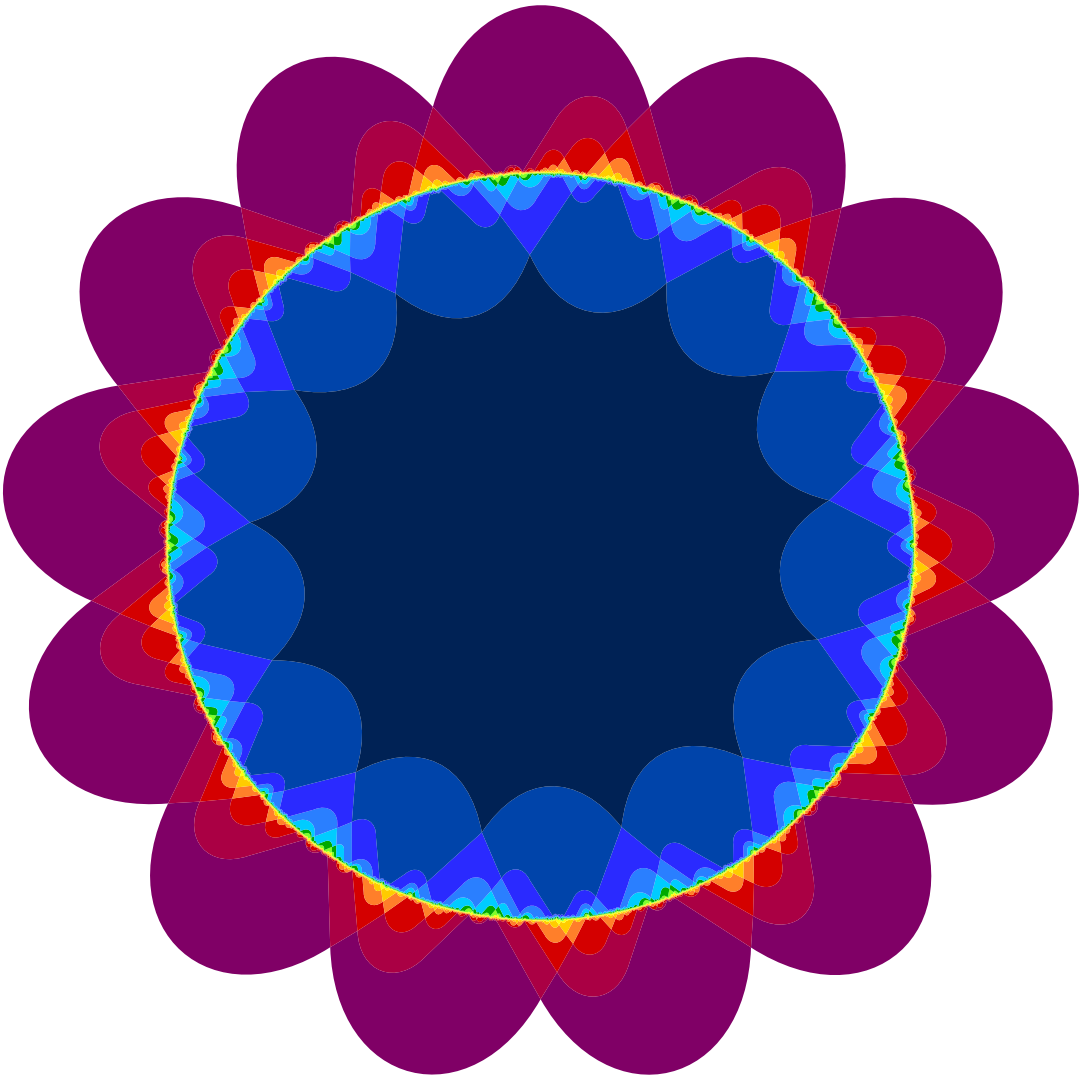

Figure 6.10: The first discovered simple symmetric 13-Venn diagram.

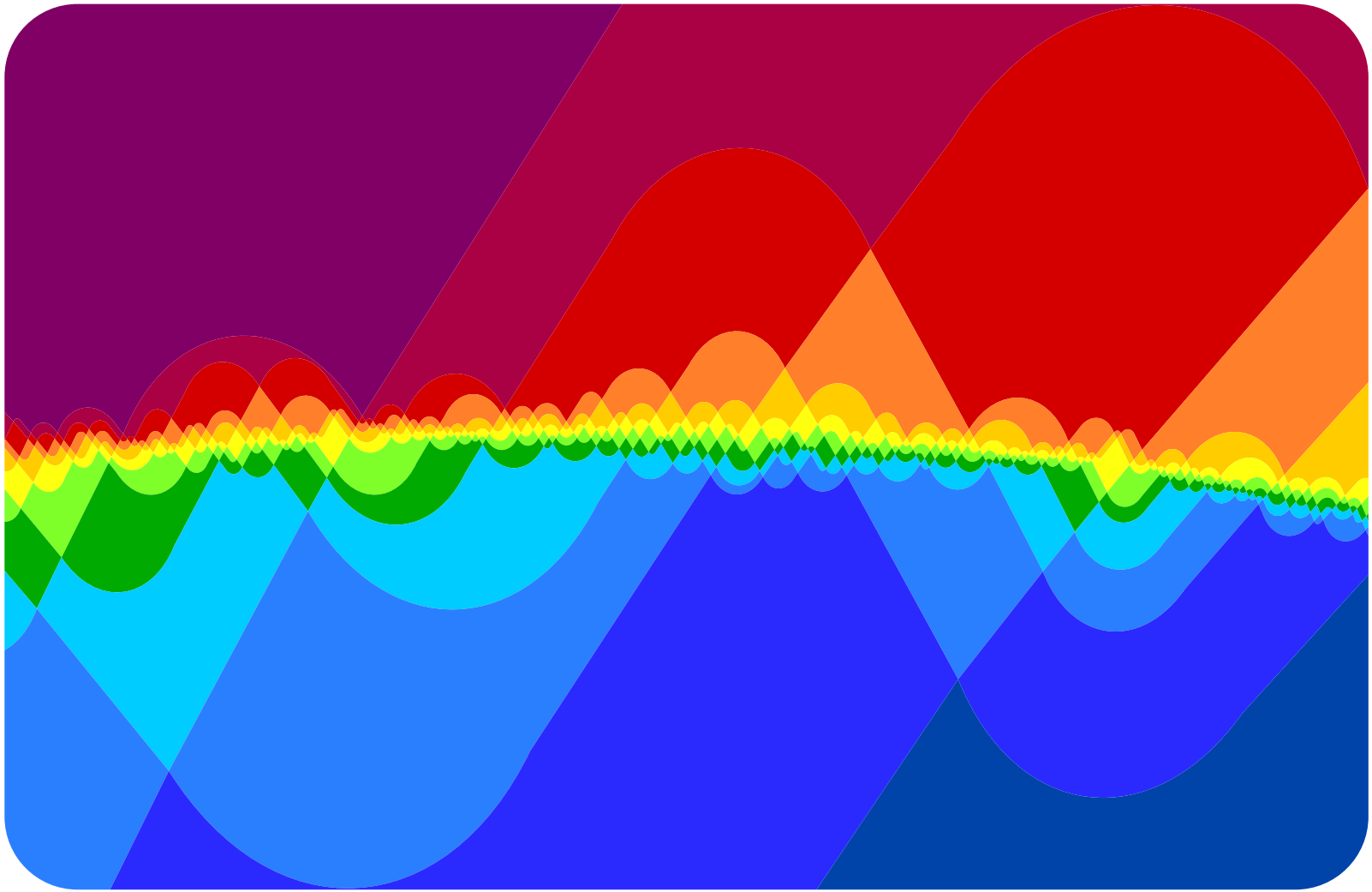

Figure 6.11: A blow up of part of the first simple symmetric 13-Venn diagram.

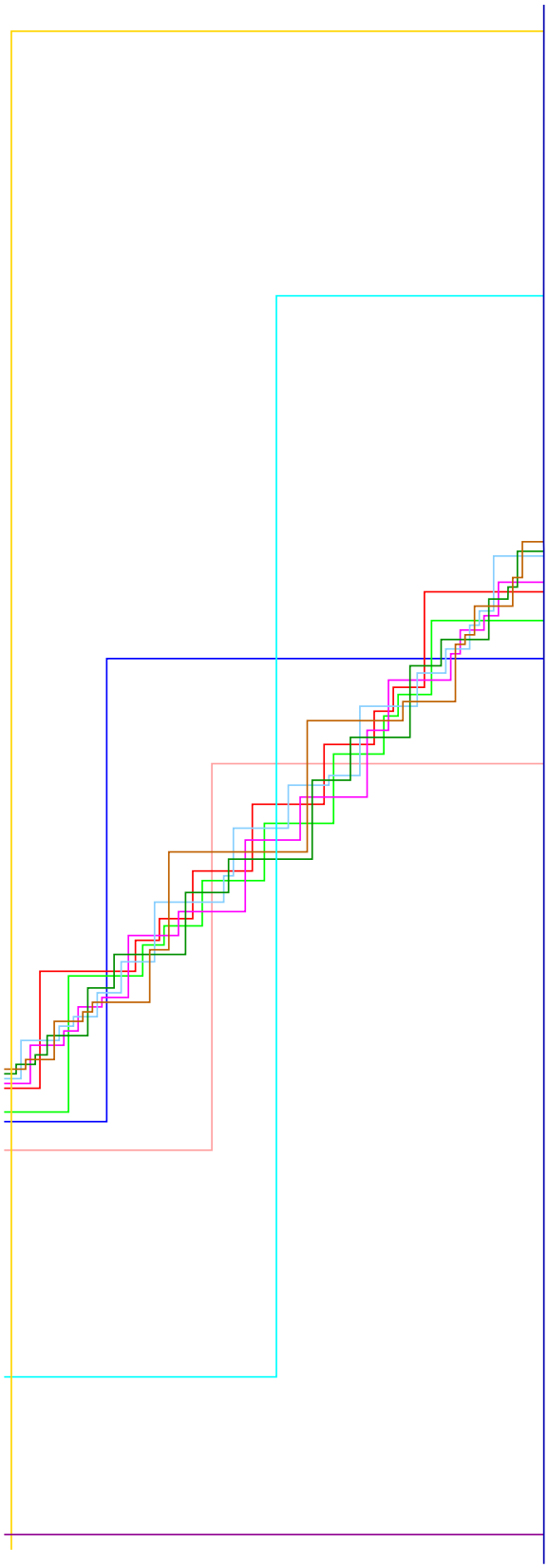

Figure 6.12: The last component of the first half of the cluster of the 13-Venn diagram of Figure 6.10

6.4 Final thoughts

Utilizing the crosscut symmetry helped in finding symmetric Venn diagrams on 11 and 13 curves. So, it is natural to try to exploit further symmetries of diagrams. In the past, attention has focused on polar symmetry. However, it did not help in finding 11-Venn diagrams (in fact, no simple polar symmetric 11-Venn diagrams are yet known), but it is natural to wonder whether it might be fruitful to search for diagrams that are both polar symmetric and crosscut symmetric. However, the theorem proven below proves that there are no such diagrams for primes larger than 7.

Define a *k-point* in a simple monotone Venn diagram to be an intersection point that is incident to two k-regions (and thus also one $(k-1)$-region and one $(k+1)$-region).

Lemma 6.4.1. *Given a cluster of a simple symmetric monotone n-Venn diagram that also has crosscut symmetry, the number of k-points on the left side of the crosscut, for* $1 \leq k < n$, *is*

$$\frac{1}{n}\left(\binom{n-1}{k} + (-1)^{k+1}\right).$$

Proof. Let R_k denote the number of k-regions on the left side of the crosscut. There is a one-to-one correspondence between the k-regions on the left side and $(k+1)$-region on the right side of the crosscut and we know that the total number of k-regions in the cluster is $\binom{n}{k}/n$. Therefore, we can compute the number of k-regions on the left side of the crosscut from the following recurrence relation.

$$R_k = \begin{cases} 1, & \text{if } k = 1 \\ \binom{n}{k}/n - R_{k-1}, & \text{if } 1 < k < n-1. \end{cases} \tag{6.1}$$

Unfolding the recurrence (6.1), we have $nR_k = \sum_{0 \leq j \leq k-1}(-1)^j\binom{n}{k-j} = \binom{n-1}{k} + (-1)^{k+1}$. Every k-point in a simple monotone Venn diagram indicates the ending of one k-region and starting of another one. Therefore, we have the same number of k-points and k-regions on the left side of the crosscut, so both of these are counted by R_k. □

Theorem 6.4.2. *There is no monotone simple symmetric n-Venn diagram with crosscut and polar symmetry for* $n > 7$.

Proof. Let V be a monotone simple symmetric n-Venn diagram which has been drawn in the cylindrical representation with both polar and crosscut symmetry, and let S be a cluster of V with crosscut C. Since the diagram is polar symmetric, S remains fixed under a rotation of π radians about some axis through the equator. Under the polar symmetry action, a crosscut must map to a crosscut, and since there are n crosscuts and n is odd, one crosscut must map to itself, and so one endpoint of this axis can be taken to be the central point, call it x, of some crosscut (the other endpoint of the axis will then be midway between two crosscuts).

Now, consider a horizontal line ℓ that is the equator (and thus must include x). Let $m = (n-1)/2$. The line ℓ cuts every m-region on the left side of C and every $(m+1)$-region on the right side of the crosscut. Because of the crosscut symmetry of V, each $(m+1)$-region on the equator (and so in the interior of C) corresponds to the image of some m-region on the equator (and so in the exterior of C) with the same number of bounding edges. Therefore, for V to be polar-symmetric, every m-region on the left side of the crosscut must be symmetric under a flip about the horizontal line ℓ, and thus each such region must have an even number of bounding edges. The number of bounding edges cannot be 2, because otherwise it is not a Venn diagram. Thus an m-region on ℓ must contain at least one $(m-1)$-point. One of those $(m-1)$-points might lie on C and thus not be counted by R_{m-1}, but all other points are counted and so we must have $R_m \leq R_{m-1} + 1$. However,

$$\begin{aligned} R_m - R_{m-1} &= \frac{1}{n}\left(\binom{2m}{m} - \binom{2m}{m-1} + 2(-1)^{m+1}\right) \\ &= \frac{1}{n}(c_m + 2(-1)^{m+1}), \end{aligned}$$

where c_m is a Catalan number. An easy calculation then shows that $R_m \leq R_{m-1} + 1$ only for the primes $n \in \{2, 3, 5, 7\}$. □

Chapter 7

Conclusions and open problems

The main focus of this thesis was on generating and constructing simple monotone Venn diagrams. Several representations of these diagrams were introduced in Chapter 3 and different backtracking search algorithms were implemented based on these representations in Chapter 4. Using these algorithms we could enumerate all simple monotone 6-Venn diagrams and all simple monotone 7-Venn diagrams that are rotationally symmetric.

Of the three representations of the simple monotone Venn diagrams introduced here, the crossing sequence works better with backtracking search algorithms because it allows us to compute the ranks of regions along the way. Therefore, it is possible to detect duplicate regions as soon as possible and eliminate non-valid cases.

The non-monotone Venn diagrams have not been as well explored as their monotone counterparts. Ruskey and Weston in their survey of Venn diagrams [46] reported 33 simple symmetric non-monotone 7-Venn diagrams but the total number of diagrams of this type is unknown. Searching for simple non-monotone crosscut symmetric Venn diagrams is another interesting problem in this area.

In Chapter 5 we introduced simple bounded Venn diagrams. Separate inductive approaches for constructing involutional simple bounded n-Venn diagrams with half-turn symmetry were provided for n even and for n odd, greater than 3. These constructions prove the existence of a simple symmetric spherical n-Venn diagram with isometry group order eight for $n = 2, 3, 4$ and for any $n \geq 6$.

Figure 7.1(a) shows an example of a simple non-monotone bounded Venn diagram of four curves. This diagram has the reflective symmetry; the axis of reflection is indicated by the dotted line. The associated permutation of the diagram is $\rho = (1\ 2\ 4\ 3)$. So, by Lemma 5.3.1 it can be used to construct a simple non-monotone 6-Venn di-

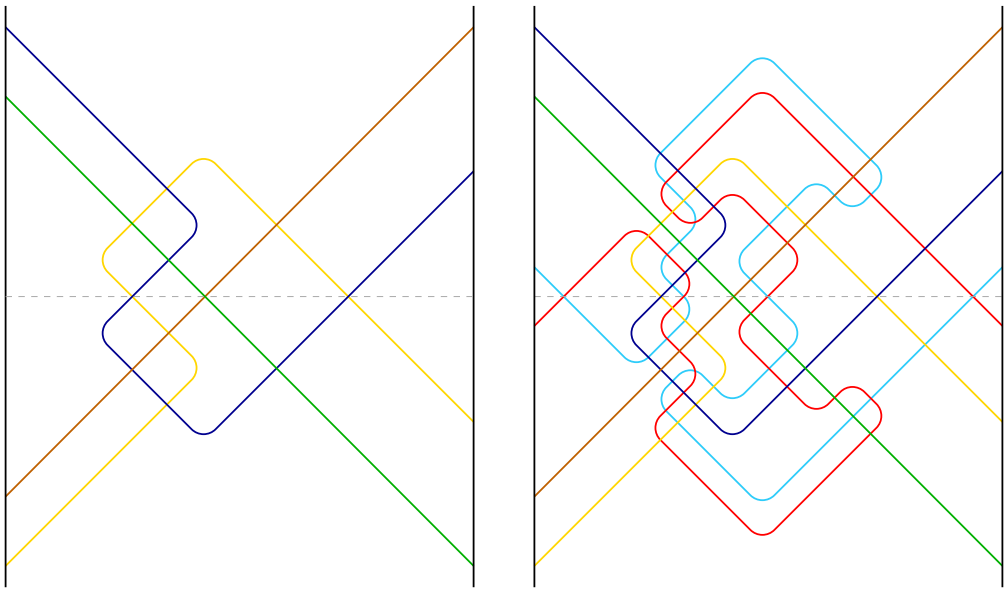

(a) (b)

Figure 7.1: Examples of non-monotone simple bounded Venn diagrams with reflective symmetry. (a) $n = 4$, (b) $n = 6$.

agram with the symmetry group of order eight. An extension of this diagram to a simple non-monotone bounded Venn diagram of six curves with the same properties is shown in Figure 7.1(b). It would be interesting to find a general inductive approach of constructing simple bounded Venn diagrams of this type, analogous to the method provided in Chapter 5.

Previous to this research, the largest prime for which a simple symmetric Venn diagram was known was seven. Taking crosscut symmetry into account in the backtracking search enabled us to find the simple symmetric 11-Venn diagrams. Restricting the search space further using iterated crosscut symmetry, we also found the first simple symmetric Venn diagrams of 13 curves. However, it is impractical to apply the same techniques introduced here in finding simple symmetric n-Venn diagrams for any prime $n \geq 17$ without developing stronger restriction rules.

In searching for simple symmetric 13-Venn diagrams with iterated crosscut symmetry, we used the α-sequence of a simple symmetric 11-Venn diagram (Figure 6.8) as a prefix which in turn contains the α-sequence of the simple symmetric 7-Venn Hamilton as a prefix. So, it is natural to ask if it is possible to generalize this idea for any prime number of curves.

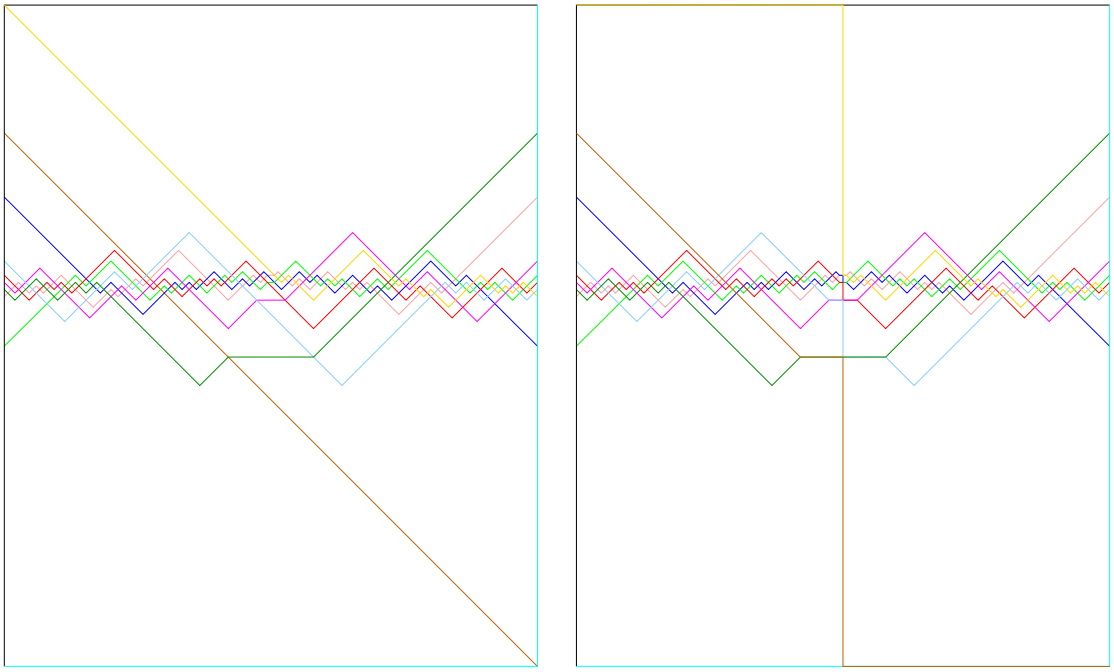

Figure 7.2: (a) Part of two adjacent clusters of Newroz with the crosscut drawn vertically on the left and on the right. The zig-zag starts at the diagonal in the NW corner, and exits at the diagonal in the SE corner. (b) A slightly modified version, showing dihedral symmetry.

Conjecture 7.0.3. *Given any pair of prime numbers n and m where $n > m \geq 3$, there exist simple symmetric Venn diagrams V_n and V_m having iterated crosscut symmetry with crossing sequences $S_n = \rho_n, \alpha_n, \delta_n, \alpha_n^{r+}$ and $S_m = \rho_m, \alpha_m, \delta_m, \alpha_m^{r+}$ such that α_m is a prefix of α_n.*

It is interesting how close our crosscut symmetric diagrams are to having dihedral symmetry. Given a crosscut symmetric n-Venn diagram, by removing $n(n-1)/2$ edges per sector, the remaining diagram can be drawn with dihedral symmetry (Figure 7.2(a)); the edges to be removed are the diagonal edges that intersect a vertical bisector of the figure. By slightly modifying those removed edges we can get a Venn diagram with dihedral symmetry (Figure 7.2(b)). However, in the diagram of Figure 7.2(b) there are curves that intersect at infinitely many points, and there are exactly $n(n-3)/2 = 4$ points where 3 curves meet.

Conjecture 7.0.4. *There is no simple n-Venn diagram with dihedral symmetry if $n > 3$.*

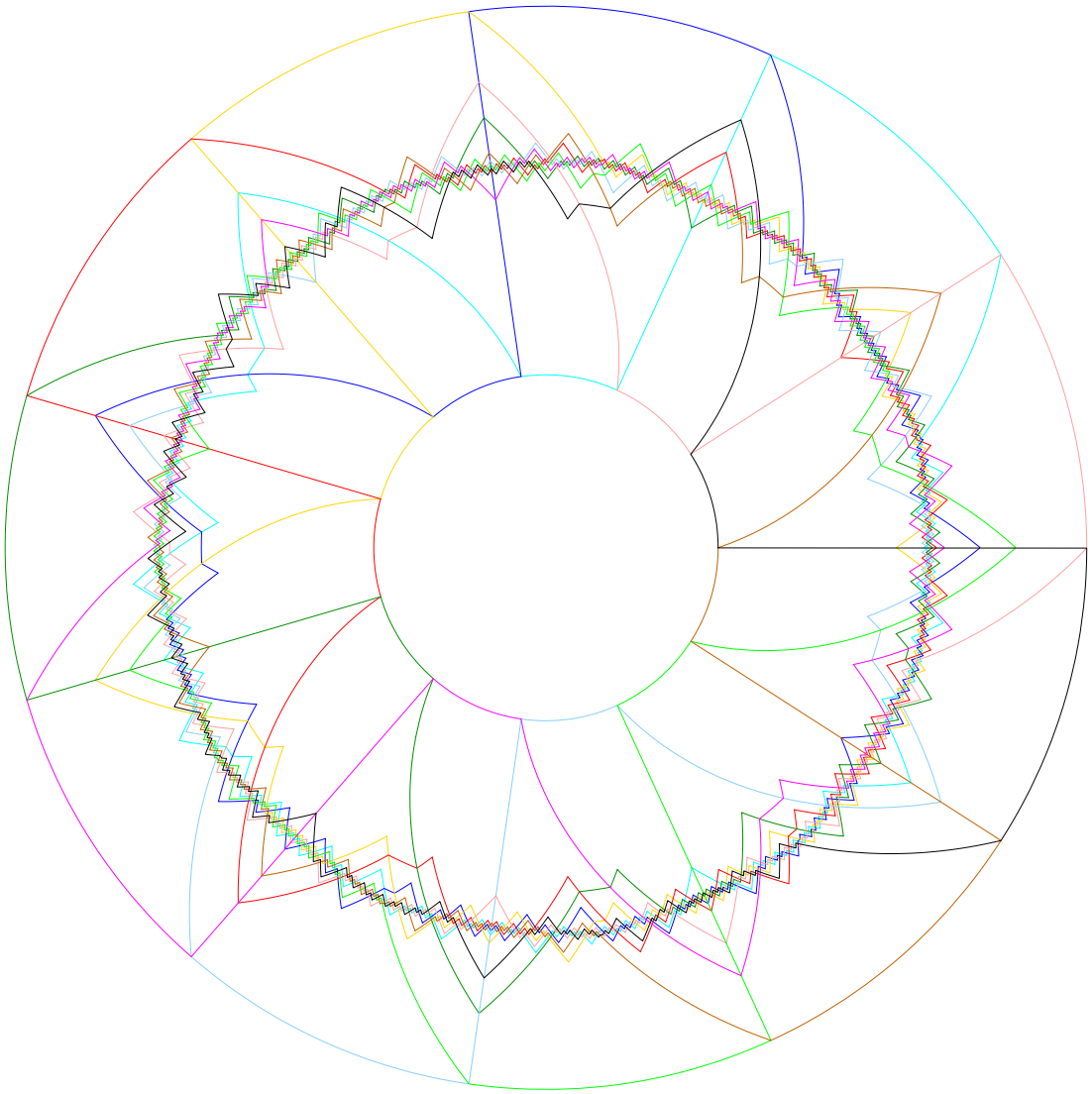

Figure 7.3: Newroz drawn with the crosscuts drawn along rays emanating from the center of the diagram, and with as much dihedral symmetry as possible.

Bibliography

[1] Daniel E. Anderson and Frank L. Cleaver. Venn-type diagrams for arguments of n terms. *Journal of Symbolic Logic*, 113–118, 1965.

[2] Jörg Arndt. *Matters Computational: Ideas, Algorithms, Source Code*. Springer-Verlag, New York, 1st edition, 2010.

[3] Margaret E. Baron. A note on the historical development of logic diagrams: Leibniz, Euler and Venn. *The Mathematical Gazette*, 53(384):113–125, 1969.

[4] Lynette J. Bowles. Logic diagrams for up to n classes. *The Mathematical Gazette*, 370–373, 1971.

[5] Gunnar Brinkmann and Brendan D. McKay. Fast generation of planar graphs. *MATCH Commun. Math. Comput. Chem*, 58(2):323–357, 2007.

[6] Bette Bultena, Branko Grunbaum, and Frank Ruskey. Convex drawings of intersecting families of simple closed curves. In *In 11th Canadian Conference on Computational Geometry*, 18–21, 1998.

[7] Bette Bultena and Frank Ruskey. Venn diagrams with few vertices. *Electronic Journal of Combinatorics*, 5:Research Paper 44, 21 pp. (electronic), 1998.

[8] Tao Cao, Khalegh Mamakani, and Frank Ruskey. Symmetric monotone Venn diagrams with seven curves. In *Fun with Algorithms*, LNCS 6099, 331–342. Springer, 2010.

[9] Jeremy Carroll, Frank Ruskey, and Mark Weston. Which n-Venn diagrams can be drawn with convex k-gons? *Discrete Comput. Geom.*, 37(4):619–628, 2007.

[10] Kiran B. Chilakamarri, Peter Hamburger, and Raymond E. Pippert. Hamilton cycles in planar graphs and Venn diagrams. *J. Combin. Theory Ser. B*, 67(2):296–303, 1996.

[11] Kiran B. Chilakamarri, Peter Hamburger, and Raymond E. Pippert. Venn diagrams and planar graphs. *Geometriae Dedicata*, 62:73–91, 1996.

[12] Kiran B. Chilakamarri, Peter Hamburger, and Raymond E. Pippert. Analysis of Venn diagrams using cycles in graphs. *Geometriae Dedicata*, 82:193–223, 2000. 10.1023/A:1005288325189.

[13] Dwight Duffus, Jeremy McKibben-Sanders, and Kyle Thayer. Some quotients of chain products are symmetric chain orders. *Electronic Journal of Combinatorics*, 19:#P46, 11 pages, 2012.

[14] A. W. F. Edwards. Seven-set Venn diagrams with rotational and polar symmetry. *Combin. Probab. Comput.*, 7(2):149–152, 1998.

[15] Anthony William Fairbank Edwards. Venn diagrams for many sets. *New Scientist*, 7:51–56, Jan 1989.

[16] Anthony William Fairbank Edwards. *Cogwheels of the mind: the story of Venn diagrams*. Johns Hopkins University Press, Baltimore, 2004.

[17] Leonard Euler. Letters to a German princess, on different subjects in physics and philosophy, 1795.

[18] Patrick Fowler, Daniel Horspool, and Wendy Myrvold. Vertex spirals in fullerenes and their implications for nomenclature of fullerene derivatives. *Chemistry: A European journal*, 13:2208–2217, 2007.

[19] Theodore W. Gamelin and Robert Everist Greene. *Introduction to topology*. Dover Publications, 1999.

[20] Martin Gardner. *Logic machines and diagrams*. McGraw-Hill New York, 1958.

[21] Jerrold Griggs, Charles E. Killian, and Carla D. Savage. Venn diagrams and symmetric chain decompositions in the Boolean lattice. *Electronic Journal of Combinatorics*, 11(1):Research Paper 2, 30 pp. (electronic), 2004.

[22] Branko Grünbaum. Venn diagrams and independent families of sets. *Mathematics Magazine*, 48:12–23, 1975.

[23] Branko Grünbaum. Venn diagrams. I. *Geombinatorics*, 1(4):5–12, 1992.

[24] Branko Grünbaum. Venn diagrams. II. *Geombinatorics*, 2(2):25–32, 1992.

[25] Branko Grünbaum. The search for symmetric Venn diagrams. *Geombinatorics*, 8(4):104–109, 1999.

[26] P. Hamburger, Gy. Petruska, and A. Sali. Saturated chain partitions in ranked partially ordered sets, and non-monotone symmetric 11-Venn diagrams. *Studia Sci. Math. Hungar.*, 41(2):147–191, 2004.

[27] Peter Hamburger. Doodles and doilies, non-simple symmetric Venn diagrams. *Discrete Math.*, 257(2-3):423–439, 2002.

[28] Peter Hamburger. Pretty drawings. More doodles and doilies, symmetric Venn diagrams. *Util. Math.*, 67:229–254, 2005.

[29] Peter Hamburger and Raymond E. Pippert. Simple, reducible Venn diagrams on five curves and Hamiltonian cycles. *Geometriae Dedicata*, 68:245–262, 1997.

[30] Peter Hamburger and Attila Sali. Symmetric 11-Venn diagrams with vertex sets $231, 242, ..., 352$. *Studia Scientiarum Mathematicarum Hungarica*, 40(1-2):1–2, 2003.

[31] Peter Hamburger and Attila Sali. 11-doilies with vertex sets of sizes 275, 286,..., 462. *AKCE International Journal of Graphs and Combinatorics*, 1(2):109–133, 2004.

[32] Godfrey Harold Hardy and Edward Maitland Wright. *An introduction to the theory of numbers*. Oxford University Press, sixth edition, 2008.

[33] David W. Henderson. Venn Diagrams for More than Four Classes. *Amer. Math. Monthly*, 70(4):424–426, 1963.

[34] Michael Henle. *A combinatorial introduction to topology*. Dover publications, 1994.

[35] J. E. Hopcroft and J. K. Wong. Linear time algorithm for isomorphism of planar graphs: preliminary report. In *Sixth Annual ACM Symposium on Theory of Computing (Seattle, Wash., 1974)*, pages 172–184. Assoc. Comput. Mach., New York, 1974.

[36] J.E. Hopcroft and R.E. Tarjan. A v log v algorithm for isomorphism of triconnected planar graphs. *Journal of Computer and System Sciences*, 7(3):323 – 331, 1973.

[37] K.K. Jordan. The necklace poset is a symmetric chain order. *Journal of Combinatorial Theory A*, 117:625–641, 2010.

[38] Charles E. Killian, Frank Ruskey, Carla D. Savage, and Mark Weston. Half-simple symmetric Venn diagrams. *Electronic Journal of Combinatorics*, 11(1):Research Paper 86, 22 pp. (electronic), 2004.

[39] Donald E. Knuth. *The Art of Computer Programming, Volume 4A, Combinatorial algorithms*. Addison-Wesley Professional, 2011.

[40] Jacek P. Kukluk, Lawrence B. Holder, and Diane J. Cook. Algorithm and experiments in testing planar graphs for isomorphism. *Journal of Graph Algortihms and Applications*, 8(3):313–356, 2004.

[41] Khalegh Mamakani, Wendy Myrvold, and Frank Ruskey. Generating simple convex Venn diagrams. *Journal of Discrete Algorithms*, 2012.

[42] Trenchard More, Jr. On the construction of Venn diagrams. *J. Symb. Logic*, 24:303–304, 1959.

[43] Reviel Netz. *The shaping of deduction in Greek mathematics: A study in cognitive history*. Cambridge University Press Cambridge, 1999.

[44] Eleanor Robson. *Mathematics in ancient Iraq: a social history*. Princeton University Press, 2008.

[45] Frank Ruskey. Combinatorial generation. *Preliminary working draft. University of Victoria, Victoria, BC, Canada*, 2003.

[46] Frank Ruskey and Mark Weston. A survey of Venn diagrams. *Electronic Journal of Combinatorics*, 11(#R86):22 pages, 2004.

[47] Frank Ruskey and Mark Weston. Spherical Venn diagrams with involutory isometries. *Electronic Journal of Combinatorics*, 18(#R191):14 pages, 2011.

[48] Ian Stewart. *Why beauty is truth: A history of symmetry*. Basic Books (AZ), 2008.

[49] Jacobo Torán and Fabian Wagner. The complexity of planar graph isomorphism. *Bull. Eur. Assoc. Theor. Comput. Sci. EATCS*, (97):60–82, 2009.

[50] Tomas M. Trzeciak. Stereographic and cylindrical map projections. `http://www.texample.net/tikz/examples/map-projections/`, August 2008.

[51] John Venn. On the diagrammatic and mechanical representation of propositions and reasonings. *The London, Edinburgh, and Dublin Philosophical Magazine and Journal of Science*, 10(59):1–18, 1880.

[52] S. Wagon and P. Webb. Venn symmetry and prime numbers: a seductive proof revisited. *American Mathematical Monthly*, 115:645–648, 2008.

[53] L. Weinberg. A simple and efficient algorithm for determining isomorphism of planar triply connected graphs. *Circuit Theory, IEEE Transactions on*, 13(2):142–148, 1966.

[54] Douglas B. West. *Introduction to Graph Theory*. Prentice-Hall, second edition, 2001.

[55] Mark Weston. *Symmetries of Venn Diagrams on the Sphere*. PhD thesis, University of Victoria, British Columbia, 2009.

[56] Hassler Whitney. A theorem on graphs. *Ann. of Math. (2)*, 32(2):378–390, 1931.

[57] Peter Winkler. Venn diagrams: some observations and an open problem. In *Proceedings of the fifteenth Southeastern conference on combinatorics, graph theory and computing (Baton Rouge, La., 1984)*, volume 45, 267–274, 1984.